

AD A060429

18 AFAPL TR-78-41

19

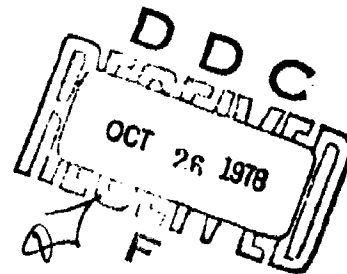
LEVEL

2

6 MAGNETOHYDRODYNAMIC LIGHTWEIGHT CHANNEL DEVELOPMENT.

10 R. W. Swallow, O. K. Sonju, D. E. Meader G. T. Heskey

Maxwell Laboratories, Inc.
200 West Cummings Park
Woburn, Massachusetts 01801



DDC FILE COPY

11 Jun 78

12 170 p.

DDC

9 Final Report.

28 Nov 75 - Dec 77, 31

Approved for public release; distribution unlimited.

15 F 33615-76-C-2001

26 3145

17 26

AIR FORCE AERO PROPULSION LABORATORY
AIR FORCE WRIGHT AERONAUTICAL LABORATORIES
AIR FORCE SYSTEMS COMMAND
WRIGHT-PATTERSON AIR FORCE BASE, OHIO 45433

18 10 16 033
410 218

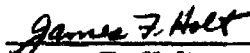
mt

NOTICE

When Government drawings, specifications, or other data are used for any purpose other than in connection with a definitely related Government procurement operation, the United States Government thereby incurs no responsibility nor any obligation whatsoever; and the fact that the government may have formulated, furnished, or in any way supplied the said drawings, specifications, or other data, is not to be regarded by implication or otherwise as in any manner licensing the holder or any other person or corporation, or conveying any rights or permission to manufacture, use, or sell any patented invention that may in any way be related thereto.


This report has been reviewed by the Information Office, (ASD/OIP) and is releasable to the National Technical Information Service (NTIS). At NTIS, it will be available to the general public, including foreign nations.

This technical report has been reviewed for publication.


James F. Holt
Project Engineer


Richard L. Verga
Technical Area Manager
MHD Energy Conversion

FOR THE COMMANDER


Philip E. Stover
Chief, High Power Branch

Copies of this report should not be returned unless return is required by security considerations, contractual obligations, or notice on a specific document.

REPORT DOCUMENTATION PAGE		READ INSTRUCTIONS BEFORE COMPLETING FORM
1. REPORT NUMBER AFAPL-TR-78	2. GOVT ACCESSION NO.	3. RECIPIENT'S CATALOG NUMBER
4. TITLE (and Subtitle) MAGNETOHYDRODYNAMIC LIGHTWEIGHT CHANNEL DEVELOPMENT		5. TYPE OF REPORT & PERIOD COVERED Final Technical Report 28 Nov 75 - 31 Dec 77
6. AUTHOR(s) Swallow, D. W., Sonju, O. K., Meader, D. E., Heskey, G. T.		7. PERFORMING ORG. REPORT NUMBER
8. PERFORMING ORGANIZATION NAME AND ADDRESS Maxwell Laboratories, Inc. 200 W. Cummings Park Woburn, Massachusetts 01801		9. CONTRACT OR GRANT NUMBER(s) F33615-76-C-20014
10. CONTROLLING OFFICE NAME AND ADDRESS Air Force Systems Command Air Force Aero Propulsion Laboratory Wright-Patterson Air Force Base, Ohio 45433		11. PROGRAM ELEMENT, PROJECT, TASK AREA & WORK UNIT NUMBERS 31452635 6 - -
12. MONITORING AGENCY NAME & ADDRESS (if different from Controlling Office)		13. REPORT DATE June 1978
		14. NUMBER OF PAGES 158
		15. SECURITY CLASS. (of this report) Unclassified
		16. DECLASSIFICATION/DOWNGRADING SCHEDULE
17. DISTRIBUTION STATEMENT (of this Report) Approved for public release; distribution unlimited.		
18. DISTRIBUTION STATEMENT (of the abstract entered in Block 20, if different from Report)		
19. SUPPLEMENTARY NOTES		
20. KEY WORDS (Continue on reverse side if necessary and identify by block number) MHD Generators Burst Power Supplies Fast Start Power Supplies High Performance MHD Generator Lightweight Megawatt Power Supplies Flightweight MHD Compact MHD Generators Lightweight MHD		
21. ABSTRACT (Continue on reverse side if necessary and identify by block number) A lightweight, high performance MHD channel and diffuser were designed, built, and tested. The hardware was designed for testing with toluene and oxygen at the Air Force Aero Propulsion Laboratory energy conversion facility (KIVA-1) at Wright-Patterson Air Force Base. The design power level of 200 kW dc was obtained during the 125 tests of the test evaluation program.		

Block 19. (Continued)

Cesium Seeding of MHD Gases
Toluene Fueled MHD
Filament Wound, Epoxy Coated Fiberglass
Direct Energy Conversion Systems

Block 20. (Continued)

The MHD channel design was a diagonal conducting wall generator with calcia stabilized zirconia electrodes and a filament wound epoxy coated fiberglass outer shell. The diffuser design utilized thin wall copper construction with external cooling tubes. These designs resulted in a significant reduction of the masses of the channel and diffuser. The masses of the channel and diffuser were 40 kg and 24 kg, respectively, which compared favorably to previous channels and diffusers of similar performance characteristics with masses of 160 kg and 150 kg, respectively.

The novel design features of the channel construction technique included the use of a filament wound, epoxy coated fiberglass structural shell, the presence of an RTV layer to provide the pressure seal, and the minimization of the use of the copper material in the electrode frames. This fabrication procedure combined to provide a lightweight channel capable of withstanding sustained operation under a wide variety of operating conditions.

FOREWORD

This final report was submitted by Maxwell Laboratories, Inc. under Contract No. F33615-76-C-2001. The effort was sponsored by the Air Force Aero Propulsion Laboratory, Air Force Systems Command, Wright-Patterson AFB, Ohio under Project 3145, Task 314526 and Work Unit 31452635 with Dr. James F. Holt/AFAPL/POP-1 as Project Engineer. Dr. Daniel W. Swallom and Dr. Otto K. Sonju of Maxwell Laboratories, Inc. were technically responsible for the work.

The authors of this report appreciate the assistance given to them by the many individuals who contributed to the work performed on this report as well as the guidance given to them by Dr. James F. Holt and the facility operating team of the Air Force Aero Propulsion Laboratory.

ACCESSION for	
REC	White Section <input checked="" type="checkbox"/>
DOC	Buff Section <input type="checkbox"/>
UNCLASSIFIED	
DATE: 10/10/76	
BY: A	

TABLE OF CONTENTS

SECTION		PAGE
I	INTRODUCTION	1
II	LIGHTWEIGHT MHD CHANNEL AND DIFFUSER DESIGN AND ANALYSIS	
	1. Objectives and Approach	4
	2. Channel/Diffuser Design Alternatives	8
	a. Introduction	8
	b. Channel Internal Area Profile	8
	c. Channel Electrode Frames Configuration	9
	d. Channel Exterior Shell Construction	15
	e. Final Channel Design	18
	f. Diffuser Design	21
	3. Performance Analysis	
	a. Structural Analysis	27
	b. Thermal Analysis	36
	c. Hydraulic Analysis	40
	d. Magnetohydrodynamic Analysis	44
	4. Cooling System Design	48
	a. Channel	50
	b. Diffuser	52
	c. Manifolds	53
III	FABRICATION OF THE LIGHTWEIGHT MHD CHANNEL AND DIFFUSER	
	1. Introduction	54
	2. Component Manufacture	55
	3. Electrode Frame Assembly	65
	a. Brazing the Current Collector Screens to the Cooling Tubes	67
	b. Soldering the Copper Cooling Fins to the Cooling Tubes	68
	c. Assembling the Corner Blocks to the Cooling Tubes	68

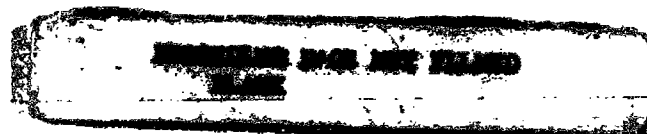


TABLE OF CONTENTS

SECTION	PAGE
<ul style="list-style-type: none"> d. Attaching the Frame Anchors to the Outer Edges of the Frames e. Installing Taps at the Corners of the Frames f. Water Flow and Leak Testing g. Dry Assembling of the Electrode Frames on the Alignment Mandrel 	69
4. Ceramic Emplacement	70
<ul style="list-style-type: none"> a. Electrode Ceramic b. Insulator Ceramic 	76
5. Final Frame Assembly, Case Fabrication and Finishing Operations	78
<ul style="list-style-type: none"> a. Final Frame Assembly b. Case Fabrication Assembly c. Finishing Operations 	89
6. Cooling System	91
<ul style="list-style-type: none"> a. Channel Cooling b. Diffuser Cooling 	96
7. Diffuser Fabrication	97
<ul style="list-style-type: none"> a. Shell Fabrication b. Pressure Taps c. Cooling Tubes d. Ceramic Felt e. Silicone Rubber Blanket 	102
 IV	
MHD GENERATOR TESTING PROGRAM	
1. Water Flow Tests	104
<ul style="list-style-type: none"> a. Introduction b. Test Set-Up and Operation c. Channel Flow Tests d. Diffuser Flow Tests 	105
2. Vacuum Tests	106

TABLE OF CONTENTS

SECTION	PAGE
3. AFAPL Experimental Test Program	107
a. Facility Description	107
b. Test Plan Summary	110
c. Thermal Tests	113
d. Low Magnetic Field Tests	116
e. Power Tests	116
f. Vibration Measurements	121
V RELIABILITY AND MAINTAINABILITY ANALYSIS	
1. Introduction	132
2. Electrode System	133
3. Cooling System	133
4. Gas Seals	136
5. Channel and Diffuser Cases	136
6. Instrumentation and Electrical	136
VI CONCLUSIONS AND RECOMMENDATIONS	140
APPENDIX - SAFETY AND HAZARDS ANALYSIS CHANNEL AND DIFFUSER	142
REFERENCES	155
LIST OF ABBREVIATIONS, ACRONYMS, AND SYMBOLS	156

LIST OF ILLUSTRATIONS

FIGURE		PAGE
1	Lightweight Channel/Diffuser System Installed at the AFAPL MHD Facility	3
2	Channel Design Evolution	6
3	Initial Electrode Frame Coolant Flow Model and Flow Test Set-Up	11
4	Second Electrode Frame Prototype	12
5	Final Electrode Design Utilizing Continuous Cooling Tube	14
6	Typical Cross Section of Electrode Wall and Insulator Wall	16
7	Completed Prototype Electrode Frame	17
8	Final Lightweight Channel Design Configuration	19
9	Lightweight Diffuser Shell	22
10	Diffuser Assembly During Fabrication	25
11	Lightweight MHD Diffuser	26
12	Coefficient of Thermal Expansion and Modulus of Elasticity for OFHC (CDA-102)	28
13	Yield Strength and Ultimate Tensile Strength of Annealed OFHC (CDA-102)	29
14	Fatigue Curve for Annealed OFHC (CDA-102) For Combined Thermal and Mechanical Strains	30
15	Frame Section Properties for Stress Analysis	32
16	Composite Case Fatigue Curve	34
17	Design Axial Heat Flux Distribution for the Channel and Diffuser	38
18	Electrode Frame Temperature Distribution	39
19	Pressure Loss for 6 mm I.D. Copper Tubing	41

LIST OF ILLUSTRATIONS

FIGURE		PAGE
20	Magnetic Field Distribution for 2.3 Tesla Center Field for the AFAPL Magnet	45
21	Variable Area Profile Characteristics of the Channel	46
22	Axial Voltage Profile in the Diagonal Wall Channel for 10.9 Ohm Load	49
23	Lightweight MHD Channel After Filament Winding	56
24	Electrode Frame Assembly	58
25	Completed Electrode Frame	59
26	Tube Radius Bending Fixture	60
27	Electrode Cooling Tube Flattening Fixture	61
28	Electrode Cooling Tube 45 Degree Bending Fixture	62
29	Channel Fabrication Mandrel	66
30	Partial Dry Assembly of the Frames on the Mandrel	71
31	Typical Cross Section of Electrode Wall	72
32	Channel Wall Construction Details	73
33	Electrode and Insulator Ceramic Samples	75
34	Electrode Frame with Electrode Ceramic Emplaced	77
35	Emplacement of the Alumina Insulator Material	79
36	Lightweight MHD Channel with Ceramic Emplaced	80
37	Final Frame Fitup in Process	82
38	Final Assembly of Frames on the Mandrel	83
39	Lightweight MHD Channel Before Filament Winding	88
40	Inlet End of Lightweight Channel	94
41	Finished Lightweight MHD Channel	95
42	Inlet and Exit Ends of Lightweight Diffuser Shell	98

LIST OF ILLUSTRATIONS

FIGURE		PAGE
43	Diffuser Cooling Tube Tooling	100
44	Lightweight MHD Diffuser	101
45	Completed Lightweight MHD Diffuser	103
46	Schematic Illustration of the Major Systems of the AFAPL MHD Generator Facility	108
47	Cooling System for the Channel and Diffuser	109
48	Lightweight Channel/Diffuser System Installed at the AFAPL MHD Facility	112
49	Axial Heat Flux Distribution for Test LWC 003	114
50	Axial Static Pressure Distribution for Test LWC 012	115
51	Schematic of the Electrical Wiring Diagram	117
52	Axial Voltage Distribution for Test LWC 007	118
53	Static Pressure Distribution for Test LWC 007	119
54	Magnetic Field Distribution for 2.3 Tesla Center Field for the AFAPL Magnet	122
55	Axial Voltage Distribution for Test LWC 122	123
56	Axial Pressure Distribution for Test LWC 091	124
57	Interior of Lightweight Channel at Test Program Conclusion	125
58	Schematic of Accelerometer Placement	126
59	Power Spectral Density for Test LWC 013	129
60	Summation Power Spectral Density for Test LWC 013	129
61	Difference Power Spectral Density for Test LWC 013	130

LIST OF TABLES

TABLES		PAGE
1	Electrode Cooling Data	43
2	Dimensional Comparisons of AFAPL Channels and Diffusers	47
3	Cooling System Summary	51
4	Operating Conditions	111
5	Electrode System RMA	134
6	Cooling System RMA	135
7	Gas Seals RMA	137
8	Channel and Diffuser Cases RMA	138
9	Instrumentation and Electrical RMA	139

SECTION I

INTRODUCTION

This is the Final Report of Contract No. F33615-76-C-2001, "Magneto-hydrodynamic Lightweight Channel Development," between the Air Force Aero Propulsion Laboratory (AFAPL) and Maxwell Laboratories, Inc. (MLI). The period of performance for the work was from November 1975 through December 1977.

The main objectives of this technical effort were to design, fabricate and test a 200 kW_e lightweight MHD channel and a lightweight diffuser. The hardware was designed for testing at the MHD energy conversion facility located in Building 71, Area B, Wright-Patterson Air Force Base, Ohio. These objectives were achieved as over 125 tests of the hardware were completed, and the design output power level of 200 kW dc was obtained.

The MHD channel design was a diagonal conducting wall generating with calcia stabilized zirconia electrodes and a filament wound epoxy coated fiber-glass outer shell. The diffuser design used thin wall copper construction with external cooling tubes. Both designs emphasized utilizing lightweight design and construction techniques to the greatest extent possible. This resulted in being able to greatly reduce the mass of the channel and the diffuser. The channel mass, including all of the tubes, fittings, and connectors, was 40 kg; and the diffuser mass, including the barbed fittings and tubing, was 25 kg. The previous hardware of similar size and electrical characteristics had a channel mass of approximately 160 kg and a diffuser mass of approximately 150 kg. Thus, the hardware developed for this contract provided a reduction in component mass by factors of 4-6, and more importantly, demonstrated the feasibility of a completely new or novel channel construction technique.

The novel design features of the channel construction technique included the use of the filament wound, epoxy coated fiberglass structural shell, the presence of an R TV layer to provide the pressure seal, and the minimization of the use of the copper material in the electrode frames. This fabrication procedure combined to provide a lightweight channel capable of withstanding sustained operation under a wide variety of operating conditions. The diffuser design used thin copper sheets to form the four walls of the diffuser. Cooling was provided by external cooling tubes which were brazed to the outside of the diffuser. Figure 1 shows a photograph of the hardware installed at the MHD facility.

The technical effort extended through various phases including design, fabrication, and testing. A chronology of the significant program events is listed below.

- | | |
|--------------------------------------|---------------|
| ● Program Start | November 1975 |
| ● Design Frozen | May 1976 |
| ● Component Manufacturing
Started | June 1976 |
| ● Channel/Diffuser Completed | October 1976 |
| ● Flow and Pressure Tests Completed | November 1976 |
| ● Channel/Diffuser Shipped to AFAPL | November 1976 |
| ● Vibration Analysis Completed | January 1977 |
| ● MHD Test Program Started | May 1977 |
| ● MHD Test Program Completed | December 1977 |



Figure 1. Lightweight Channel/Diffuser System Installed at the AFAPL MHD Facility.

SECTION II
LIGHTWEIGHT MHD CHANNEL AND DIFFUSER
DESIGN AND ANALYSIS

1. OBJECTIVES AND APPROACH

The design and fabrication of a lightweight, high performance channel and diffuser presented two problem areas which must be resolved simultaneously - the lightweight and compact wall structure limitation and the high performance requirement. The lightweight requirement was satisfied by using the high strength-to-weight filament wound, fiber reinforced epoxy resin for the channel wall (i.e., the pressure vessel) and by minimizing the volume of heavy materials in the channel electrode frames and in the diffuser walls. The high performance requirement demanded careful attention to the design of the method used to cool the channel and diffuser walls. This requirement was met by constructing the electrode frames and the diffuser walls of copper, primarily because of its high coefficient of thermal conductivity, and by cooling the members with high velocity water, thereby optimizing the rate of heat removal from the walls. This represents the first step in the development of MHD channels using this design concept. At the present time this concept is being carried further with the development of a 30 MW MHD channel under Air Force Contract No. F33615-76-C-2104.

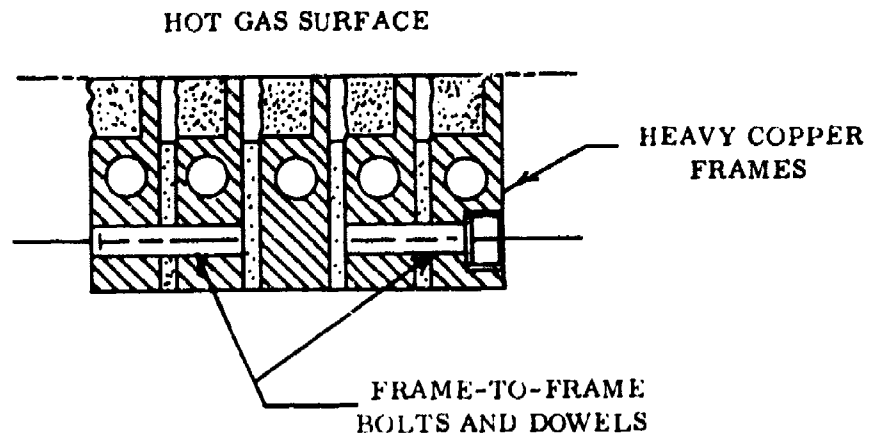
In many existing MHD generators, the electrode frames of the MHD channels were constructed by machining the trapezoidal central region out of solid copper plates.¹ This approach resulted in a rather heavy and thick wall construction, which was not competitive from an overall system design point of view. The successful achievement of this lightweight design resulted from a careful analysis of the construction requirements of the MHD channel.

¹ R. V. Shanklin, J. K. Lytle, R. A. Nimmo, L. W. Buechler, and H. W. Hehn
"KIVA-I Extended Duration MHD Generator Development", AFAPL-TR-75-27,
June 1975.

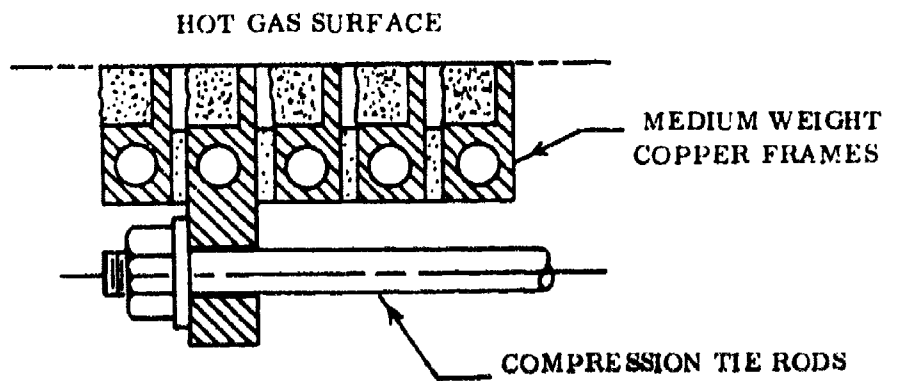
The details of the various designs which were evaluated are illustrated in Figure 2. Figure 2a illustrates a non-optimum design which has been tested in the past.^{1,2} This design utilized heavy copper frames which were bolted and doweled together. The seals were installed between adjacent frames such that the assembled frames served as the electrodes and the pressure vessel or structural wall. The cooling passages were typically drilled along all four sides and then plugged as appropriate. The welded or brazed plugs provided a potential source of water leaks. The sharp corners resulted in higher pressure drops than a smoothly bent tube. In order to provide reliable gas seals, the electrode frame must be relatively thick to insure structural integrity.

Figure 2b shows a "medium" weight design where the weight reduction was achieved by the use of external compression tie rods to clamp together a set of "medium" weight frames. Since no bolts were used between adjacent frames, less material was required for each frame turn. This provided a significant reduction of the channel mass. Again, the electrode frames served as the electrode elements and the pressure vessel or structural wall. However, when the wall thickness was reduced, gas sealing became a problem with this design. A more detailed analysis of this sealing problem showed that the mechanical integrity of this design dictated a minimum wall thickness. Finally, even though the channel mass has been reduced with the "medium" weight design, the bulkiness of the channel has not been reduced. Hence, the volumetric filling factor of the warm bore of the magnet has not been significantly reduced from the approach shown in Figure 2a.

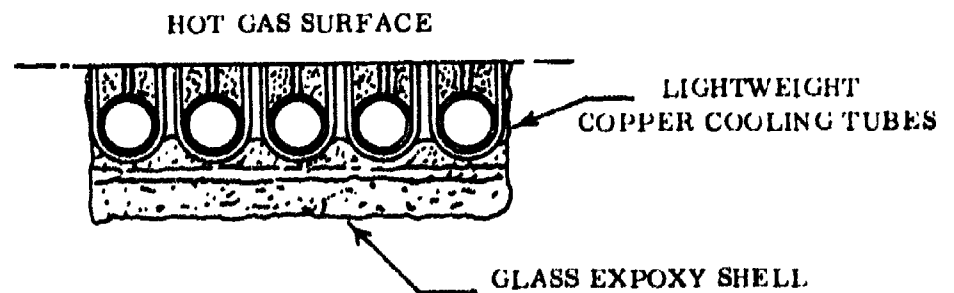
²T. R. Brogan, A. M. Aframe, and J. Hill, "Preliminary Design of a Magneto-hydrodynamic Channel for the USSR U-25 Facility", Final Report, Contract #14-32-001-1733, November 1974.



(a) Heavy Weight



(b) Medium Weight



(c) Light Weight

Figure 2. Channel Design Evolution

The most significant reduction of the channel mass and volume was achieved by separating the pressure vessel wall function from the electrode frame function. This approach is shown in Figure 2c. With this lightweight design, the electrode frame utilized a lightweight thin copper, cooling tube, and the pressure vessel wall utilized a high strength-to-mass, non-metallic composite material such as filament wound, fiberglass or "Kevlar" reinforced epoxy resin. No interelectrode frame gas sealing was required for this design - a feature which was extremely important for reliable operation. In addition, the surfaces of the electrode frames did not have to be machined to either high precision dimensional flatness tolerances or critical surface finish requirements. Once the manufacturing process has been fully developed, this simplification in the manufacturing techniques has the potential to significantly reduce the fabrication cost of the electrode frames.

In addition to the advantages obtained by reducing the channel mass and volume, other significant gains were achieved. Some of these advantages were: 1) potential for low cost fabrication; 2) increased reliability; 3) finer segmentation of the electrodes; 4) integral cooling passages without braze or weld joints or connections at elevated temperatures; 5) no gas sealing problems; 6) no critical tolerances inside the entire channel; 7) minimal thermal expansion problems since close tolerances of the mating surfaces of dissimilar materials were not required; 8) flexibility and simplicity of construction; and 9) mechanical simplicity. Since the overall channel design objective was a reduction of channel mass and volume along with increased reliability, decreased fabrication complexity and increased design flexibility, the general design approach selected was required to satisfy all of these objectives.

Paragraph 2 of this section describes the channel/diffuser design alternatives. The performance analysis is described in paragraph 3. The cooling system design is described in paragraph 4.

2. CHANNEL/DIFFUSER DESIGN ALTERNATIVES

a. Introduction

The lightweight channel involved three areas of significant design alternatives: the channel internal area profile, the electrode frames configuration, and the exterior shell construction.

b. Channel Internal Area Profile

Two of the existing AFAPL heat sink channels were constructed with contoured side peg walls and plane or flat surfaced top and bottom electrode walls. The walls were attached to each other with adjustable fastening hardware so that the top and bottom walls could be "opened" or "closed" to cause a 20% change in the exit area. Previous performance tests with the heat sink channel demonstrated that the area profile had been optimized.³ Since the main objective of this lightweight channel program was not to optimize the channel performance but rather to demonstrate the feasibility of lightweight channel design and fabrication, there were no channel performance reasons to change the area profile. However, there were some changes to the area profile which were made in order to simplify the fabrication of the lightweight channel.

A key feature in achieving the lightweight channel construction was the use of a fiberglass filament wound reinforced epoxy resin shell that was fabricated in place around the outside of the electrode frames. The high strength-to-weight ratio of the shell was the result of the continuous glass filaments being wound around the channel. These filaments formed the four walls without any seams or joints along the edges of the channel. Consequently, there was no practical way of providing a variable area profile.

³ O. K. Sonju, J. Teno, J. W. Lothrop, and S. W. Petty, "Experimental Research on a 400 kW High Power Density MHD Generator", AFAPL-TR-71-5, May 1971.

Another change to the area profile which simplified the fabrication was the elimination of the contoured surfaces of the heat sink channel side walls. The lightweight channel side walls and the top and bottom walls were designed with flat surfaces. This modification allowed the use of identical or duplicate corner features of the electrode frames and significantly reduced the complexity of the electrode frames fabrication. Previous performance tests with a channel of this internal contour also demonstrated satisfactory performance.¹

c. Channel Electrode Frames Configuration

The electrode frames configuration involved two regions of the channel - the transition frames at the entrance and exit of the channel, and the generating frames which comprised the main body of the channel.

The original concept for this channel program was a design for the transition regions which utilized a set of "U" shaped electrode frames to form the angular transition between the perpendicular ends of the channel and the diagonal generating electrode frames. These transition frames were all oriented at the same angle of inclination as the diagonal generating frames, but each frame had a different depth of the "U" shape. These transition frames were considered to be too complicated to fabricate within the scope of this program. Instead, the angle transition was achieved by designing the entrance and exit ducts with inclined ends that matched the diagonal electrode frames.

The initial design concept of the generating electrode frames was based on the use of straight sections of cooling tubes along the sides, tops, and bottoms of the frames. These four sections were to be connected together at the corners of the frames by soldering them into square corner blocks with drilled holes for the

internal cooling passages. The tubing was to be circular in cross section with a small diameter tube used along the sides of the frames because of the space limitations of the narrow cross section of the frame. The first model frame with the connected tubes was fabricated and flow tested and is shown in Figure 3. The flow test results showed an excessively high pressure drop because of the small diameter tubes.

In an attempt to reduce the pressure drop, a second model frame with connected tubes was fabricated with larger diameter tubing which was flattened to an oval cross section along the sides of the frame as shown in Figure 4. The flow tests for this frame produced pressure drops that were acceptable. However, the process of fabricating the second model frame demonstrated that the complex external geometry and the critical internal cooling passages of the corner blocks resulted in very high machining costs. In addition, previous experience with MHD generator channels had shown that solder joints in cooling tubes which were exposed to repeated thermal cycling were frequently a source of leaks. However, the connected tube design did have the advantage that the frame internal opening height and width dimensions could be closely controlled. This was accomplished by assembling the loose tubes and corner blocks on a sizing mandrel and temporarily tack welding the tubes to the corner blocks. This process maintained the frame dimensions while the frames were removed from the mandrel and the tube to corner block joints were permanently joined by high temperature soldering or brazing. However, the advantages did not outweigh the disadvantages.

The next stage in the electrode frame design development was an attempt to use a single continuous piece of copper tubing to form the complete cooling passage for one frame. This approach would have had the advantage of eliminating any joints in the cooling passage which would significantly increase the reliability of the electrode frames. However, this design concept proved to present a number of problems or disadvantages which caused it to be abandoned. Attempts

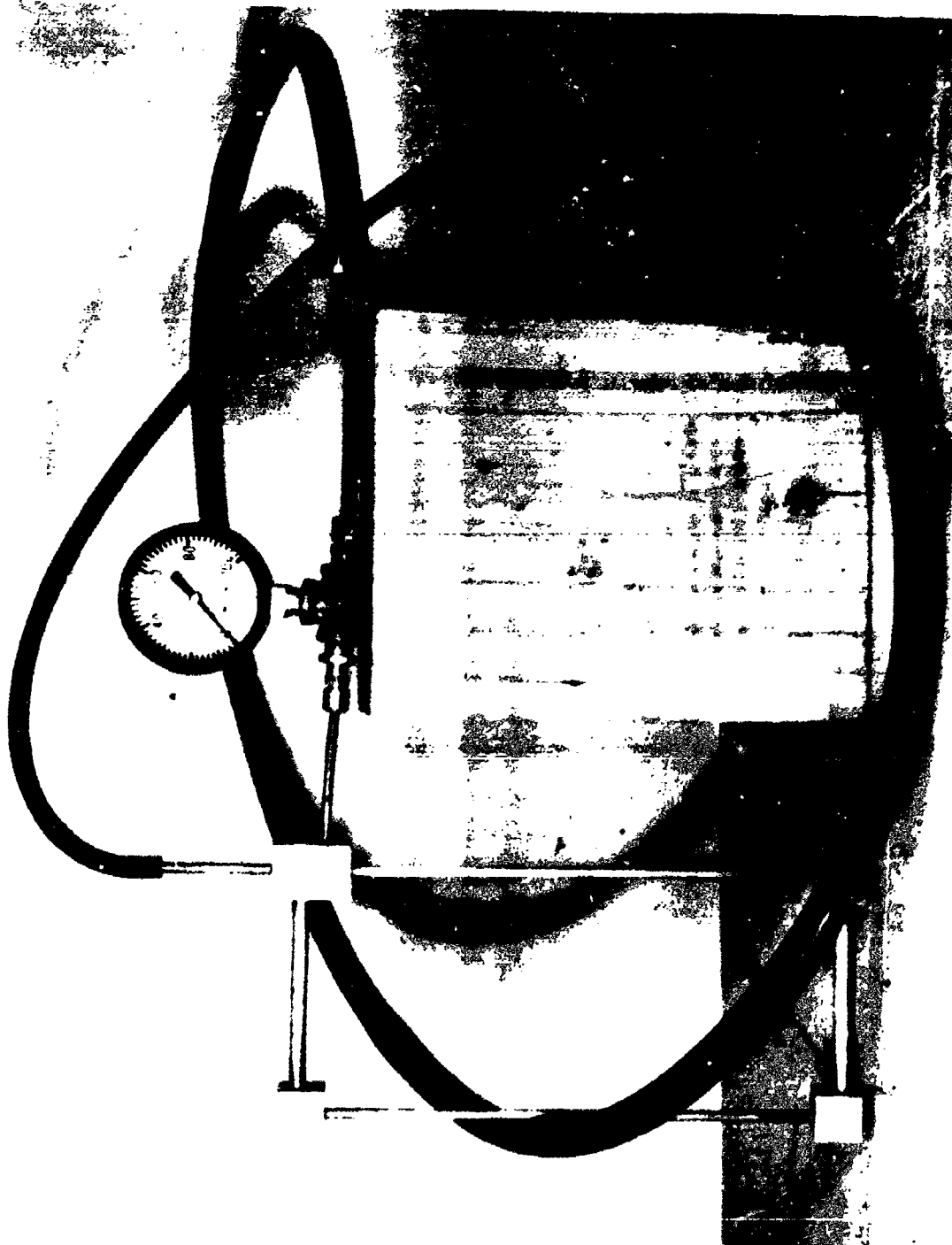


Figure 3. Initial Electrode Frame Coolant Flow Model and Flow Test Set-Up.

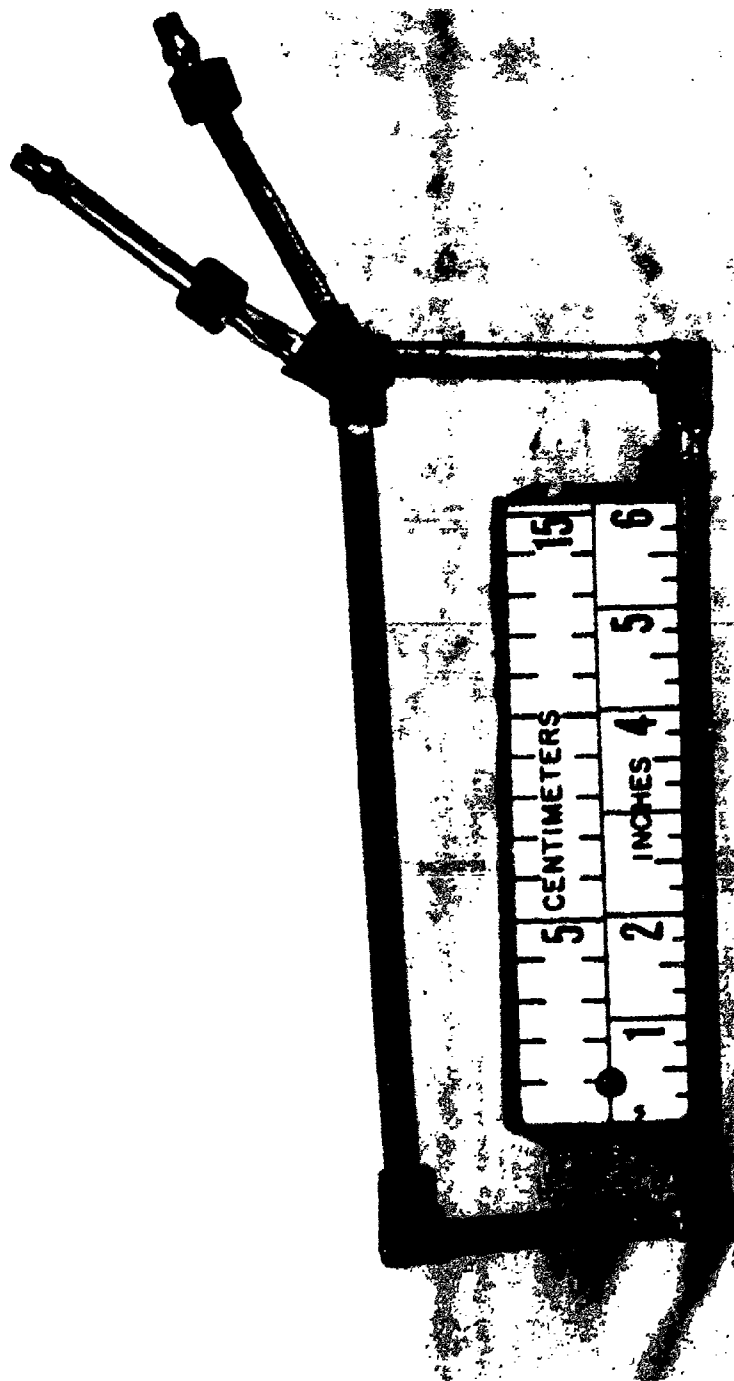


Figure 4. Second Electrode Frame Prototype.

to form one continuous tube across the top of the channel, down one side, across the bottom and then up the other side proved to be impractical within the scope of this program. The three-dimensional geometry that was required for the tubes to make the transition around the corners of the channel in addition to the requirement for flattening the tube cross section along the sides of the channel would require extensive and complex tooling and techniques to successfully form the single continuous tube. In addition the "closed loop" continuous tube approach eliminated any possibility of adjusting the frame opening internal height and width dimensions to fit a sizing mandrel within close tolerances. Another disadvantage of the closed loop approach, particularly with the smaller electrode frames of this channel, was that the frame internal opening width and height dimensions were too small to allow ready access to the hot gas surfaces of the electrodes. This size limitation would have restricted fabrication operations such as cutting the Inconel current collector screens to equal the height of the adjacent cooling fins.

The final design concept that was selected for the lightweight channel frames utilized two continuous cooling tubes for each frame. One tube formed the top cross member and one side of the frame, and the other tube formed the bottom cross member and the opposing side member of the frame as shown in Figure 5. This design required separate corner blocks, but the blocks were not part of the frame cooling passages. Instead, the corner blocks now functioned as heat transfer and structural members only.

This "two tube" approach eliminated the problems and disadvantages involved with the single tube approach. Forming the tube proved to be less difficult because of the access to the tube from all directions. The inlet and outlet ends of the tubes were designed with a definite space between the adjacent tubes. This design allowed the two halves of each frame to be adjusted relative to each other when they were placed on the sizing mandrel and the corner blocks to be made to compensate for the variations in the spacing of the tubes. This approach also allowed access to

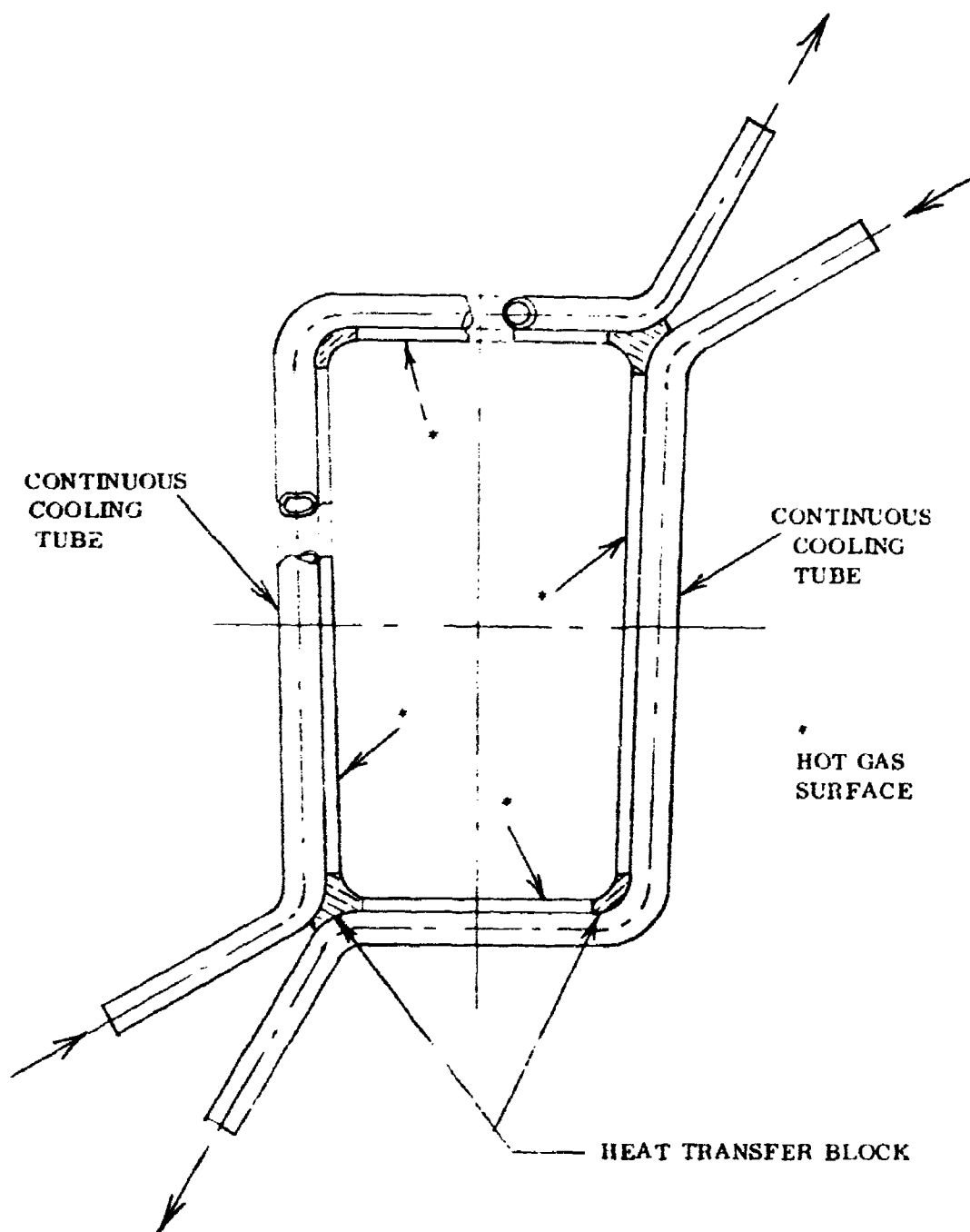


Figure 5. Final Electrode Design Utilizing Continuous Cooling Tube.

the hot gas surfaces of the frames for performing various fabrication operations while the frames existed as two halves, i.e. before joining the halves together at the two corners of the channel.

The hot gas surface regions of the electrode frames consisted of the Inconel current collector screens and the copper cooling fins which were attached to the cooling tube as shown in Figure 6. The construction of the electrode wall sections of the frames is shown in Figure 6a. The cooling tube was circular in cross section in this region. The Inconel screen was folded into a double layer and was attached to the cooling tube by high temperature brazing with the folded edge of the screen in contact with the tube. The copper cooling fins were premachined and formed to fit the tube and were attached to the tube by soldering. The space between the cooling fins and the electrode screen was then filled with the zirconia electrode ceramic. The construction of the insulator wall sections of the frame is shown in Figure 6b. The features of these sections were essentially the same as the electrode wall sections, except that the cooling tube cross section was oval or flattened to form a narrower width frame in this region, and the cooling fins were premachined and formed to match the flattened tube section.

This approach with the two continuous tubes for each frame was selected for the lightweight channel design, and a completed prototype frame is shown by the photograph of Figure 7.

d. Channel Exterior Shell Construction

The major design alternatives that were considered for the fabrication of the channel exterior shell construction were the materials to be selected for the fiber reinforcing material and the plastic matrix material. These materials were combined to produce the fiber reinforced composite shell structure. The primary properties of the composite materials that were of concern were the strength values of the reinforcing filaments, the resistance of the plastic matrix materials to heat

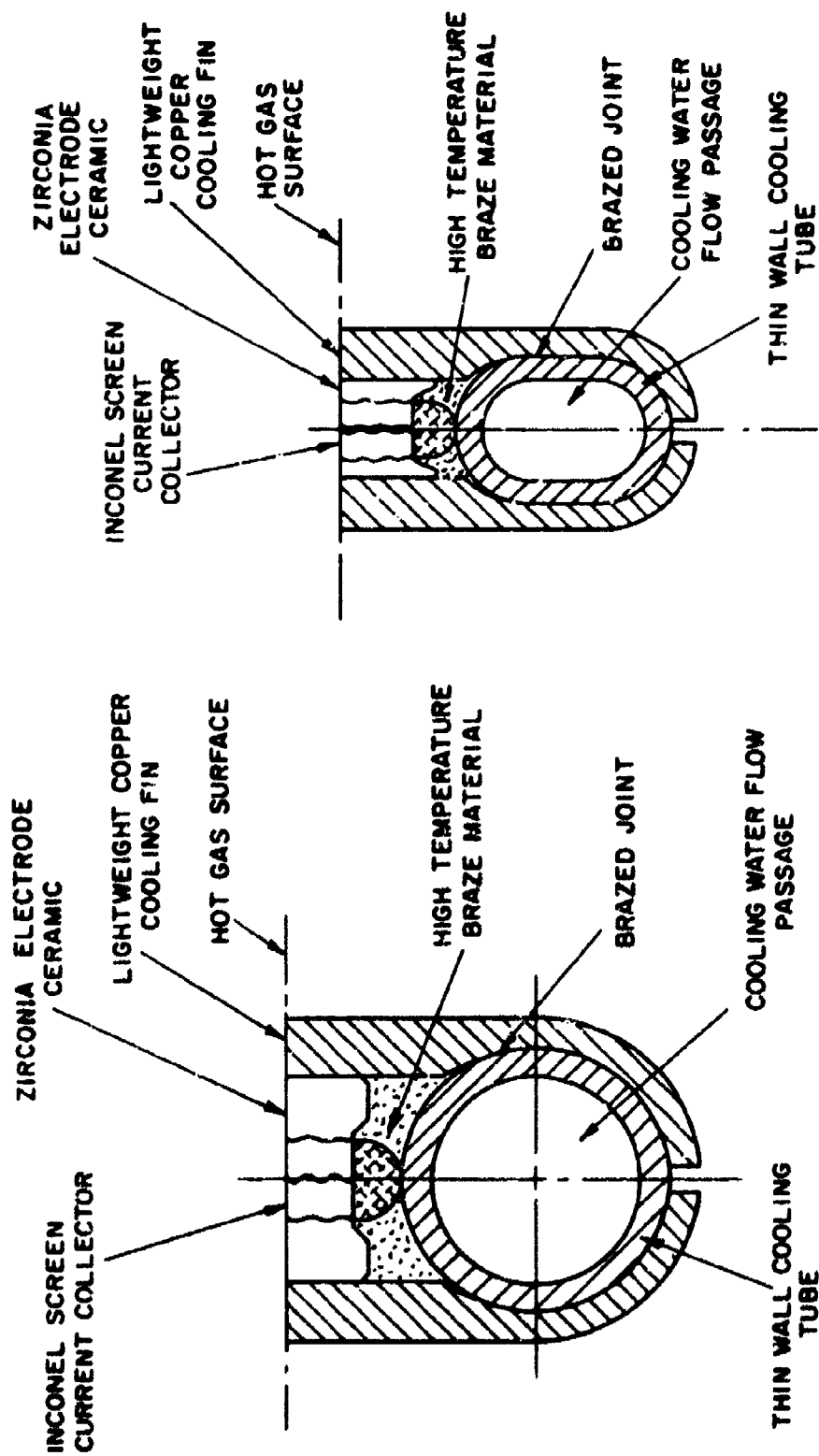


Figure 6. Typical Cross Section of Electrode Wall and Insulator Wall.

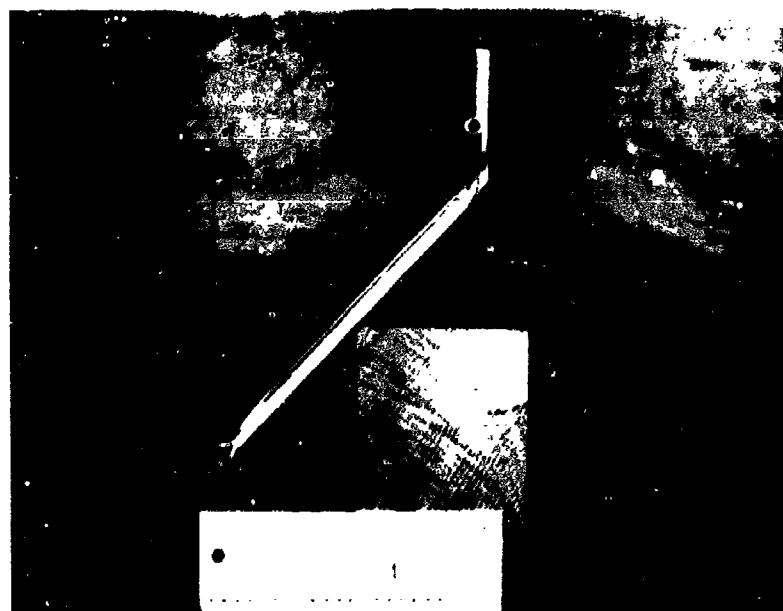
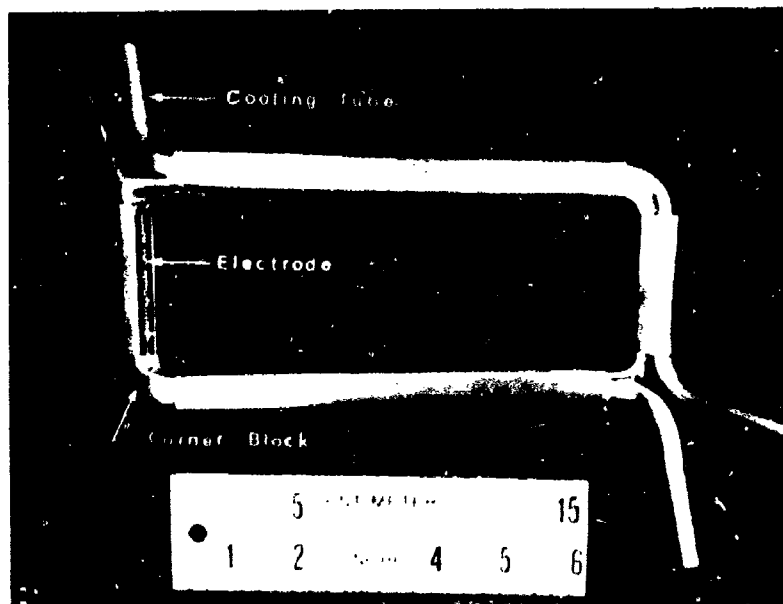


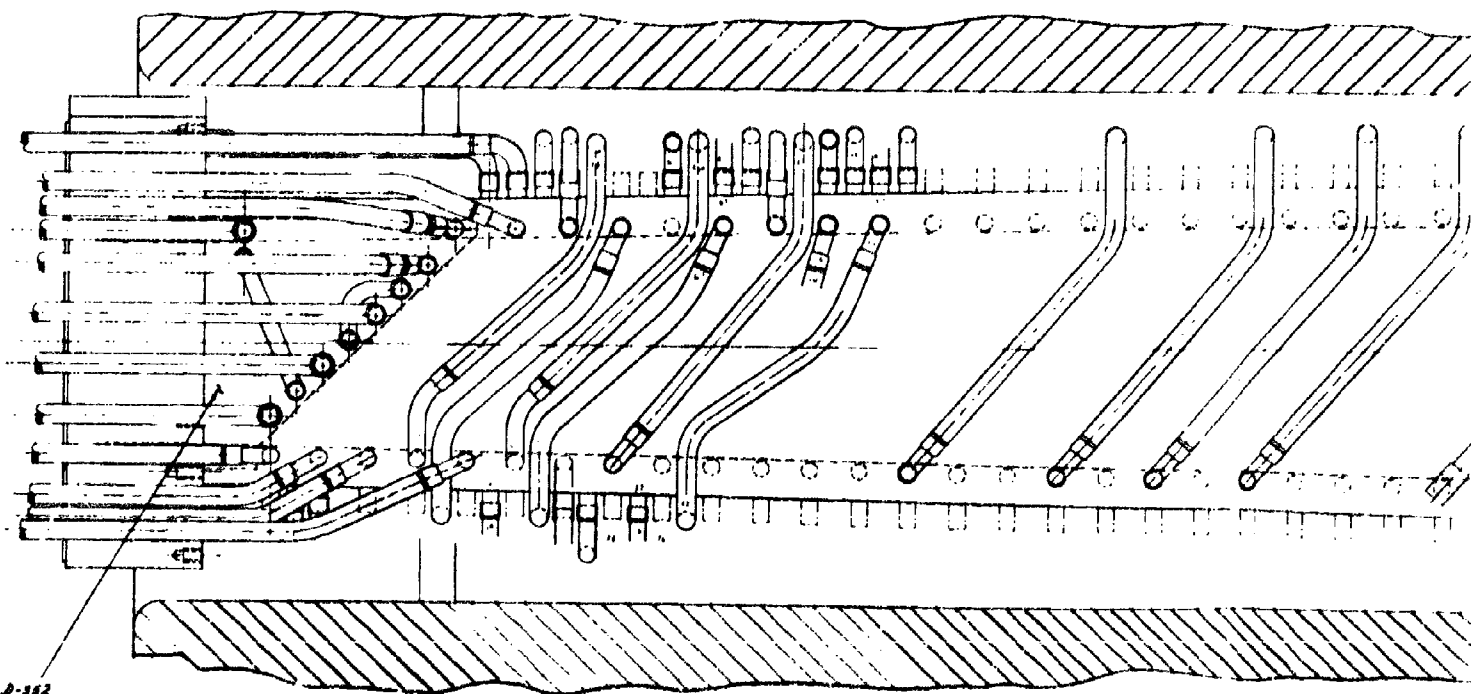
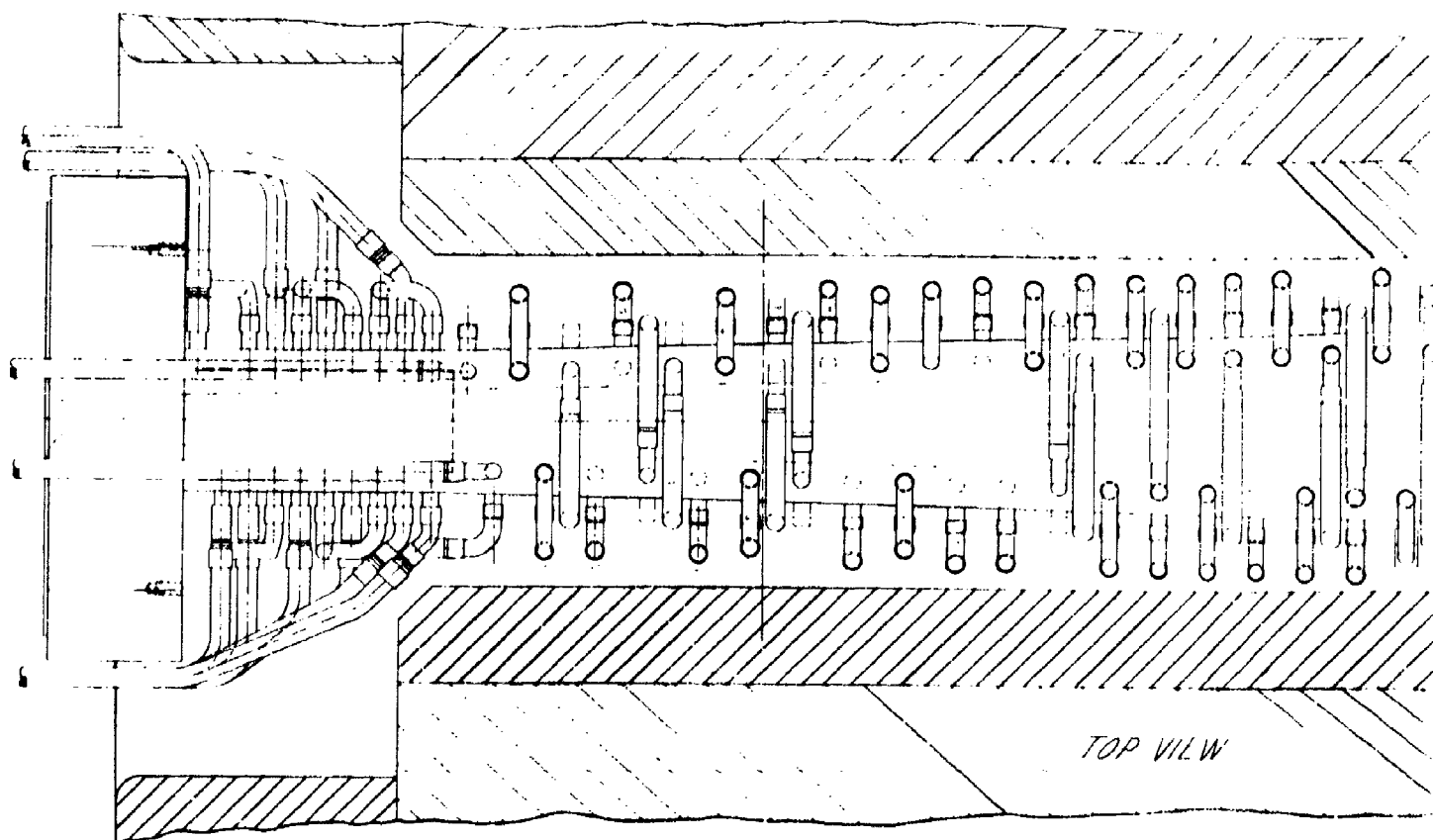
Figure 7. Completed Prototype Electrode Frame.

distortion, and the maximum recommended service temperature. Previous material studies and modeling work had investigated the use of silicone resins as the plastic matrix material.⁴ Although the silicone resin has higher temperature ratings than epoxy resins, the process of fabricating the composite material proved to be complicated. Since the heat resistance requirements of lightweight channel were considered to be well within the capabilities of conventional epoxy resins, a standard commercially available epoxy resin was selected. For the selection of the fiber reinforcing material, there are other filaments or fibers that have properties superior to the E-glass selected, such as the aromatic polyamide fibers (DuPont "Kevlar"). This polyamide fiber had a tensile strength that was 20% better than E-glass, stiffness that was twice that of E-glass, and a density that was 43% lower than E-glass. Although the properties of Kevlar were significantly better than glass fibers, Kevlar nevertheless was a relatively new material to use with the fabrication techniques that were required to optimize its utilization in a composite material. Since the structural requirements of the lightweight channel were well within the range of conventional materials, the more commonly used glass fibers were selected for the lightweight channel shell.

e. Final Channel Design

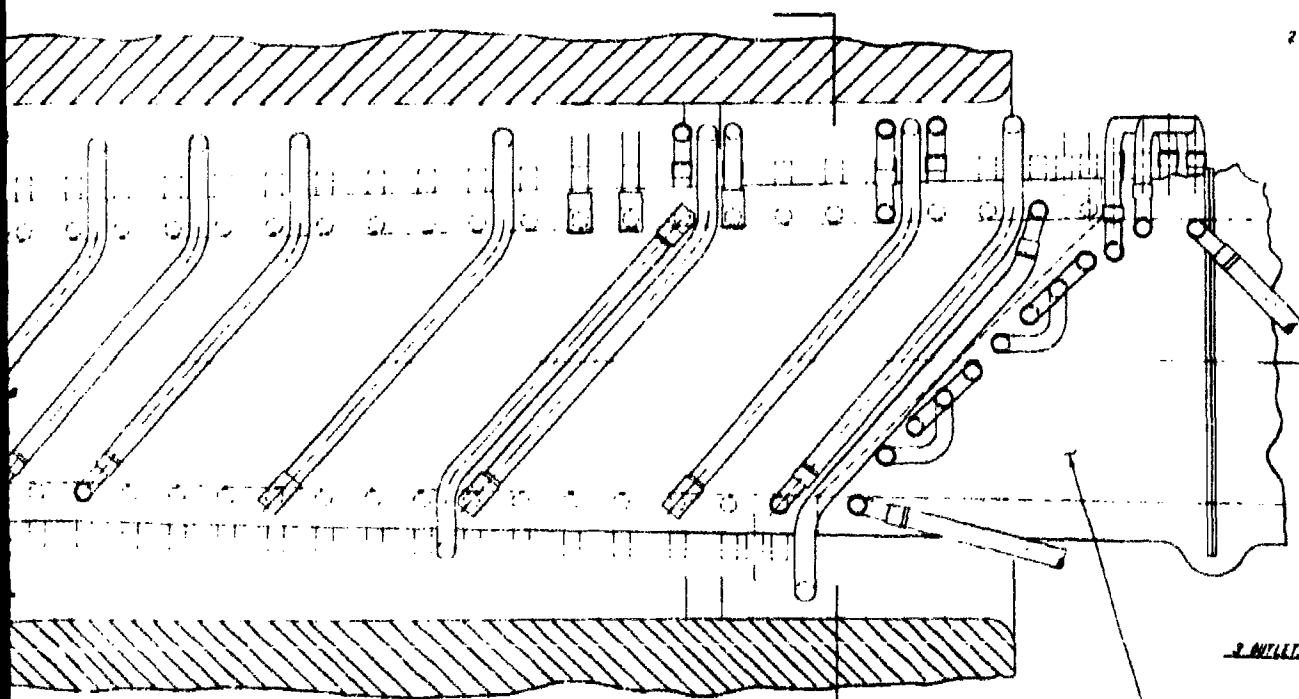
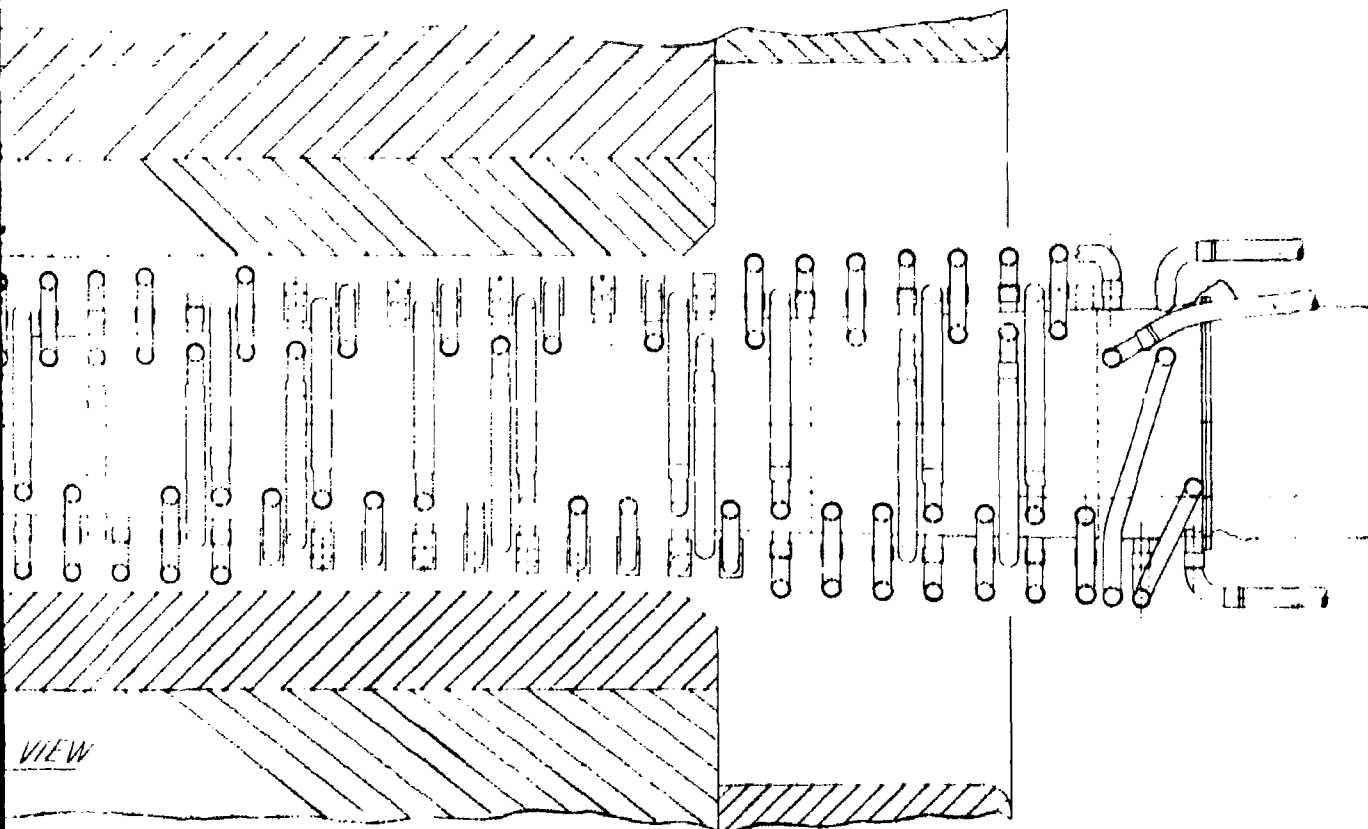
The final lightweight channel design configuration is shown in Figure 8. The internal gas side contour was designed with an entrance width of 24.9 mm and height of 99.8 mm. The exit width was 72.6 mm, and exit height was 140 mm. The overall length, including the inlet and exit ducts, was 1054 mm. The side walls and the top and bottom walls were designed with flat surfaces that diverged from the entrance to exit dimensions over a length of 1003 mm. A length of 51 mm at the exit end was designed with the walls parallel to match the entrance

⁴ O. K. Sonju, J. Teno, R. Kessler, L. Lontai, and D. E. Meader, "Status Report of the Design Study Analysis and the Design of a 10 MW Compact MHD Generator System," AFAPL-TR-74-47, Part II, June 1974.



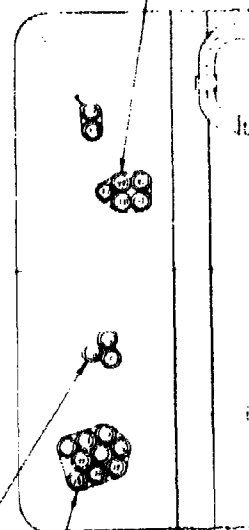
D-182

RIGHT SIDE VIEW



2 WELDS

5 WELDS



2 INLETS

2 INLETS

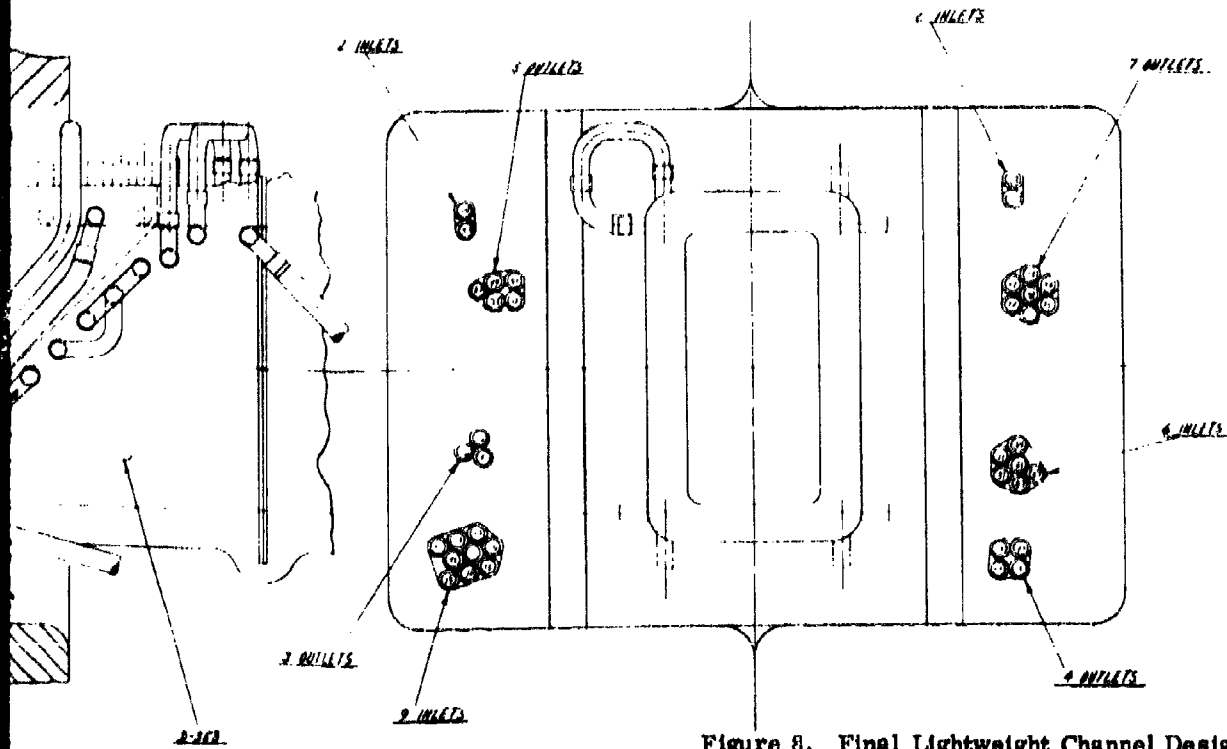
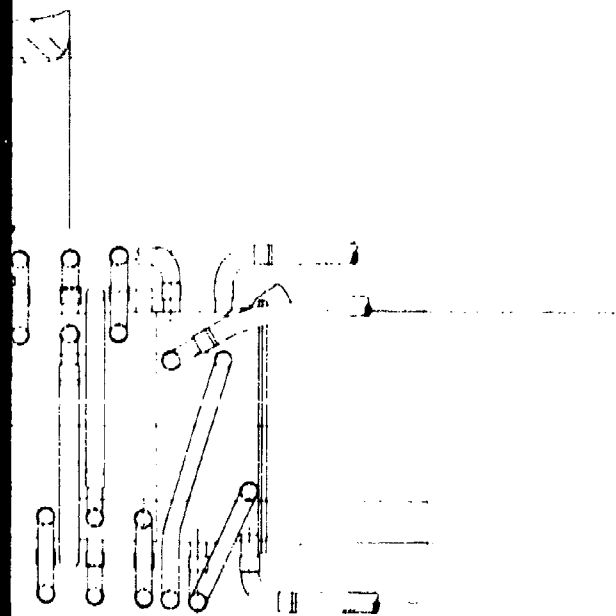


Figure 8. Final Lightweight Channel Design Configuration.

3

contour of the diffuser. The actual mass of the lightweight channel without any cooling tubes attached was 27.7 kg, and with the cooling tubes attached, the mass was 40 kg. This is compared to an estimated mass of approximately 160 kg for a conventional channel utilizing electrode frames machined from solid copper plates with drilled cooling passages.

f. Diffuser Design

The diffuser was designed to meet the hot gas flow pressure and temperature requirements and to demonstrate lightweight diffuser fabrication techniques. The internal geometry of the diffuser was based on the existing APL diffuser. Sufficient test data was available to demonstrate that the actual pressure recovery coefficient was within the margin of error of the calculated value.

The internal passage was designed with a constant width of 72.6 mm and a total length of 965 mm. A straight supersonic/subsonic section of 140 mm height and 483 mm length was connected to a subsonic section which diverged to a height of 198 mm over a length of 482 mm. This geometry is shown in Figure 9, which is a photograph of the lightweight diffuser shell without the cooling tubes attached.

In cases where minimum mass has not been a design goal, diffusers have typically been designed with thick plate copper walls with the cooling passages formed by drilling holes in the plates parallel to the hot gas surfaces. In order to minimize the mass, the diffuser was designed with thin copper sheet walls forming a minimum mass shell. The copper cooling tubes were soldered to the outside of the shell to form the cooling system which removes the expected thermal load imposed on the diffuser by the hot plasma.

The diffuser shell was designed with 1.2 mm thick copper sheets. Copper was used because of its outstanding thermal conductivity and the ease of attaching cooling tubes by brazing or soldering processes. A design verification model was

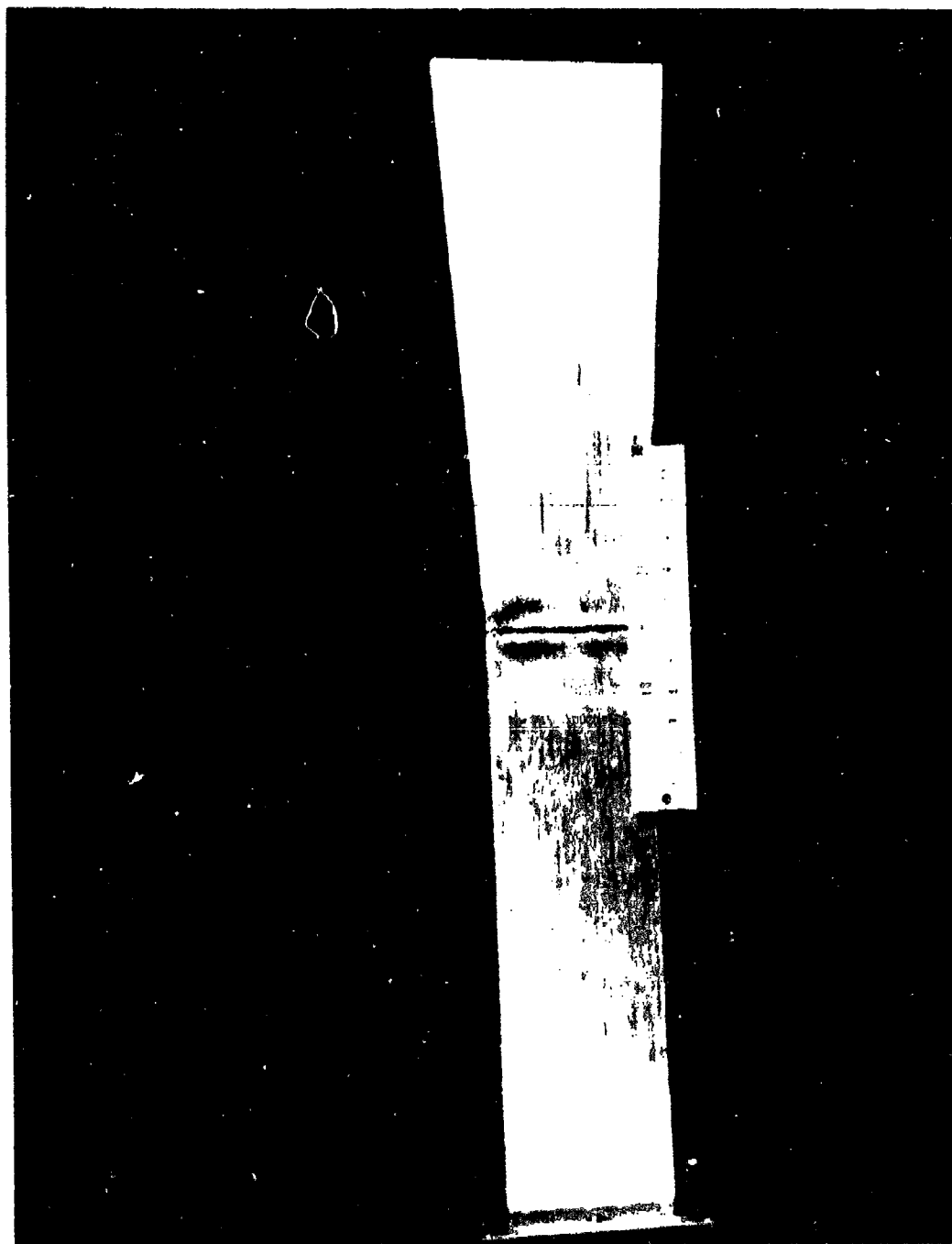


Figure 9. Lightweight Diffuser Shell.

fabricated in an attempt to use sheets of 0.85 mm copper, but the process of brazing the tubes to the sheet caused excessive buckling between the tubes which would have caused excessive disturbances in the gas flow along the walls.

The cooling tubes were originally designed so that each tube formed one complete turn around the diffuser, but several problems occurred during fabrication which caused a redesign so that each tube only formed a half-turn around the diffuser shell. The original design was based on circular cross section tubing that would be formed around the shell at assembly to ensure a close fit between the tubes and the shell walls. However, a detailed thermal analysis of the temperature gradients in the tubes and shell showed that one side of the cooling tube was required to be flattened in order to increase the heat transfer area between the wall and the tubes. This resulted in a "D" shaped tube cross section which was more difficult to form around the shell. By changing the design to "half-turn" tubes, the fabrication was completed without requiring the additional costs of designing and fabricating more complex tube forming tooling.

In addition to providing the means of cooling the diffuser, the cooling tubes also served as structural members to stiffen the thin copper walls to withstand the pressure gradient present because of the high velocity gas flow. The diffuser internal static pressure during operation varies from 0.1 atmosphere at the entrance to 1.0 atmosphere at the exit. The tubes were designed to function as stiffening ribs or beams and were positioned transversely to the diffuser axis to minimize the length of unsupported span. This procedure minimized the required tube cross sectional material requirement.

The spacing of the tubes was determined by the combined requirements of the thermal and structural specifications. The tube diameter was selected to achieve the desired water flow velocity and pressure drop. The spacing was then determined by the expected operating temperature of the shell wall, which reached

a maximum at points midway between adjacent tubes. Finally, the spacing of the tubes was analyzed to verify the structural integrity of the wall.

The spacing between the tubes was expected to increase along the length of the diffuser in the gas flow direction because of the decreasing pressure gradient across the diffuser wall; however, the space between the tubes had to be decreased because of the increasing heat loads along the axial length. Figure 10 is a photograph showing the process of attaching the tubes to the shell.

The diffuser was designed with six pressure taps which were equally spaced along the horizontal centerline of one side of the diffuser. Each tap consisted of a small diameter brass rod that was soldered to the diffuser shell between adjacent cooling tubes. A small diameter hole passed through both the rod and the shell wall.

The outer surfaces of the shell-tube wall were then covered with a layer of lightweight ceramic felt insulation. This insulation was covered with a thin layer of RTV silicone rubber to protect the cooling tubes from damage and reduce the rate of heat transfer to the surrounding equipment.

The final lightweight diffuser is shown in the photograph of Figure 11. The actual mass of the diffuser as shown was 23.6 kg. This is compared to an estimated mass of approximately 150 kg for a conventional, thick walled diffuser design. If full turn cooling tubes were used, the diffuser weight would have been reduced by approximately 3% by eliminating the extra set of inlet and outlet connections.

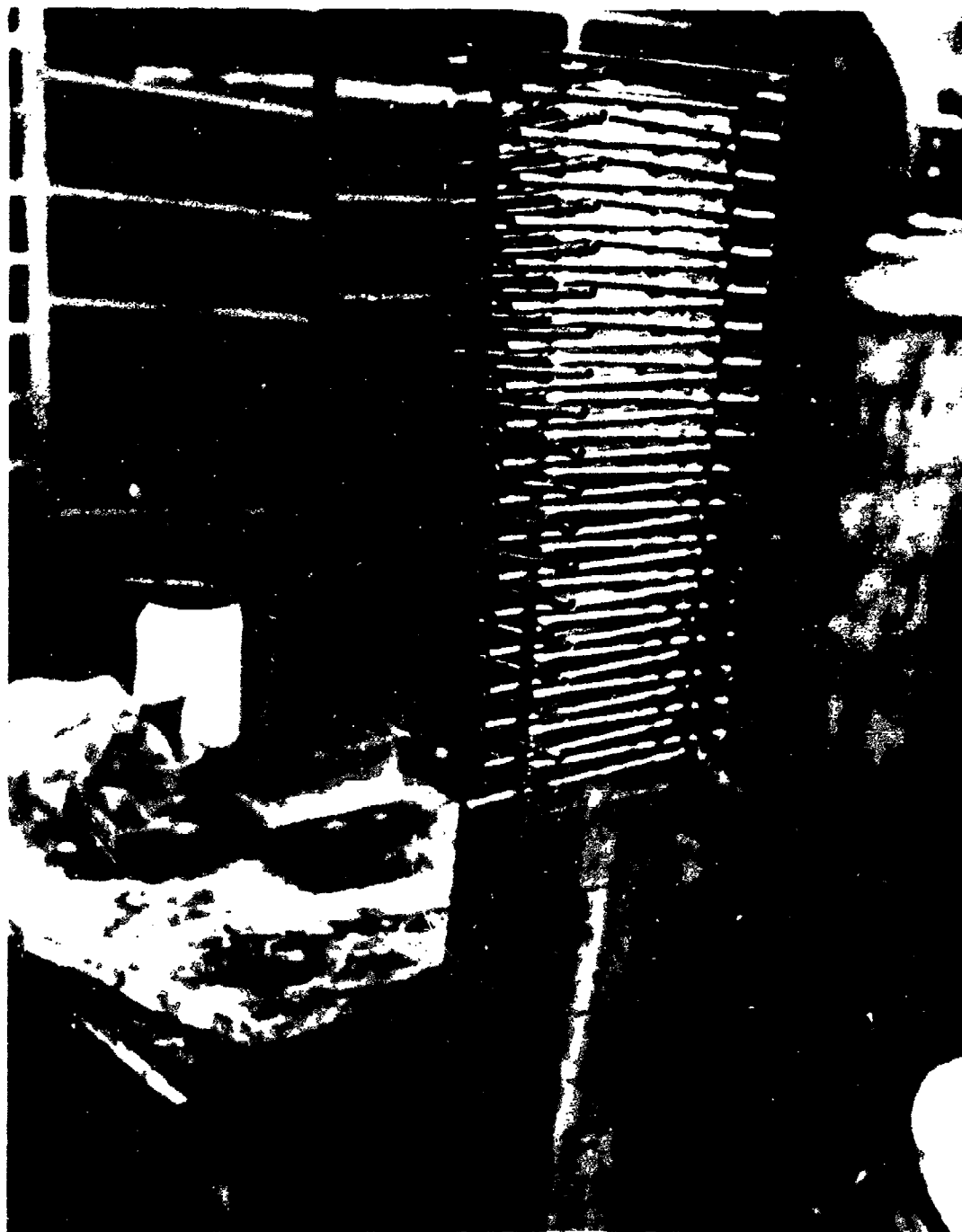


Figure 10. Diffuser Assembly During Fabrication.

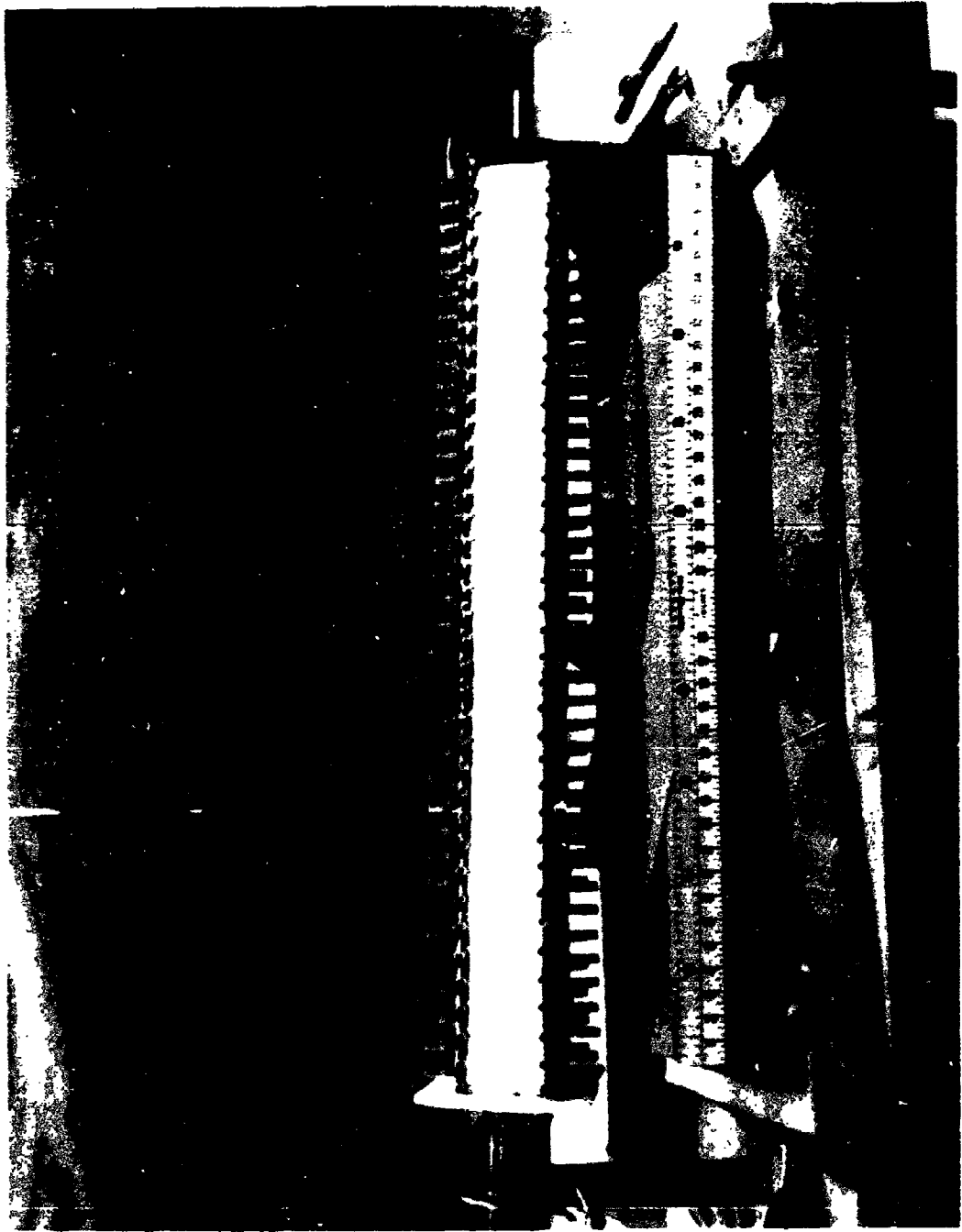


Figure 11. Lightweight MHD Diffuser.

3. PERFORMANCE ANALYSIS

a. Structural Analysis

The structural analysis of the lightweight channel included an investigation of the electrode frames and the fiberglass case. First, the analysis of the copper electrode frames is presented. Then, the results of the analysis of the filament wound fiberglass case are discussed.

The structural analysis of the electrode frames required the thermal and mechanical properties of oxygen-free high-conductivity (OFHC) copper. Figure 12 shows the coefficient of thermal expansion and the Young's modulus of elasticity for oxygen-free high-conductivity copper. In Figure 13, the ultimate tensile strength and yield strength of OFHC copper are given. The thermal expansion, Young's modulus of elasticity and strength data were obtained from Copper Data Association (CDA) data sheets. The fatigue curve for combined strains for OFHC copper is shown in Figure 14.^{5,6}

The calculation of the frame fatigue life under combined loads was performed by adding the strain components and entering the appropriate fatigue curve. In the curve of Figure 14, use was made of the fact that repeated thermal loading on a restrained bar will have a lower life than an applied mechanical strain at the maximum temperature of the thermal loading.

⁵ Coffin, L. F., Internal Stresses and Fatigue in Metals, G. Rosswalter and W. Grube, Elsevier Publishing Co., 1959.

⁶ Majors, H., "Comparison of Thermal Fatigue with Mechanical Fatigue Cycling," ASTM STP 165, 1954.

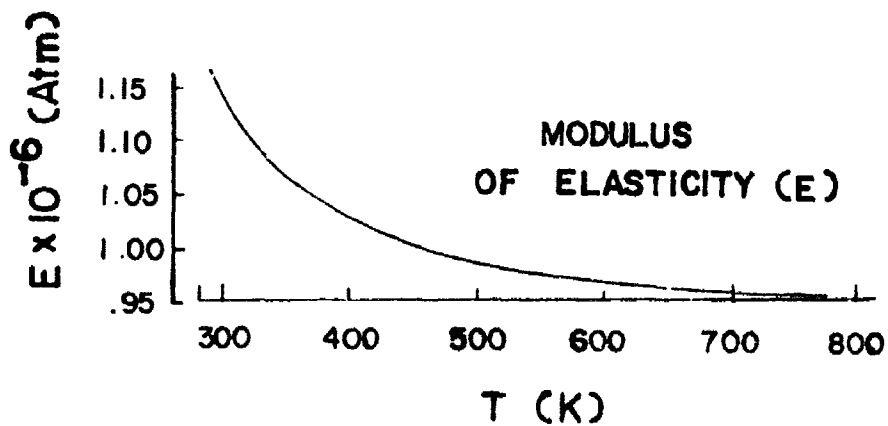
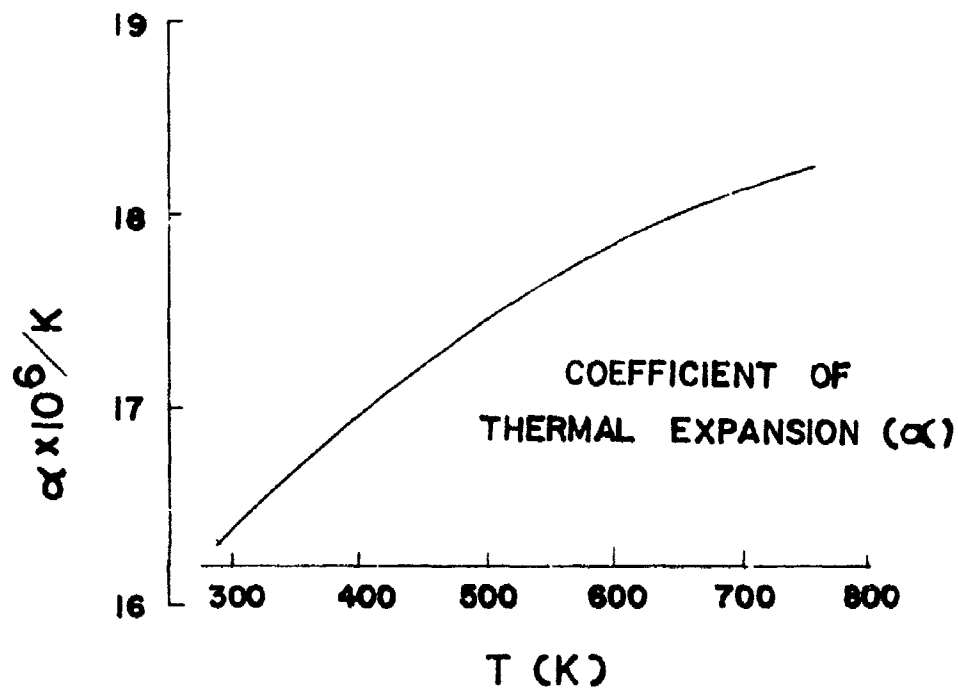


Figure 12. Coefficient of Thermal Expansion and Modulus of Elasticity for OFHC (CDA-102).

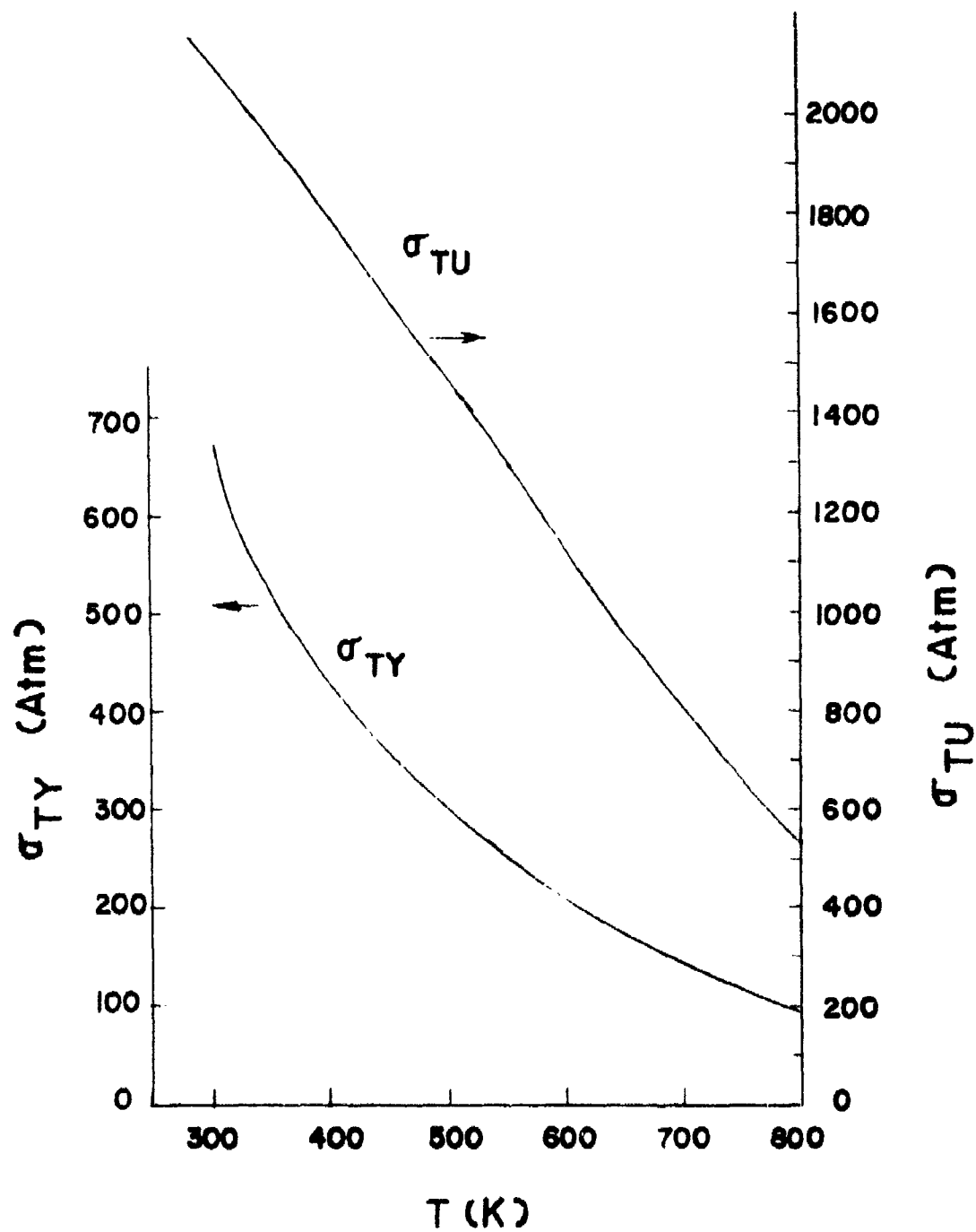


Figure 13. Yield Strength and Ultimate Tensile Strength of Annealed OFHC (CDA-102).

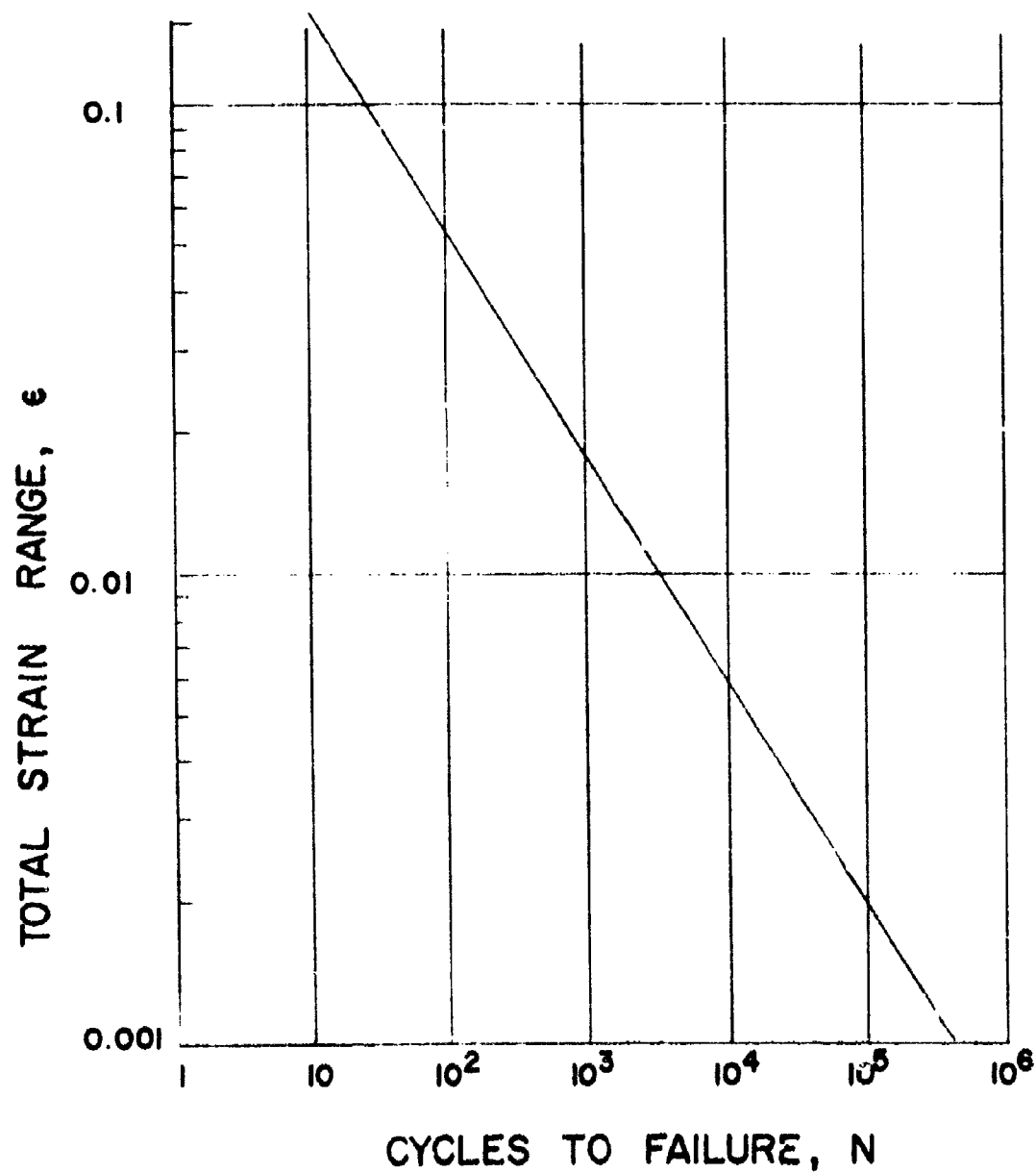


Figure 14. Fatigue Curve for Annealed OFHC (CDA-102) for Combined Thermal and Mechanical Strains.

Some conservatism resulted from the demonstration that the combination of thermal and mechanical effects followed an interaction relation which yielded longer life than the simple added strains method.⁷

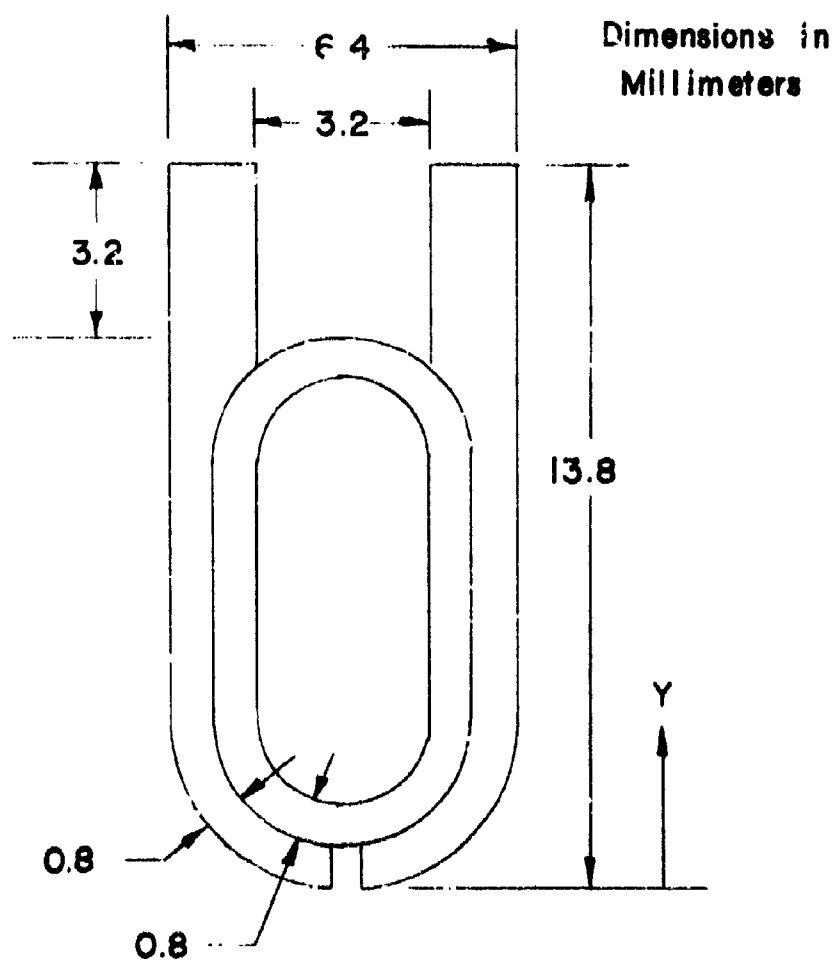
The maximum pressure deliverable to the critical coolant tubes with a 7.9 mm O.D. x 0.79 mm wall thickness was assumed to be 7 atm. The resultant circumferential membrane stress, σ_1 , was 28 atm.

The axial stress, σ_2 , was less than $\sigma_1/2$ because of the presence of the frame. The maximum tube wall temperature was assumed to be 395 K at the circumferential location where the tube was not in contact with the frame. Therefore, the circumferential membrane strain, ϵ_1 , was 4.1×10^{-4} . This calculation was on the conservative side because the lateral shrinkage of the wall, $\nu\sigma_2/E$, was neglected.

Based on the static loading, the factor of safety was 10, while for the fatigue life, with $N_{all} > 10^6$ cycles, the factor of safety is greater than 100 if 1000 loadings were assumed for design purposes. These conditions existed close to the bending neutral axis of the frame/tube combination.

At the extremes of the cross section, the thermal stresses and longitudinal bending at the gas face controlled the factor of safety. All diagonal frames were assumed to be simply supported over a maximum span of 198 mm. Near the corners, the maximum bending moment was assumed to be one-tenth of the product of the electrode frame loading and the electrode frame length. The maximum pressure difference was approximately 0.8 atm. With a frame side member width of 630 mm, the bending moment was 2.58 N-m. The section modulus, Z , for the gas face, as shown in Figure 15 was 80 mm^3 , and the bending stress, σ , was 398 atm.

⁷ Manson, S.S., "The Challenge to Unify Treatment of High Temperature Fatigue," ASTM STP 520, 1973.



$$A = 41.9 \text{ mm}^2$$

$$\bar{y} = 5.64 \text{ mm}$$

$$I_{xx} = 450 \text{ mm}^4$$

$$Z_{xx} = 80 \text{ mm}^3$$

$$\rho = 1.77 \text{ mm}$$

Figure 15. Frame Section Properties for Stress Analysis.

The upper surface temperature was 590 K. Consequently, the modulus of elasticity was approximately 10^6 atm, and the strain was 4.0×10^{-4} . The bending deflection, which has been approximated by $0.017 \text{ pwL}^4 / \text{EI}_{xx}$, was 0.033 mm.

The critical frames were in the region of the channel entrance where the transverse temperature gradients were the greatest. Each frame was assumed to be completely restrained internally against curvature because of these transverse temperature gradients. At the entrance the frame transverse temperature difference was assumed, conservatively, to be 220 K for which the thermal strain, ϵ , was $\propto \Delta T/2$, or 0.002 mm. The bending strain was negligible. For this condition the total number of cycles was greater than 10^6 cycles, and the factor of safety exceeded 100.

The vibratory response was assumed to be 50 g at all frequencies. This was equivalent to a pressure on each frame of approximately 0.38 atm. Hence, the stresses caused by vibration were small.

All frames were supported by the anchors in a manner that permitted freedom of axial movement on each side. Axial forces were induced by the anchors which acted normal to the axial thermal growths. However, those forces were small compared to the column buckling load which was in the yield range.

The filament wound fiberglass case structural analysis required the fatigue life properties of the fiberglass material shown in Figure 16.^{8,9} Since this fatigue curve represented the effect of stress concentrations, even though none were present in the regions of the composite where the stresses were the greatest, the calculations resulting from this curve were conservative. The case

⁸ Dietz, A.G.H., Composite Engineering Laminates, MIT Press, 1969.

⁹ Broutman, L.J. (Ed.), Composite Materials, Vol. 5, Academic Press, 1974.

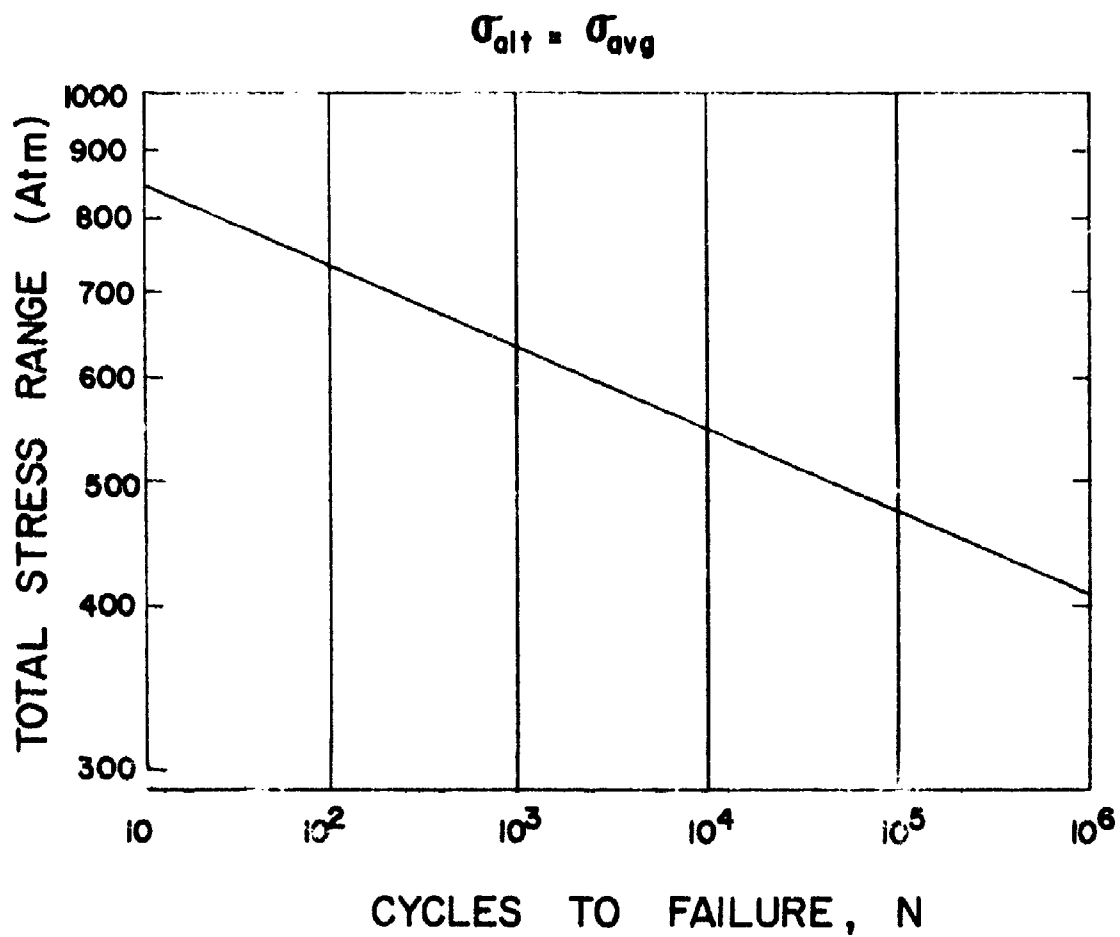


Figure 16. Composite Case Fatigue Curve.

was assumed to have a constant thickness of 9.5 mm. For the largest span of the fiberglass case (140 mm) at the peak negative pressure difference (0.80 atm), the inward center deflection was 0.40 mm. The resultant bending stress was 88 atm. Since $R/h = 1.6$, the stress was increased by 41 percent at the inner fiber because of the curved beam effect.⁹

The membrane stress was 3.1 atm. Thus, the total stress range was 91 atm. Therefore, with a fatigue life greater than 10^6 cycles, the factor of safety for fatigue was over 100. The factor of safety for static loading was over 7.4.

The entrance region of the case was assumed to be subjected to 56 K temperature rise at the inner surface as a so-called thermal shock. For the case material, the unit restraint stress per unit temperature rise was $\propto E/(1-\nu) = 3.67 \text{ atm/K}$. Therefore, for a Poissons ratio of 0.33, the stress caused by thermal shock was 206 atm.

The equivalent pressure on the combination of the case and frames at 50 g was 0.48 atm. The bending stress was 53 atm.

The natural frequency of the channel was calculated using

$$f = (\pi/2)(cr/L^2) \sqrt{W_{\text{case}} / (W_{\text{case}} + W_{\text{frames}})}$$

where r is the radius of gyration of the channel cross section.¹⁰ The sound speed, c , was assumed equal to $2.7 \times 10^6 \text{ mm/sec}$ for the composite, r was chosen at 40 mm as an average value and $L = 1000 \text{ mm}$. Then, with the ratio of the case mass to the case plus frame mass equal to 0.17, the natural frequency was calculated to be 56 Hz.

⁹ Broutman, L.J. (Ed.), Composite Materials, Vol. 5, Academic Press, 1974.

¹⁰ Jacobsen, L.S., R. S. Ayre, Engineering Vibrations, McGraw Hill, 1958.

b. Thermal Analysis

The thermal analysis of the lightweight channel was completed by recognizing the two competing thermal requirements. The zirconia surface temperature was required to be high enough to provide effective electrical current collection by each electrode, while at the same time the frame body temperature must remain low enough to maintain the integrity of the frame and the surrounding case. These two requirements required a careful design of the electrode frame details together with a practical cooling system operating under readily controllable flow conditions. These cooling requirements must be consistent with the KIVA-I facility capability. As a result of this restriction, a hydraulic analysis was also required. This hydraulic analysis is discussed in the following section. The thermal analysis included an investigation of the electrode frame and the case thermal behavior.

The electrode frame cooling tube temperatures were obtained from preliminary estimates using various water flow rates and a simplified frame cross section model for a range of average gas side heat fluxes. The water/metal surface heat transfer film coefficient was determined by:

$$h = 0.62(1 + 1.29 \times 10^{-2} T - 2.47 \times 10^{-5} T^2)(v)^{0.8}(d)^{-0.2} \left[\frac{\text{watts}}{\text{cm}^2 \text{K}} \right]$$

where T is the mean water/metal temperature in Celsius, v is the water velocity in the tube in m/sec, and d is the tube inside diameter in mm.¹¹ The approach that was used was to determine the required mass flow rate for a fixed bulk water temperature rise. This represented the minimum amount of water that was required for cooling. The heat transfer coefficient and the temperature distribution were then calculated. From these calculations the heat transfer coefficient required to prevent gas side overheating was computed. The velocity required to attain

¹¹ Kreith, F., Principles of Heat Transfer, International Textbook Co., 1961.

this heat transfer coefficient was then calculated and the resulting half-frame pressure drop was obtained. From these results the half-frame or full-frame cooling loops were established.

Figure 17 shows the actual axial heat flux distribution from previous tests at the AFAPL facility.^{1,3} These tests indicated a maximum heat flux of ~ 550 watts/cm² near the channel inlet and a minimum heat flux of ~ 100 watts/cm² in the channel exit region. The results shown in the upper curve of Figure 17 agree within about 20% with the turbulent boundary layer predictions.³

Using the MITAS finite element heat transfer program, the electrode frame temperature distribution fields were determined.¹² A typical temperature distribution plot for an axial location approximately 220 mm from the nozzle/channel interface is shown in Figure 18. This figure is for the electrode wall. An additional analysis was completed for the insulator wall, which utilized an oval cooling tube instead of the round tube used for the electrode wall. The resultant temperature distribution for the insulator wall was similar to the results shown in Figure 18. The critical regions of the electrode were the ceramic surface temperature, the Inconel screen temperature, and the screen/copper and the fin/cooling tube solder joints. Similar temperature distribution grids were also computed for other axial locations in the channel.

¹²User Information Manual for MITAS (Martin Marietta Thermal Analyzer System); Publication No. 86615000, Rev. A; Cybernet Service Control Data Network; September 1972.

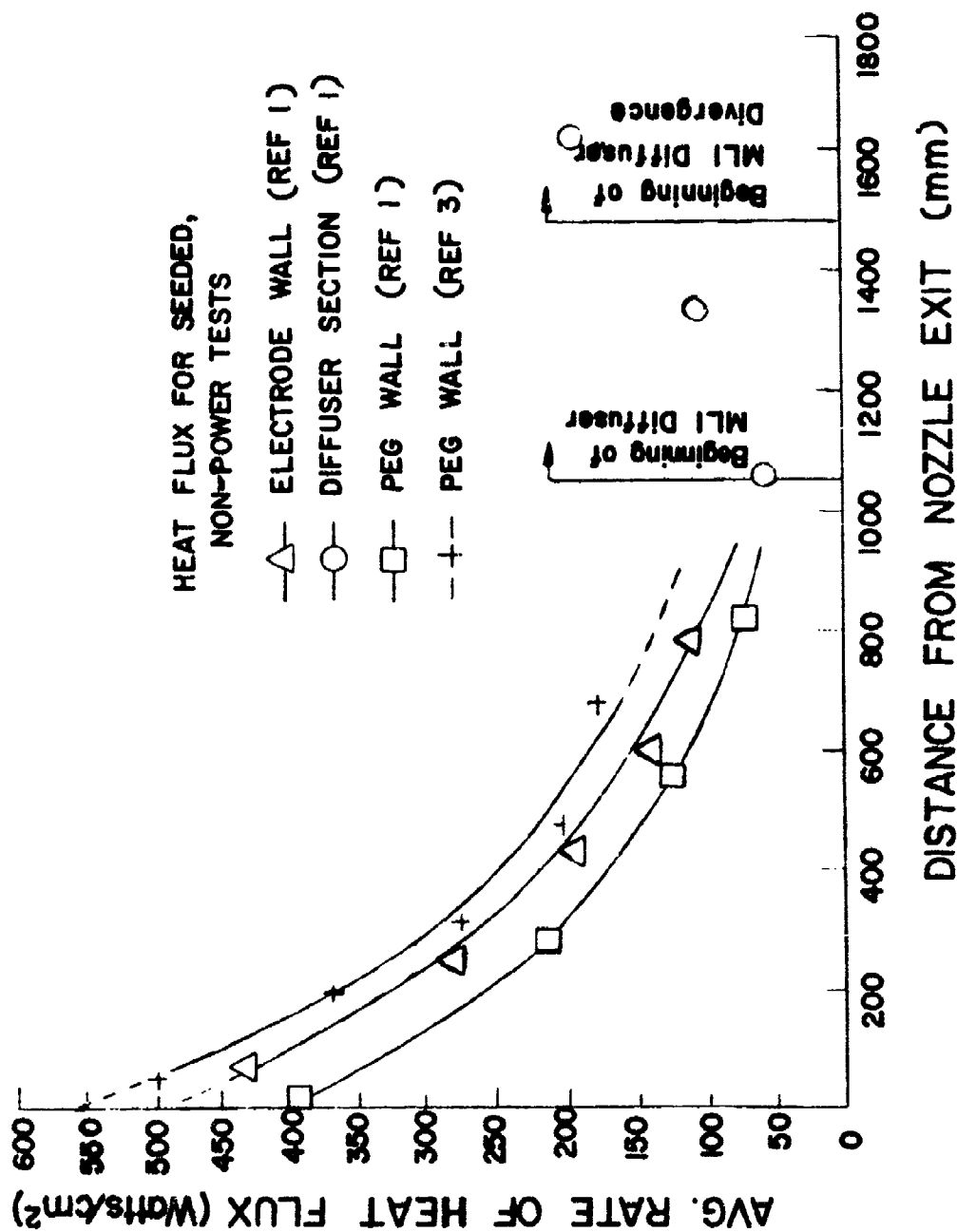


Figure 17. Design Axial Heat Flux Distribution for the Channel and Diffuser.

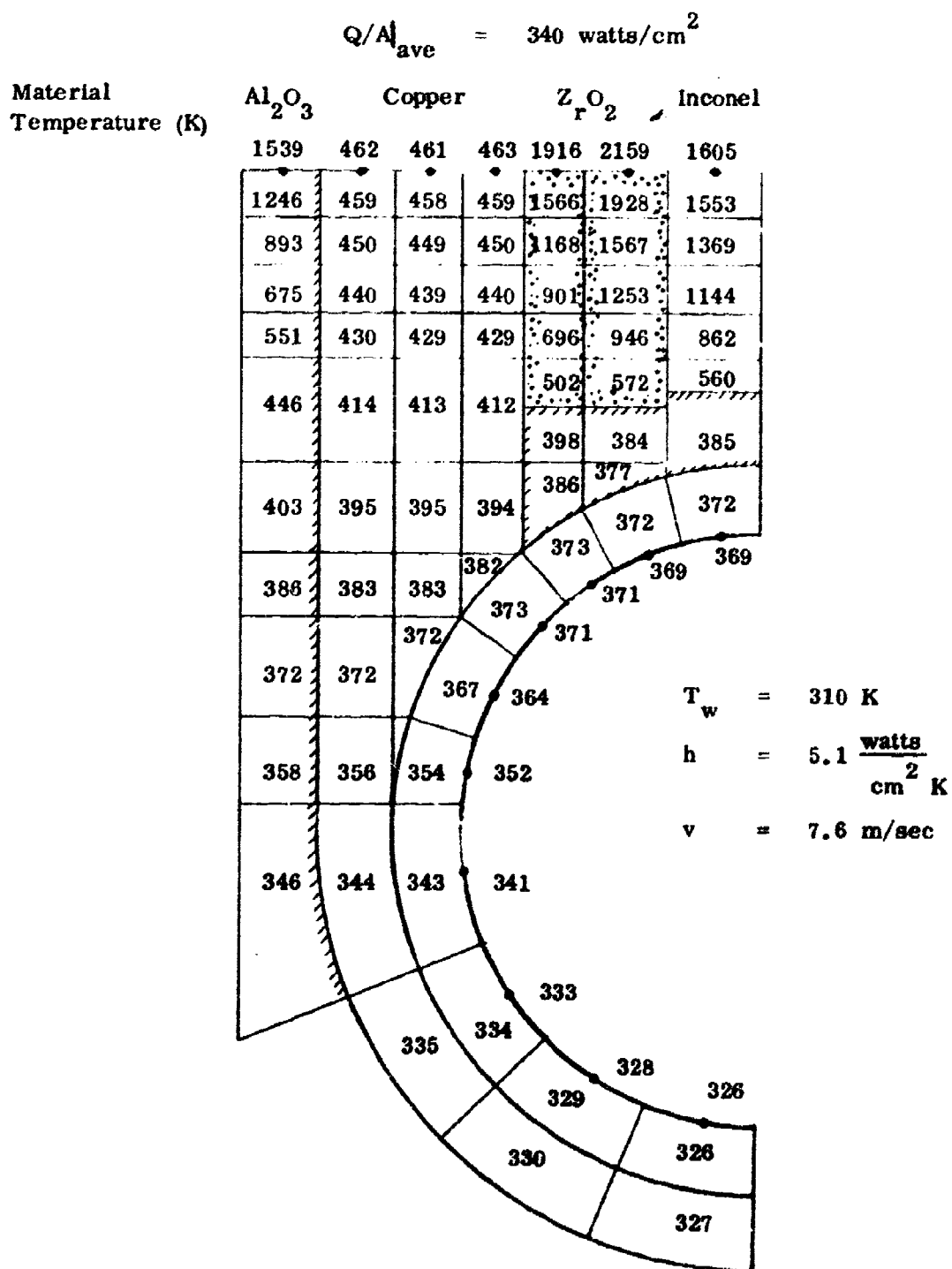


Figure 18. Electrode Frame Temperature Distribution.

c. Hydraulic Analysis

As the lightweight channel design discussed in Section II-2 illustrated, there were two water cooling loops per electrode frame. In the channel entrance region the water flowed in parallel through each of the half-frame cooling loops. Downstream, where the heat flux was lower, more than one half-frame cooling loop was connected in series. From a heat transfer standpoint, up to ten half-frame loops were connected in series. Since the number of half-frame loops controlled the final temperature at the coolant/frame interface, the connection arrangement was critical to maintain the desired temperature distribution. The hydraulics requirement, therefore, consisted of achieving a reasonable balance between the total flow requirements and the temperature distribution. The goal of the cooling system design was to maintain the cooling water flow requirements below the maximum water flow rate at the AFAPL facility and to minimize the electrode frame temperature rise.

The calculations of the pressure drop through the cooling tubes were completed by using the data on the measured pressure loss as a function of the flow velocity for the type of tubing used in the lightweight channel and diffuser. The experimental measurements for 6 mm tubing are shown in Figure 19 for straight tubes. The data for the curved tubes, orifices, and changes in section were available from various publications.¹³

The total pressure loss in the flow path between the feed and the drain manifolds consisted of the following components: inlet manifold exit to flexible hose; flexible hose friction loss; flexible hose entrance loss to frame; frame friction loss including bends; frame exit loss to flexible hose; and flexible hose to exit manifold. For the half-frames which were connected in series, further

¹³ Anon., "Flow of Fluids Through Valves, Fittings, and Pipes," Crane Company Technical Paper No. 410, 1976.

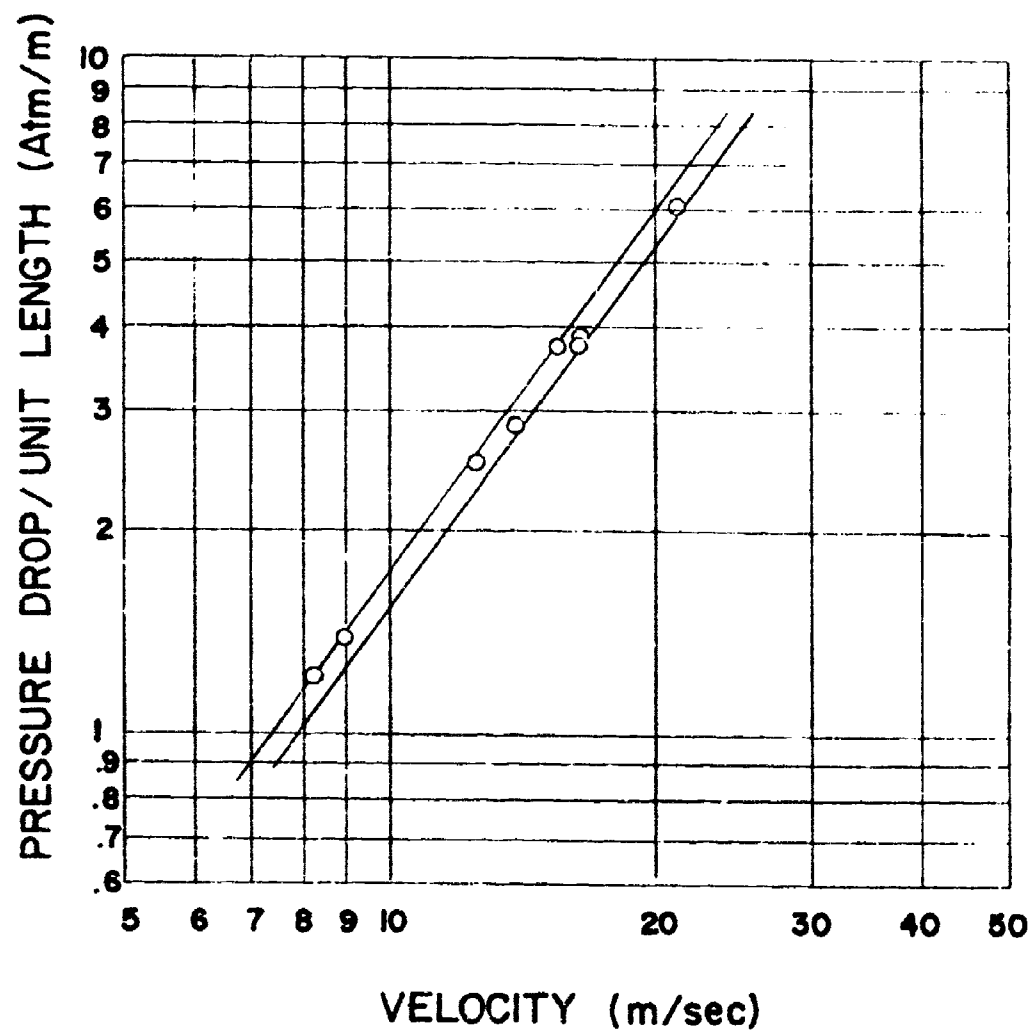


Figure 19. Pressure Loss for 6 mm I.D. Copper Tubing.

pressure losses were caused by the return loops between the half-frames and by the additional flexible tubing connecting the frames together.

As a result of applying the data generated to the analysis of the entrance region and the region 500 mm downstream from the channel/nozzle interface, the information shown in Table 1 was obtained. The difference in flow velocities resulted from the parallel and series cooling loops through the entrance and downstream electrode frames.

To assure a balanced cooling water flow distribution, the velocities and cooling loop pressure drops were determined for each of the channel half-frames. This pressure drop data along with the pressure drop data for the connections, etc. was then used to determine the cooling loop connection scheme which is described in Section II-4.

Since each of the seventy frames had two cooling loops, 140 parallel cooling loops were theoretically possible. However, the water flow requirements for cooling with all of the half-frames connected in parallel exceeded the capability of the AFAPL facility. In addition, the pressure drop across each half-frame would not have been equal, thus requiring a more complex orificing of the manifolds; and the electrode frame temperature distributions would not have been satisfactory. After a thorough analysis of the possible alternatives, thirty-one electrode frame cooling loops were selected. This connection scheme resulted in from one to ten half-frames being connected in series to satisfy hydraulic, thermal, and facility requirements.

TABLE 1. ELECTRODE COOLING DATA

Heat Load	w/cm ²	425	200
Station X	mm	100	500
Heat Load per Frame	watts	510	240
H Required to Prevent Gas Side Overheating	$\frac{\text{watts}}{\text{cm}^2\text{K}}$	4.6	2.9
Velocity	$\frac{\text{m}}{\text{sec}}$	10	5.6
Cooling Flow per Half-Frame/Frames	liters/min	19/NA	NA/11
ΔP for V Half-Frame/Frames	atm	5.4/NA	NA/6
P Required to Prevent Boiling	atm	1/NA	NA/1
Required Pressure	atm	6.4/NA	NA/7
AFAPL Systems Pressure	atm	7.8	7.8

NA = Not Applicable

d. Magnetohydrodynamic Analysis

Since the objective of this program was to design, fabricate and test a lightweight magnetohydrodynamic (MHD) generator channel/diffuser system, extensive MHD performance analysis was not completed. Furthermore, a previous technical effort maximized the channel/diffuser performance for the range of operating conditions of this channel test program.³ Except for the simplification of the fabrication process, no technical reasons existed to deviate from the successfully tested existing gas flow train design. Although an analytical calculation of the channel performance was made because of the internal contour variances discussed below, the basic inlet and outlet areas for the channel and diffuser were not changed. Figure 20 shows the experimental magnetic field at the AFAPL facility. This distribution was also used for the performance analysis calculations. The range of area ratios for the previous performance tests is shown in Figure 21.³ For the performance calculations of this effort, only the open position was considered since this was the position which produced greater performance.

A comparison with two previous channels is shown in Table 2.^{1,3} The heat sink channel, the original channel design, was the shortest of the three channels. The diagonal conducting wall channel length was increased to match the increased length of the magnet pole pieces. The lightweight channel overall length was increased to accommodate the lightweight channel entrance and exit ducts. However, the axial length of the lightweight channel electrodes was identical to the diagonal conducting wall channel.

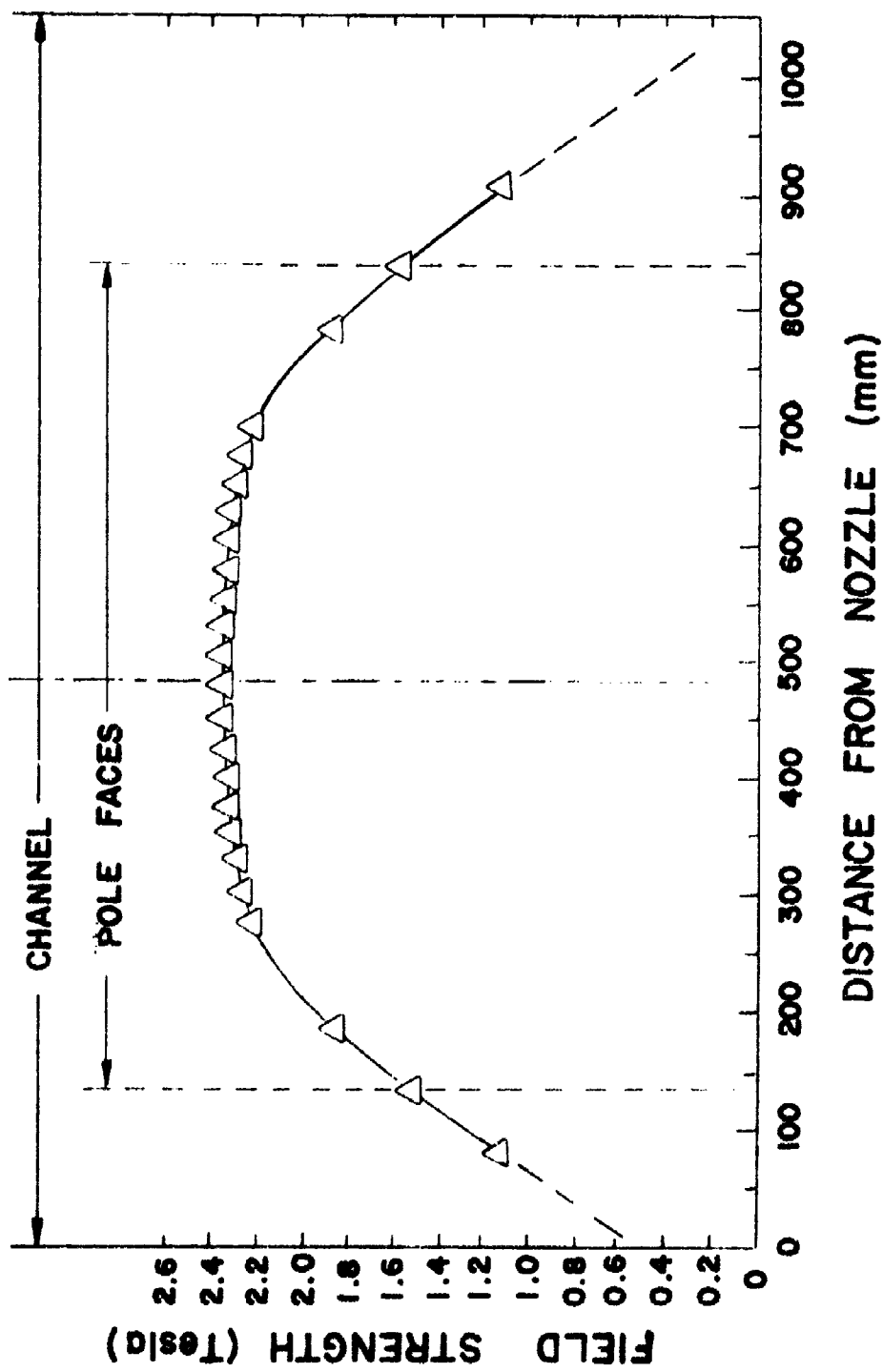


Figure 20. Magnetic Field Distribution for 2.3 Tesla Center Field for the AFAPL Magnet.

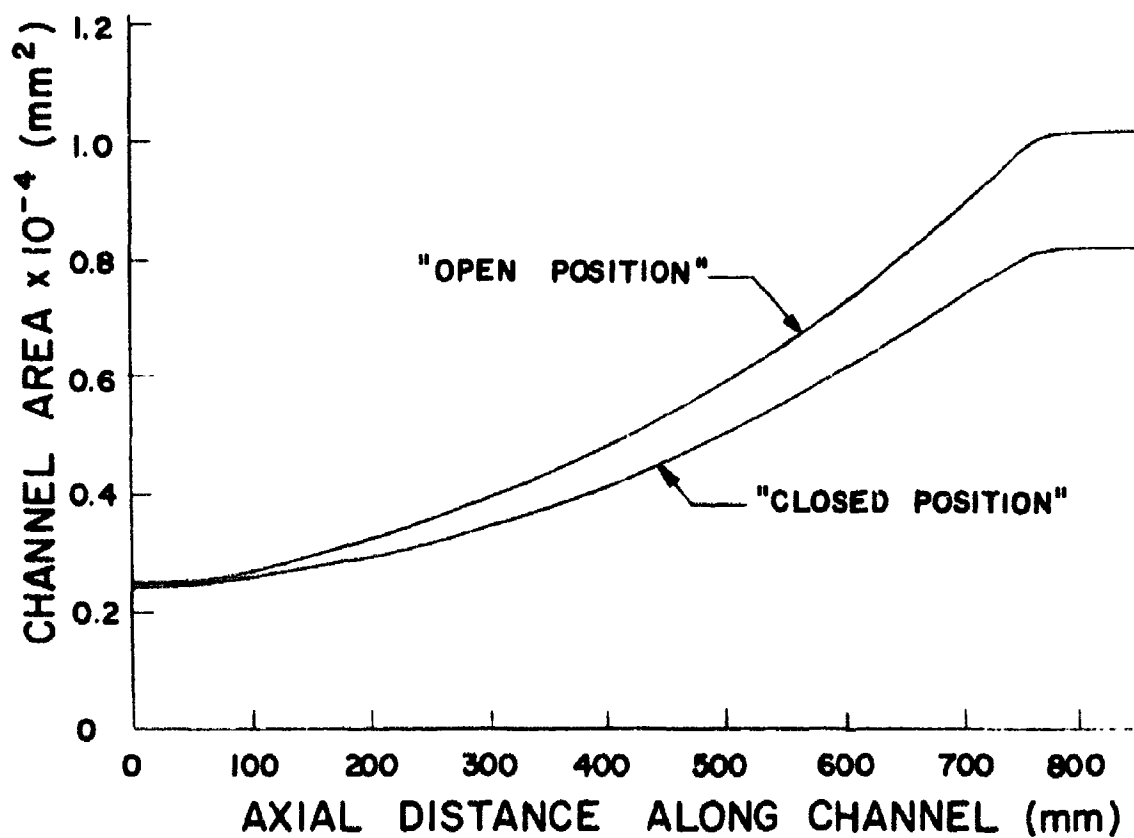


Figure 21. Variable Area Profile Characteristics of the Channel.

TABLE 2. DIMENSIONAL COMPARISONS OF AFAPL CHANNELS AND DIFFUSERS
(All Dimensions Are in Millimeters)

	Channel Entrance		Channel/Diffuser Interface		Diffuser Exit		Overall Length	
	Width	Height	Width	Height	Width	Height	Channel	Diffuser
Heat Sink	24.9	99.8	72.6	140	72.6	200	857	965
Diagonal Conducting Wall	24.9	99.8	72.6	140	72.6	200	989	965
Lightweight	24.9	99.8	72.6	140	72.6	200	1054	965

A change to the area profile which substantially simplified the fabrication effort was the elimination of the contoured surfaces of the walls perpendicular to the magnetic field. All four walls were fabricated with flat surfaces. This modification reduced the complexity of the channel construction. Previous performance analyses and tests with a channel of this internal contour demonstrated satisfactory operation.¹ Power levels obtained during these test series were 175 kW to 200 kW electrical output power in the main load. Figure 22 shows the axial voltage profile for a test with a diagonal conducting wall generator with flat, diverging walls. This series of test runs, along with a similar set run during the effort described in the previous reference,¹ demonstrated that the electrical performance of the diagonal conducting wall generator with flat instead of aerodynamically shaped walls was sufficient to achieve the required performance level.

A performance analysis to optimize the diffuser pressure recovery was not completed. Previous test programs have demonstrated that satisfactory diffuser pressure recovery was obtained with the existing design.^{1,3} The lightweight diffuser was constructed to the interior dimensions of these previous ones, but satisfying the objective of a lightweight component significantly decreased the exterior dimensions.

4. COOLING SYSTEM DESIGN

During the mechanical design of the lightweight channel, the cooling system details evolved through several states. This evolution has been described previously in Section II-2 and will not be repeated here. This section will discuss the selection

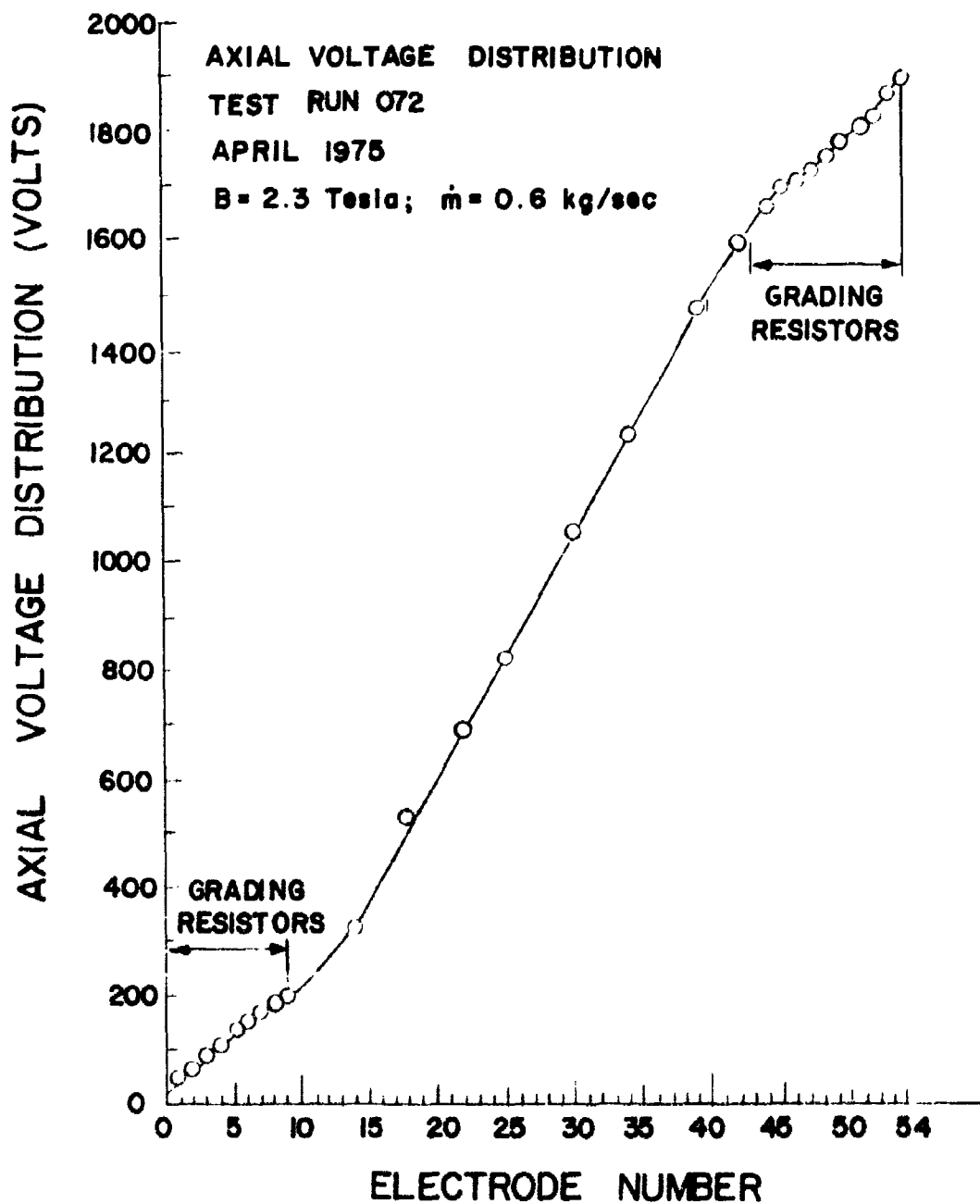


Figure 22. Axial Voltage Profile in the Diagonal Wall Channel.

of the water flow rates, the connection of the half-frame cooling loops, and the matching of the cooling requirements to the AFAPL cooling system capacity. Table 3 shows an overall cooling system summary for both the channel and the diffuser. The results shown in the table were based on the experimental heat flux curves from previous tests shown in Figure 17.^{1,3} This figure is presented in Section II-3. b and will not be repeated here.

a. Channel

Using the experimental heat transfer curves, the half-frame flow loop connections were established. Because of the high heat flux ($\sim 500 \text{ watts/cm}^2$) in the inlet region of the channel, each cooling loop consisted of only one half-frame. As the heat flux decreased downstream from the inlet, two or more half-frames were connected in series depending on the heat flux, pressure drop, and physical constraints. The correlation of the coolant flow rate, water flow velocity, the heat transfer coefficient, and pressure drop was further complicated by the individual flow path geometries. A not inconsequential restriction for a small compact generator of this type was the physical space limitations caused by the close proximity of the magnet. As many as ten half-frames (five complete frames) were connected in series at the channel exit end. The pressure drops from frame inlet to outlet in the electrode half-frame connections were approximately 6 atm for all parallel paths. As a result, the velocity and temperature increases varied from connection to connection. For cooling loops the heat transfer coefficient was calculated to insure that adequate heat removal was available. The velocity varied from 11 m/sec in the single half frame to as

TABLE 3. COOLING SYSTEM SUMMARY

Channel

Heat Load (MW)	0.55
Cooling Water Temperature, In (K)	294
Maximum Cooling Water Temperature, Out (K) (For Half-Frames)	300
AFAPL System Water Pressure (atm)	7.8
Minimum Flow Rate (liters/min)	140
Actual Flow Rate (liters/min)	450

Diffuser

Heat Load (MW)	0.80
Cooling Water Temperature, In (K)	294
Maximum Cooling Water Temperature, Out (K) (For Half-Frames)	320
AFAPL System Water Pressure (atm)	4.0
Minimum Flow Rate (liters/min)	203
Actual Flow Rate (liters/min)	525

low as 4.5 m/sec in the exit region where ten half-frames were connected in series. The corresponding range of temperature rise in the single and multiple half-frame paths was from 5 K to 40 K.

The fabricated cooling system was flow checked and leak checked to insure compliance with the design specifications. More details of the channel cooling system fabrication are provided in Section III-6. The water flow tests are described in Section IV-1.

b. Diffuser

For the design of the diffuser cooling system, a computer analysis of the diffuser wall temperature distribution was made. The results of this analysis indicated that the diffuser wall operating temperature was very sensitive to the width of the silver solder fillet between the cooling tube and the wall. Because of this characteristic, the tubing size was increased and one side of the tube wall was flattened to form a "D" shaped cross section. The flat side of the "D" was silver soldered to the diffuser wall.

The spacing of the tubing was determined by the combined requirements of the thermal and structural specifications. These considerations have been described in the Diffuser Design section, II-2.f, and will not be repeated in this section.

Each of the cooling loops of the diffuser completed a half-turn loop. However, each of these half-turn loops was connected externally to provide full turn cooling loops. Forty-four of these full turn loops were used to cool the diffuser. The spacing of the cooling loops along the axis varied to match the structural and thermal requirements of the diffuser.

c. Manifolds

The channel and diffuser manifold were designed to provide a minimum pressure drop between the cooling manifolds and connecting tubing to the channel and diffuser cooling loops. Four manifolds, two inlet and two outlet, were furnished with the channel. Similarly, the diffuser was also provided with four manifolds. The fabrication and description of the manifolds are described in Section III-6.

SECTION III

FABRICATION OF THE LIGHTWEIGHT MHD

CHANNEL AND DIFFUSER

1. INTRODUCTION

During the fabrication of the lightweight channel, a number of significant fabrication problems occurred. These problems resulted in considerable delay during the fabrication of the channel and in a few cases caused some modifications to the channel construction. The details of the specific problems are presented in the subsequent sections of this chapter.

A lack of adherence to the required dimensional tolerances of the frames was the cause of many of the frame fabrication problems. While some of the frames were produced within the design specifications, many of the frames were not within the design tolerances. These variances required a substantial amount of fitting and reworking of each of the frames as each frame was fit on the mandrel. The critical tolerance areas were the interframe gaps on all four sides of the electrode frame, the electrode frame to mandrel gap, and the electrode frame angle orientation. In addition, several other frames were poorly made; and hence, did not fit the mandrel properly. Consequently, these few frames were eliminated, and a larger interframe ceramic width resulted. However, as a result of the accumulation of the stackup tolerances, an overall channel growth in the axial direction would have occurred had these poorly made frames not been eliminated. Thus, in order to maintain the design channel length, six electrode frames were eliminated during the final assembly process. These eliminated frames resulted in the design channel length of 1054 mm.

Because of the excessive electrode frame to mandrel gaps, an appreciable amount of alumina ceramic material flowed into this region. This produced an uneven hot gas surface with regions of alumina overlapping several frames. Many

voids were present in the alumina regions between the electrode frames. The repair of this problem required an extensive amount of filing and grinding and then refilling of the ceramic areas. This handworking process produced the necessary smooth interior contour required for the proper operation of the lightweight MHD channel.

The subsequent sections of this chapter describe the various steps of the fabrication of the lightweight MHD channel from the manufacture of the machined components through the case winding and finishing operations. The fabrication of the diffuser is discussed. The description of the fabrication of the cooling system for both the channel and diffuser is also included in this chapter.

2. COMPONENT MANUFACTURE

The components of the lightweight channel were an entrance duct, an exit duct and seventy individual electrode frames that were positioned on an assembly mandrel. These components were enclosed by a fabricated-in-place fiberglass-epoxy shell to form a completed channel as shown by Figure 23.

The entrance duct was machined from a solid block of copper. The walls were drilled with a series of closely spaced cooling passages that were arranged so that no joints in the cooling passages were in contact with the hot gas surfaces. The cooling passages were connected externally by short sections of copper tubing that were brazed into the main block. A static pressure tap was provided on one side of the duct by drilling a small diameter hole through the wall and brazing a short brass connecting tube to the outside of the duct wall. All coolant passages were pressure checked for leaks before winding the fiberglass-epoxy shell around the entrance duct.

The exit duct was fabricated from thin copper sheets that were brazed together into a lightweight shell that formed the smooth internal hot gas surfaces. The walls were cooled by a series of individually formed cooling tubes that were

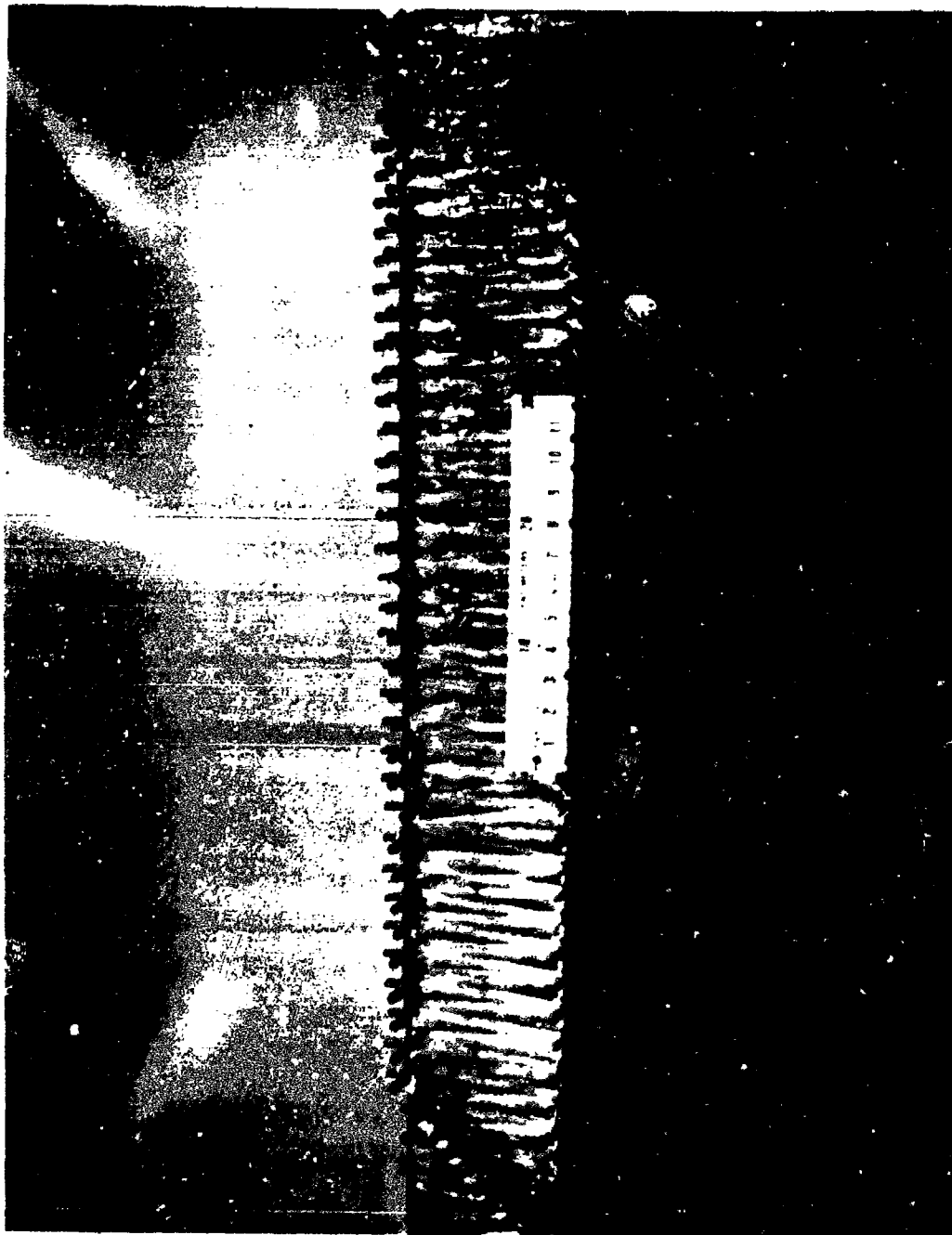


Figure 23. Lightweight: MHD Channel After Filament Winding.

brazed to the outside of the shell so that no joints in the cooling passages were in contact with the hot gas surfaces. One side of each cooling tube was flattened so that the tube had a "D" shaped cross section. The flat side of the tube was brazed to the wall of the lightweight shell so that there was sufficient heat transfer area between the tubes and the walls. A static pressure tap similar to the one used on the entrance duct was installed in one side of the exit duct.

Each electrode frame assembly consisted of continuous cooling tubes, current collector screens, cooling fins, corner blocks and frame anchors. A drawing of a typical frame is shown in Figure 24, and a photograph of a typical finished frame is shown in Figure 25. Ten of the frames were provided with pressure taps, which were equally spaced along the length of the channel.

The continuous cooling tubes shown in Figure 24, Items 1 and 2, were formed in three steps using standard size commercial copper tubing. The corner bends were formed on the special, adjustable tube forming fixture shown in Figure 26. This fixture was designed with sufficient adjustments to permit one fixture to cover the complete range of all the bend angles and of all the distances between bends that were required for the set of seventy electrode frames.

As shown in Figure 6, the side members of each frame were much thinner than the cross members. The thinner sections formed the insulator walls, Figure 6B, and the thicker sections formed the electrode walls, Figure 6A. The thinner sections required the flattening of the tubes used for the insulator walls. This was done with a special tube flattening fixture shown in Figure 27.

Sections A-A and B-B of Figure 24 show how the cross members of the frames were arranged with the current collector screens and the cooling fins positioned perpendicular to the hot gas surface, while the side members were positioned at an angle to the channel axis. In order to produce this geometry, the cross members were displaced from the side members at an angle of 45 deg. This was accomplished by using the special bending fixture shown in Figure 28.

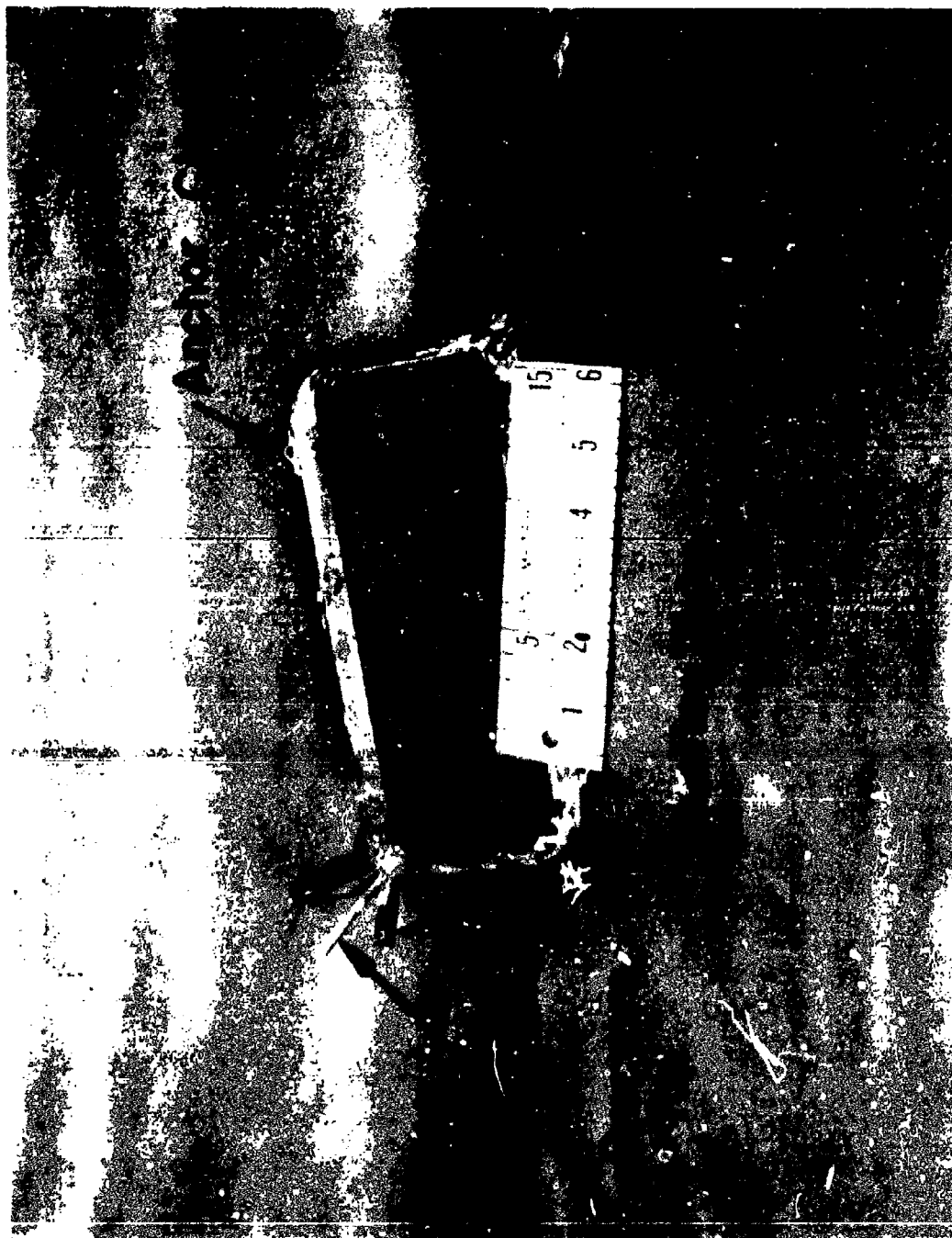


Figure 25. Completed Electrode Frame.

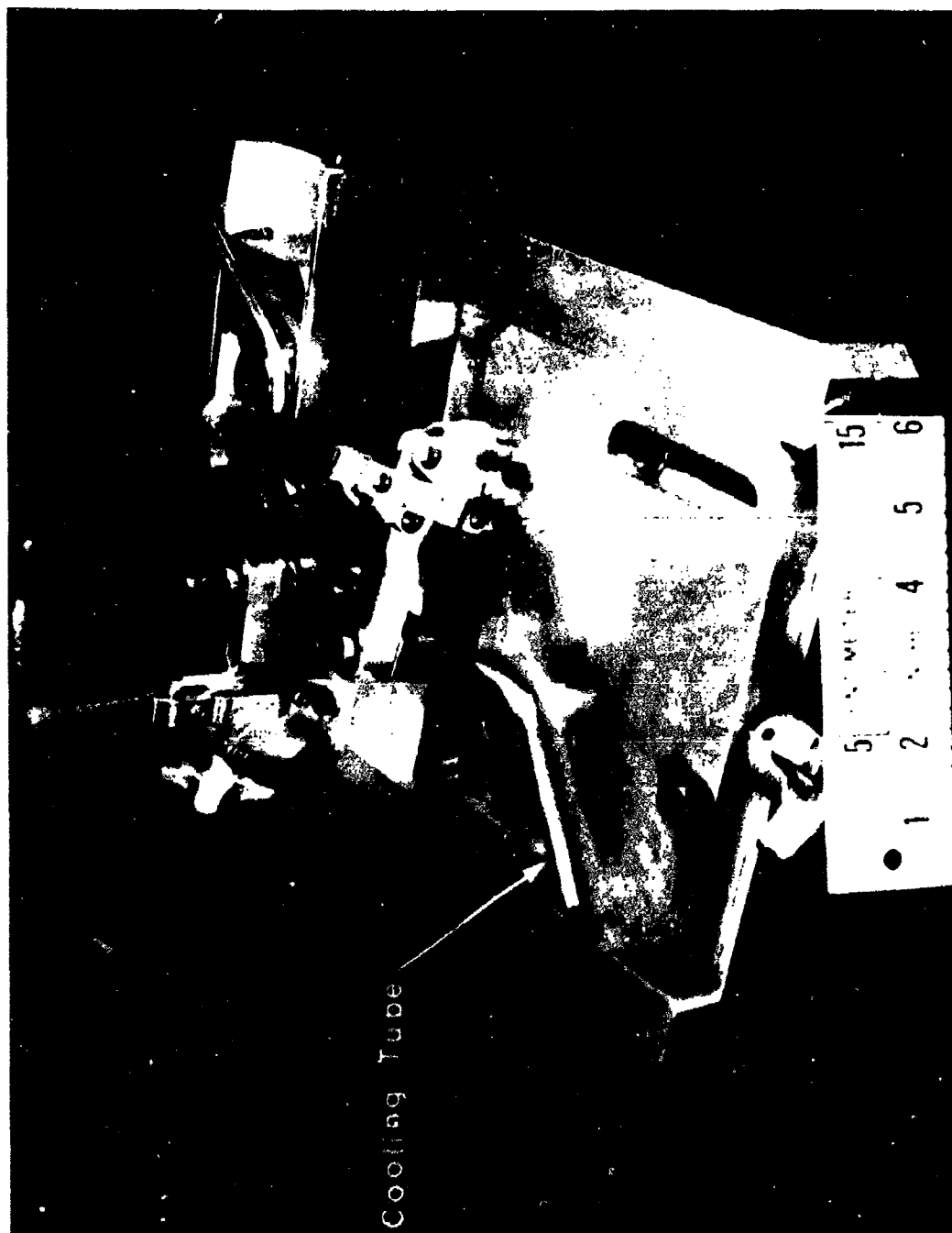


Figure 26. Tube Radius Bending Fixture.

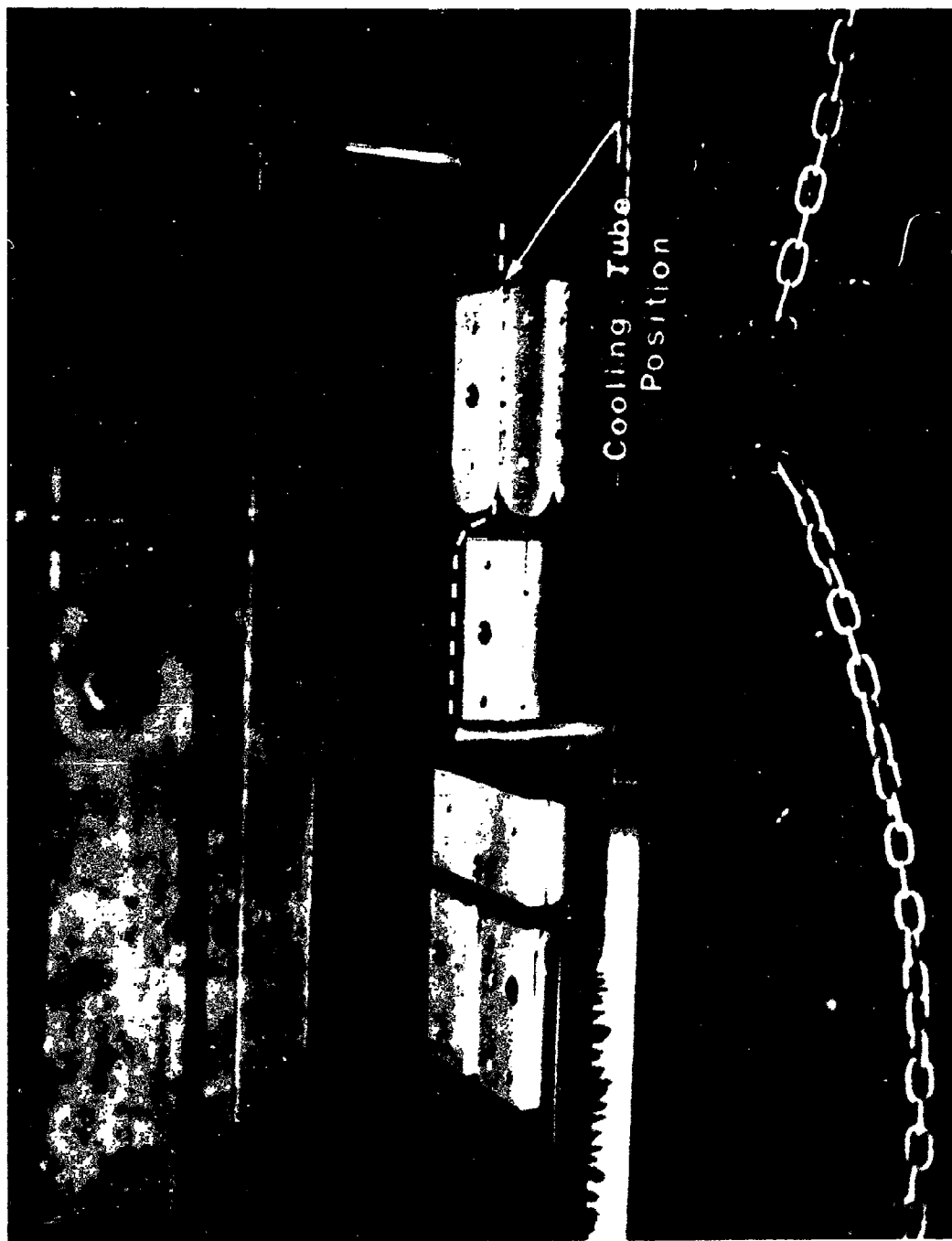


Figure 27. Electrode Cooling Tube Flattening Fixture.

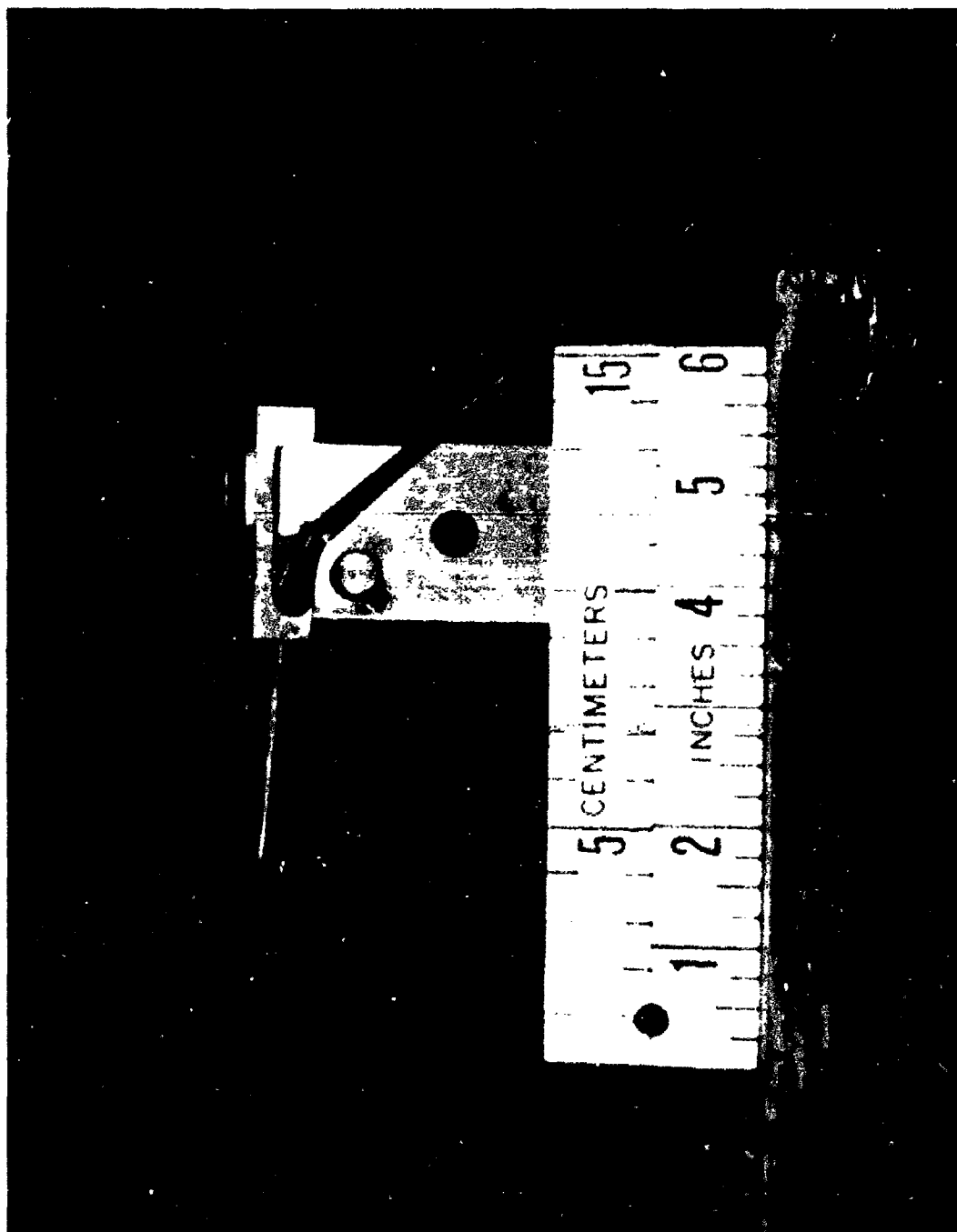


Figure 28. Electrode Cooling Tube 45 Degree Bending Fixture.

The current collector screen shown in Figures 6A and 6B was formed by folding the Inconel screen into double layers and then cutting extra width strips that were cut back to size after being attached to the cooling tubes. The screening was folded and cut on the bias (i.e. at an angle of 45 deg to the strands of the screen). This insured that each and every screening strand was attached to the cooling tube by the brazed joint, thereby forming a reliable heat transfer path from each strand to the cooling tube so that the screen was adequately cooled.

The cooling fins shown in Figures 6A and 6B were produced by machining flat sheets of copper to the required thicknesses and then forming the fins around a special die so that the internal contour of the fins matched the external contour of the cooling tubes. The outside widths of the electrode cross sections were the same for all the electrode frames. However, the widths of the grooves for the zirconia electrode ceramic were designed to be narrowest at the upstream end of the channel where the heat load on the walls was highest. As the heat load decreased along the length of the channel, the width of the grooves was increased. The variation in the widths of the grooves was accomplished by varying the thicknesses of the fins in that region of the frame cross section.

The corner blocks shown in Figure 24, Items 6, 7, 8, and 9, required a complex three-dimensional compound angle geometry. The inside surfaces had a radius which formed the inside corners of the channel. The outside surfaces of two corner blocks had a radius which conformed to the inside radius of the cooling tubes, while the opposing two corner blocks had a square corner where the tube inlet and outlet connections are formed. The upstream and downstream surfaces of the corner blocks required these compound angles so that the surfaces would lie in the same planes as the surfaces of the adjacent cooling fins.

If each corner block was individually machined out of a block of copper, extensive tooling, fixtures and measuring gauges would be required, and the costs of machining would be very high. However, a simplified process of machining

was developed which required minimal tooling and fixtures. This process resulted in a reasonable cost for machining. This simplification was primarily possible because the corner blocks were identical for all the frames (i.e. there were four types of blocks for each frame, resulting in quantities of seventy blocks of each type).

The corner blocks were formed by machining the inside corner radius and the outside radius or square corner along the length of a bar of copper long enough to make at least fifteen to twenty corner blocks. Then a slitting saw of the exact width of the insulation space between the adjacent blocks was used to cut the bars transversely at the required angles. This saw cut produced the individual blocks.

The frame anchors shown in Figure 24, Item 13, were fabricated from round copper wire that was formed to the required shape in a special forming die. The straight sections at the ends of the anchor were formed in line so that they could be soldered to the backs of the electrode frames, while the center sections were formed into a loop that projected into the glass epoxy shell and anchored the frames to the shell.

The pressure taps shown in Figure 24, Item 15, provided a passage from the hot gas surface through the frame and the shell wall so that the static gas pressure in the channel could be monitored. These pressure taps were fabricated from a small diameter brass rod which had a small hole drilled through its center.

Another manufactured item, which was not a component of the final channel but was critical to this state-of-the-art process of fabricating lightweight MHD generator channels, was the channel assembly mandrel. The critical function of the mandrel will be described in later discussions of the "Electrode Frames Assembly" and "Final Frame Assembly, Case Fabrication and Finishing Operations".

The first attempt to fabricate the mandrel was to use precision ground aluminum tooling plate to form the sides of the mandrel. The edges of the plates were machined so that the mandrel surfaces would diverge in both directions. Then the plates were joined together into a tapered box section by welding the edges of the plates together. The purpose of this design was to reduce the amount of materials required and to eliminate the machining of the mandrel surfaces. However, the process of welding caused excessive warping and distortion of the mandrel. After this attempt to assemble the mandrel by welding, there was not enough material remaining to salvage the mandrel by machining the surfaces. Consequently, another mandrel had to be fabricated.

The final mandrel shown in Figure 29 was fabricated from a solid bar of aluminum by machining the outer surface contour of the mandrel to the exact dimensions and contour of the internal contour of the generator channel hot gas surfaces. Then rotation trunnions were attached to both ends of the mandrel to be used to support the channel during the process of fabricating the fiberglass epoxy composite shell.

3. ELECTRODE FRAME ASSEMBLY

In order to assemble the component parts into the electrode frame assembly, seven major operations were required. These operations are described in detail in the following discussions. A detailed drawing of a typical frame is shown in Figure 24, and a photograph of a completed electrode frame is shown in Figure 25. The details of the electrode frame cross sections are shown in Figure 6. The wider frame sections, which formed the cross members along the channel electrode walls, are shown in Figure 6A. The narrower frame sections which form the diagonal members along the channel insulator walls, are shown in Figure 6B.

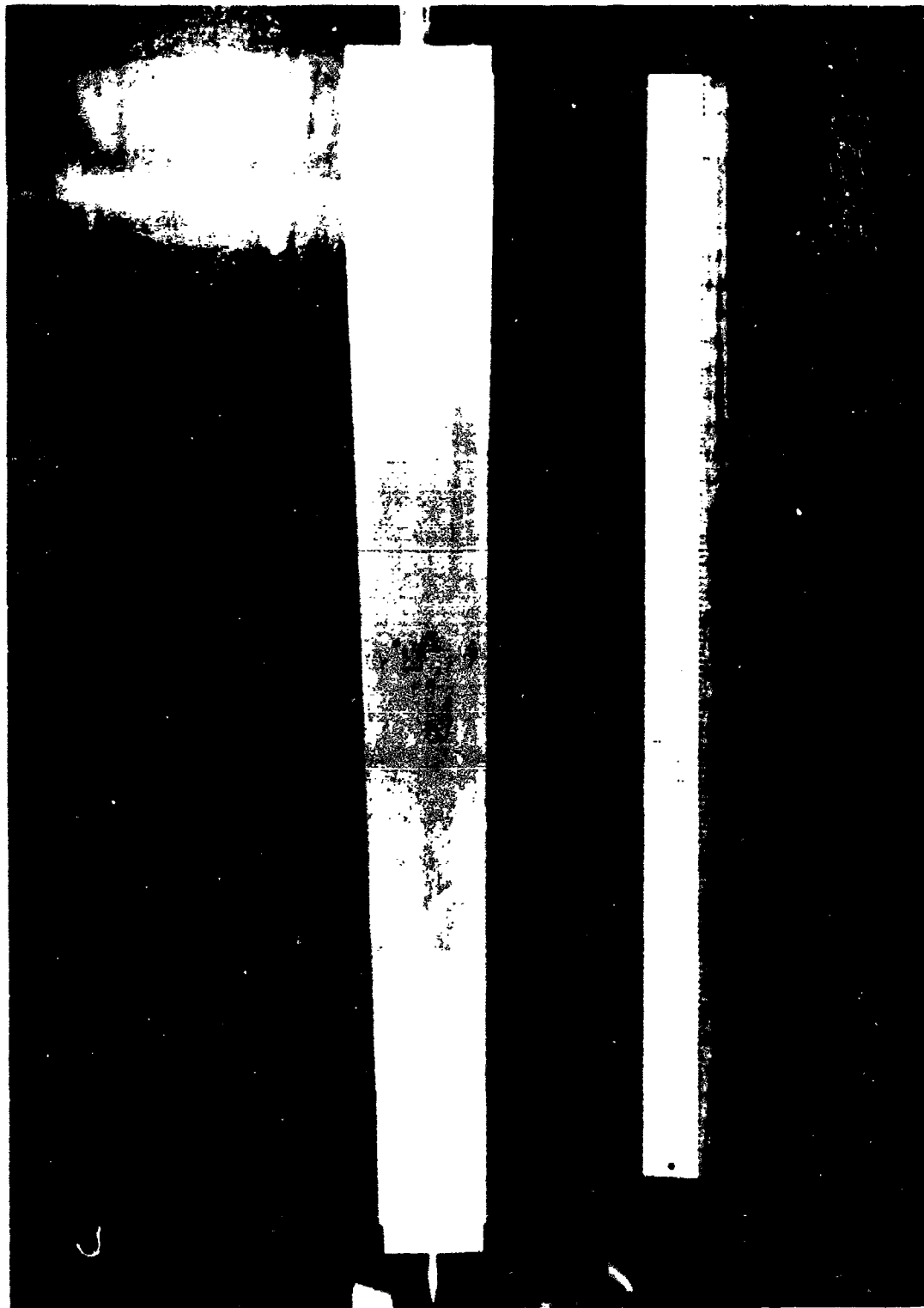


Figure 29. Channel Fabrication Mandrel.

a. Brazing the Current Collector Screens to the Cooling Tubes

The current collector screens must be precisely located along the mid-planes of the cooling tubes. The braze joint that attached the screens to the tubes must be void free and completely surround the roots of the screen strands to provide a solid braze material heat transfer path between the screens and the tubes. At the same time the upper region of the screens (region nearest the hot gas surface) must be free from braze material to allow the electrode ceramic to be in close contact with the current collector screen. At the hot gas surface the current collector screen operated at temperatures above the melting points of the braze material. Consequently, any braze material deposited on the screens in that region would melt away during the initial runs. This would leave voids between the screen and the adjacent ceramic which would interrupt the flow of electrical current between the screens and the electrode ceramic.

To begin the assembly procedure, the braze joint areas of the cooling tubes and screens were cleaned. A special alignment fixture was used to locate the screens on the midplane of the cooling tubes with the folded edge of the screen in contact with the surface of the cooling tube. The extra width, double thickness screens were then temporarily attached by tying the screens to the tubes with fine Nichrome wires along the length of the tubes. The melting temperature of the Nichrome wires was above the brazing temperature so the wires maintained their integrity during the brazing process. Next, the braze joint regions were coated with flux. The screens were then manually torch brazed to the tubes with careful attention given to the amount of braze material that was applied to ensure that a reliable heat transfer path was formed. The upper regions of the screens were coated with a braze stop-off masking material to prevent the braze material from penetrating the prohibited areas of the screens. The temporary Nichrome wires were then removed. The experience gained during this fabrication process indicated that the successful fabrication of the screen tube braze joint was critically dependent on close adherence to the brazing process developed for this application.

b. Soldering the Copper Cooling Fins to the Cooling Tubes

The outside surfaces of the cooling tubes were cleaned to remove any excess screen braze material. The fins were then fitted to the tubes to ensure a close fitting solder joint. A special alignment fixture was used to locate the fins which were then temporarily attached to the tubes with intermittent tack welds along the backs of the tubes. Next, the assemblies were removed from the fixtures and the fins were torch brazed to the tubes. The excess current collector screen widths were then trimmed to size by grinding the screens down flush with the edges of the cooling fins. A problem was encountered with various amounts of excess solder material flowing into the ceramic groove regions because of the wicking actions of the narrow slots. The excess solder was ground out by using a narrow, high speed rotary abrasive disk grinder.

c. Assembling the Corner Blocks to the Cooling Tubes

The corner blocks had several critical requirements relating to their assembly to the cooling tubes. The inside radius surface of the blocks must be precisely oriented to form the smooth internal contour of the channel along the corners between the adjacent walls. Since the corner blocks must be cooled by the tubes, a reliable heat transfer path was required. The corner blocks also functioned as structural members - tying the two halves of the frame together and reinforcing the cooling tubes in the other two corners.

Since each electrode frame had two cooling tubes, the previous operations produced "half-frames" consisting of cooling tubes with attached screens and fins. At this point each pair of half-frames with their accompanying four corner blocks was temporarily placed on the channel assembly mandrel at the correct locations. The corner blocks were temporarily tack welded to the half-frames, the combined frame assembly was removed from the mandrel, and the corner blocks were securely torch brazed to the half-frames. This process formed a continuous electrode frame. This operation was the first critical use of the assembly mandrel, which was used as the master sizing gage to achieve the fabrication tolerances of the frames.

d. Attaching the Frame Anchors to the Outer Edges of the Frames

Four electrode frame anchors were positioned on each frame. Two anchors were placed on each diagonal side member of the frame as shown in Figure 24. They were temporarily attached to the frames by tack welding, and then firmly attached by soldering the entire lengths of straight sections of both ends of the anchors to the outer edges of the electrode frames.

e. Installing Taps at the Corners of the Frames

The pressure taps were installed in ten electrode frames which were evenly spaced along the length of the channel. The predrilled brass rods were temporarily tack welded to the corner blocks, and then they were permanently attached by soldering. The predrilled hole in the brass rod was used as a guide to drill an in-line hole through the corner block. This hole provided a passage from the hot gas surface through the electrode frame to allow the measurement of the gas static pressure.

f. Water Flow and Leak Testing

Water flow and leak tests were performed on each electrode frame. No leaks were anticipated because of the "continuous cooling tube" design. However, the high rates of heat transfer present during operation required relatively high water flow velocities. Consequently, the pressure drop from inlet to outlet in each frame was measured at the flow rate required to remove the expected thermal load imposed on the channel by the hot plasma. The test results indicated satisfactory water flow velocities, and there were no leaks.

g. Dry Assembling of the Electrode Frames on the Alignment Mandrel

A dry assembly of all the electrode frames was made on the mandrel to check the frame dimensions and fit-up relative to the mandrel and to each other. The exit duct was mounted on the mandrel and then each frame was positioned at its nominal location on the mandrel. A partially completed dry assembly is shown

in Figure 30. Each frame was inspected to check the interelectrode spacing, the gap between the frames and the surface of the mandrel, and the angle of inclination between the sides of the frames and the axis of the channel. At this stage the dimensional tolerances were found to exceed the design specifications. One problem was caused by the width of the frame cross sections (reference Figure 6). The solder joints between the cooling fins and the cooling tubes were thicker than expected. This caused the overall cross section widths to be greater than the design values. The growth was compensated for by increasing the frame-to-frame pitch dimensions accordingly so that the interframe insulation space along the side walls was consistent with the design values. Although this approach improved the frame spacing along the side walls with the diagonal frame members, it simultaneously introduced other dimensional problems. Because of the diagonal geometry relationships between the side members and the cross members of the frames, the increased frame spacing along the side walls introduced greater spacing dimensions between the cross members along the top and bottom walls. Consequently, the interframe gaps were over the design dimensions. In addition, the increased frame-to-frame spacing required the frames to be offset along the channel axis from their design positions. Since the internal opening of the channel was tapered (divergent), the axial shift of the frames introduced radial dimensional variations over the design values. Consequently, considerable effort was required to optimize the positioning of the frames during the final frame assembly process.

4. CERAMIC EMPLACEMENT

Two types of refractories were used in the lightweight MHD channel: a zirconia-based electrode ceramic, and an alumina-based insulator ceramic. At high temperatures the zirconia ceramic served as a current conductor within each frame while the alumina ceramic provided electrical insulation between adjacent frames. Figures 31 and 32 show the locations of the ceramics.

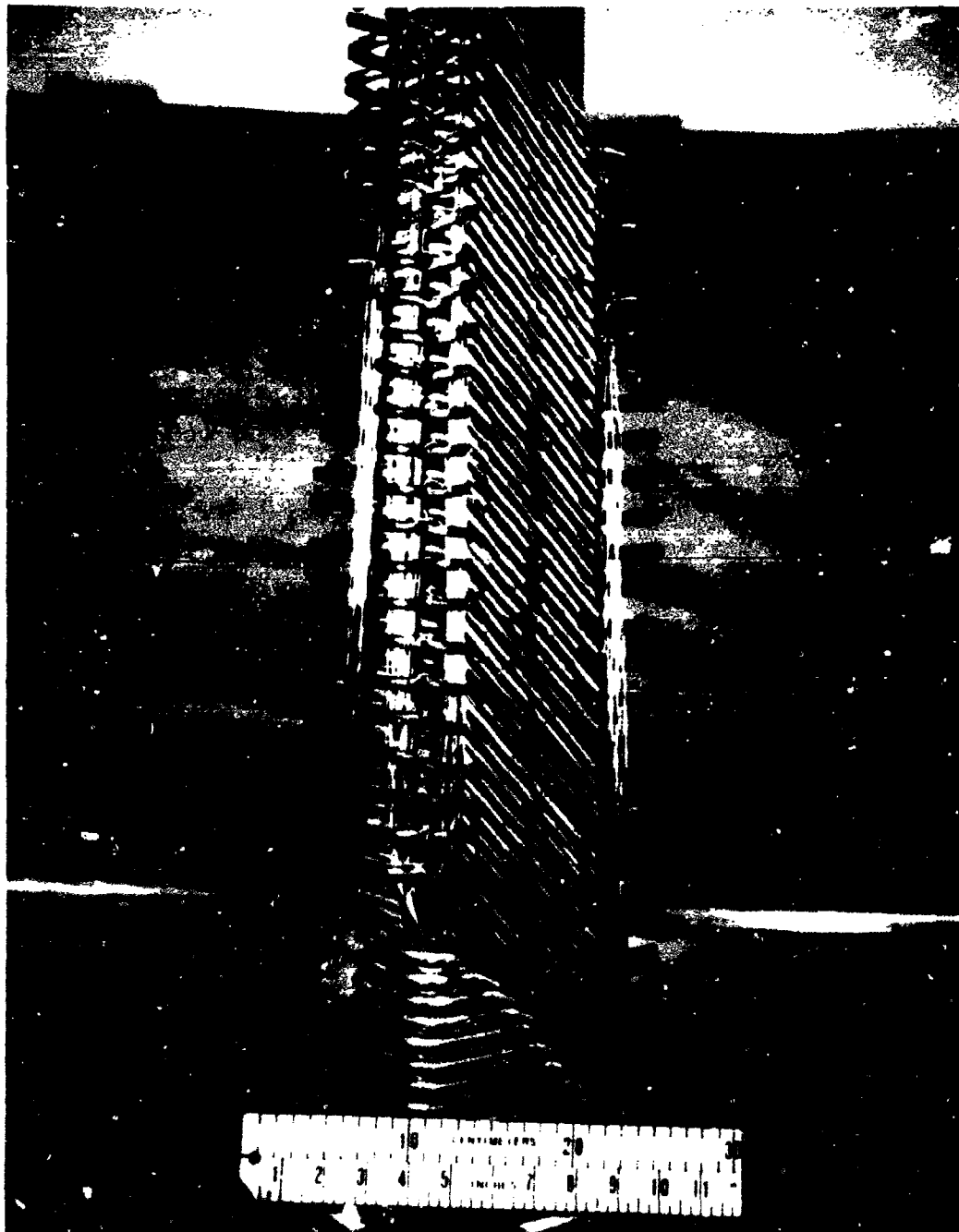


Figure 30. Partial Dry Assembly of the Frames on the Mandrel.

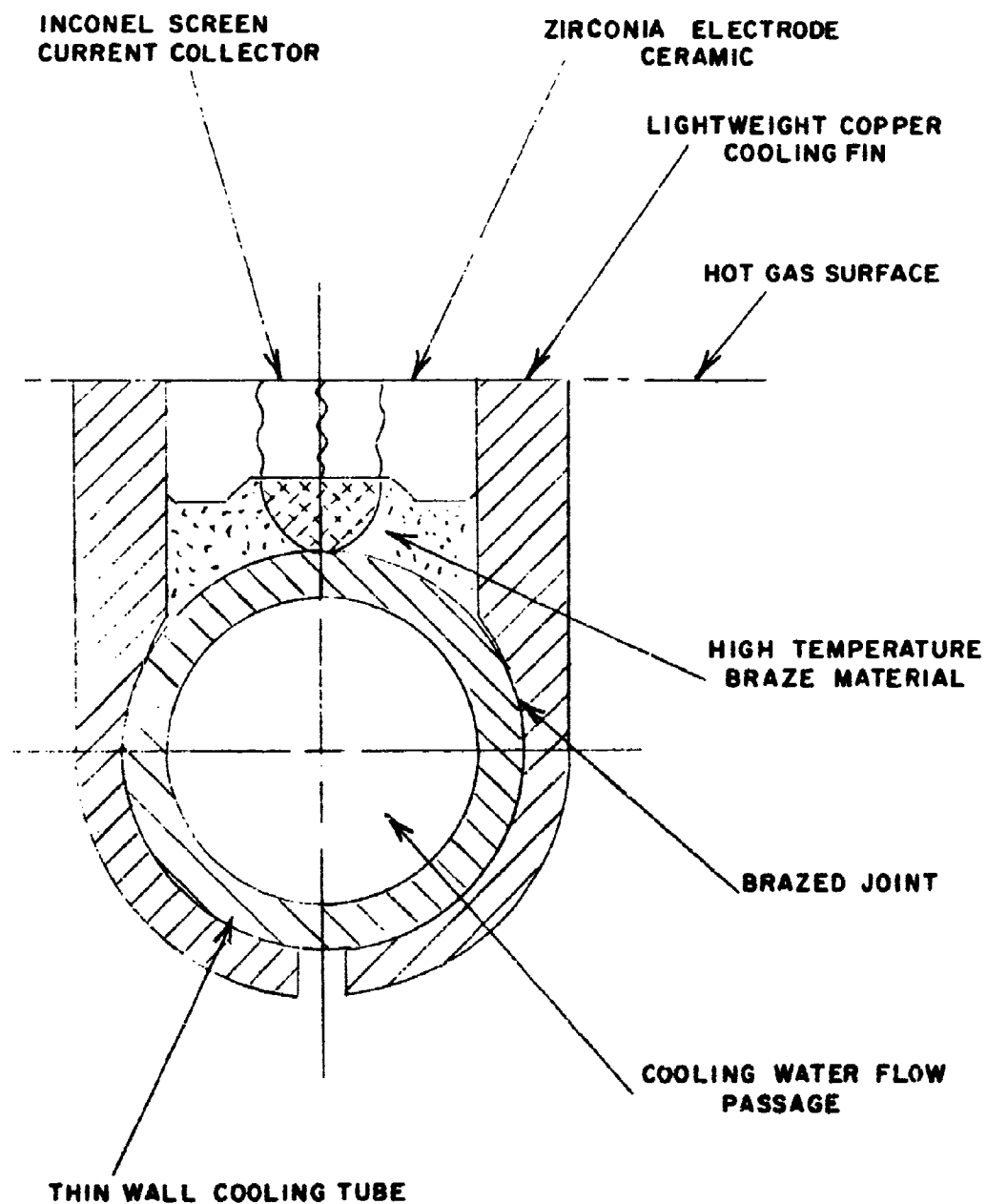


Figure 31. Typical Cross Section of Electrode Wall.

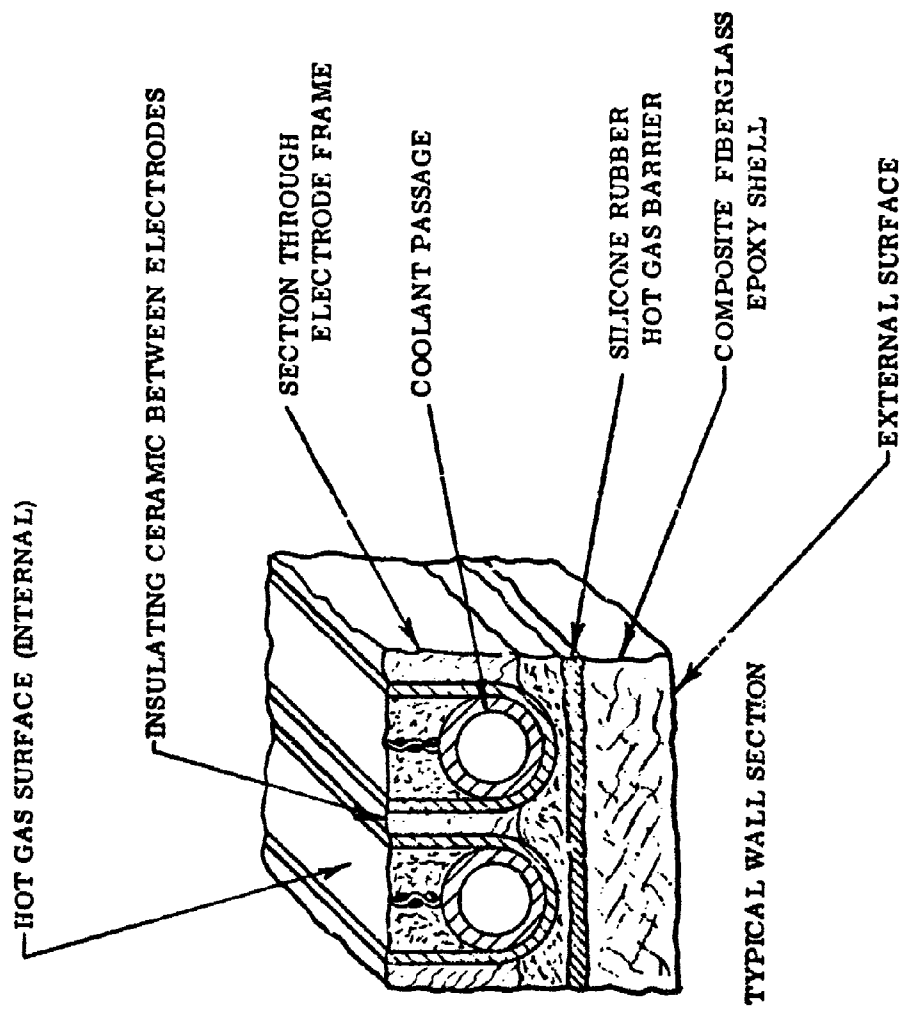


Figure 32. Channel Wall Construction Details

Substantial experimental testing was performed in order to find an optimum ratio between each ceramic and its binder. From a fabrication standpoint the ceramic/binder mixture must have a reasonably long pot-life, a viscosity consistent with the installation technique, and the correct mechanical and electrical properties to permit operation of the channel.

Several dozen sample mixes were prepared, poured into a multi-cavity mold, and baked for two hours at 330-335 K. The wafer-shaped samples, shown in Figure 33, were then weighed, visually inspected, fractured, inspected again and categorized according to strength, surface finish, and porosity. Finally, the optimum mixtures were selected.

a. Electrode Ceramic

Prior to the final assembly of the frames on the mandrel, the electrode ceramic was emplaced between the copper fins and Inconel screen on all four sides of each frame. Ideally, the ceramic must also fill the screen interstices, providing mechanical strength and efficient heat transfer. Before the emplacement all frame assemblies were degreased to promote ceramic adhesion. Wood racks were made which were capable of holding several electrode frames at a time facilitating both the filling and baking operations.

The formulation (and batch size) selected for the electrode ceramic was:

37 g	-	zirconia
6.5 g	-	zirconium di-boride (standard chemical grade)
7 ml	-	zirconia bonding liquid

After determining the mass of the zirconia and zirconium di-boride separately, the two powders were then thoroughly dry mixed together in a container. This was done by rotating the container with the container axis tilted from the vertical position. Next the bonding liquid was slowly added to the container and thoroughly mixed with a small flat metal spatula. This spatula was also used

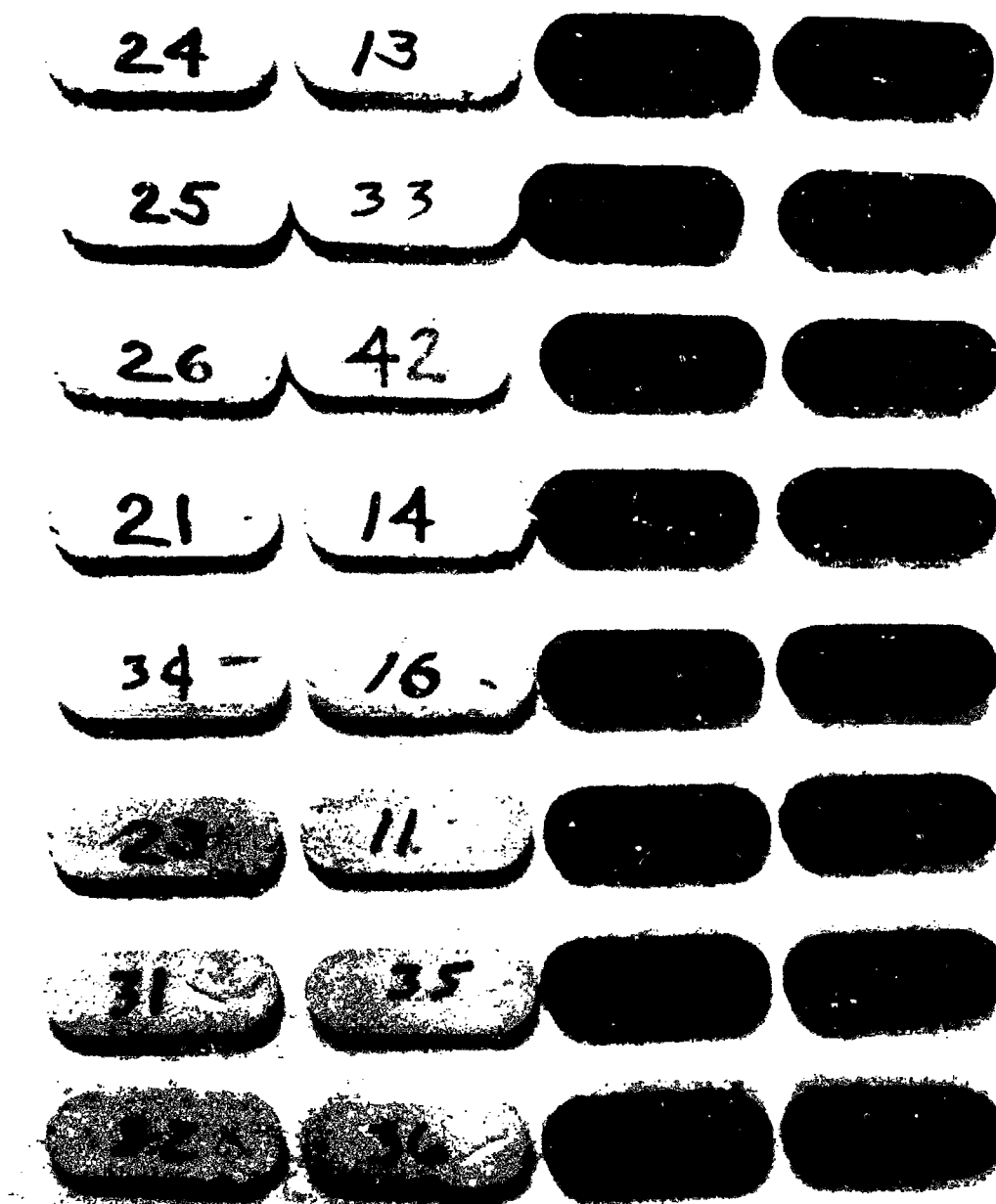


Figure 33. Electrode and Insulator Ceramic Samples.

as the emplacement tool. When the ceramic became uniform in consistency and color (purple-gray), the filling operation was initiated.

Several frames were filled simultaneously, one side at a time. The ceramic was added to the frame grooves, tamped down and leveled off. Next, the electrode frames were vibrated to eliminate the entrapped air bubbles. The vibration step was accomplished with the frames in a wooden rack. After 30 seconds the ceramic was inspected and more ceramic was added if necessary. Precautions were taken not to vibrate the ceramic too long because the bonding liquid would precipitate out of the matrix and float to the surface.

Following an air drying of about twenty minutes, the frames were rotated 90 deg to an adjacent side, and the filling process was repeated. When all sides were completed, the rack was placed in a preheated oven set at 330-355 K for two hours. Figure 34 shows several frames just after the baking operation.

The finishing operations consisted of adding more ceramic if necessary and rebaking, and then smoothing the ceramic surface with silicon-carbide cloth (220 grit) flush with the tops of the copper fins. Following a final visual inspection, the frames were then ready for the final assembly on the mandrel (see Section III-5).

b. Insulator Ceramic

The insulator ceramic was emplaced between adjacent frames, following the final fit-up of the frames on the mandrel. Ideally, the interframe gaps were filled from the hot gas surface (mandrel surface) to at least the center of the cooling tubes (see Figure 32). In addition the ceramic was emplaced around the tubes on both entrance and exit ducts to the same height as on the frames. This was done most effectively with the mandrel/frames assembly positioned horizontally in the winding fixture and oven assembly.

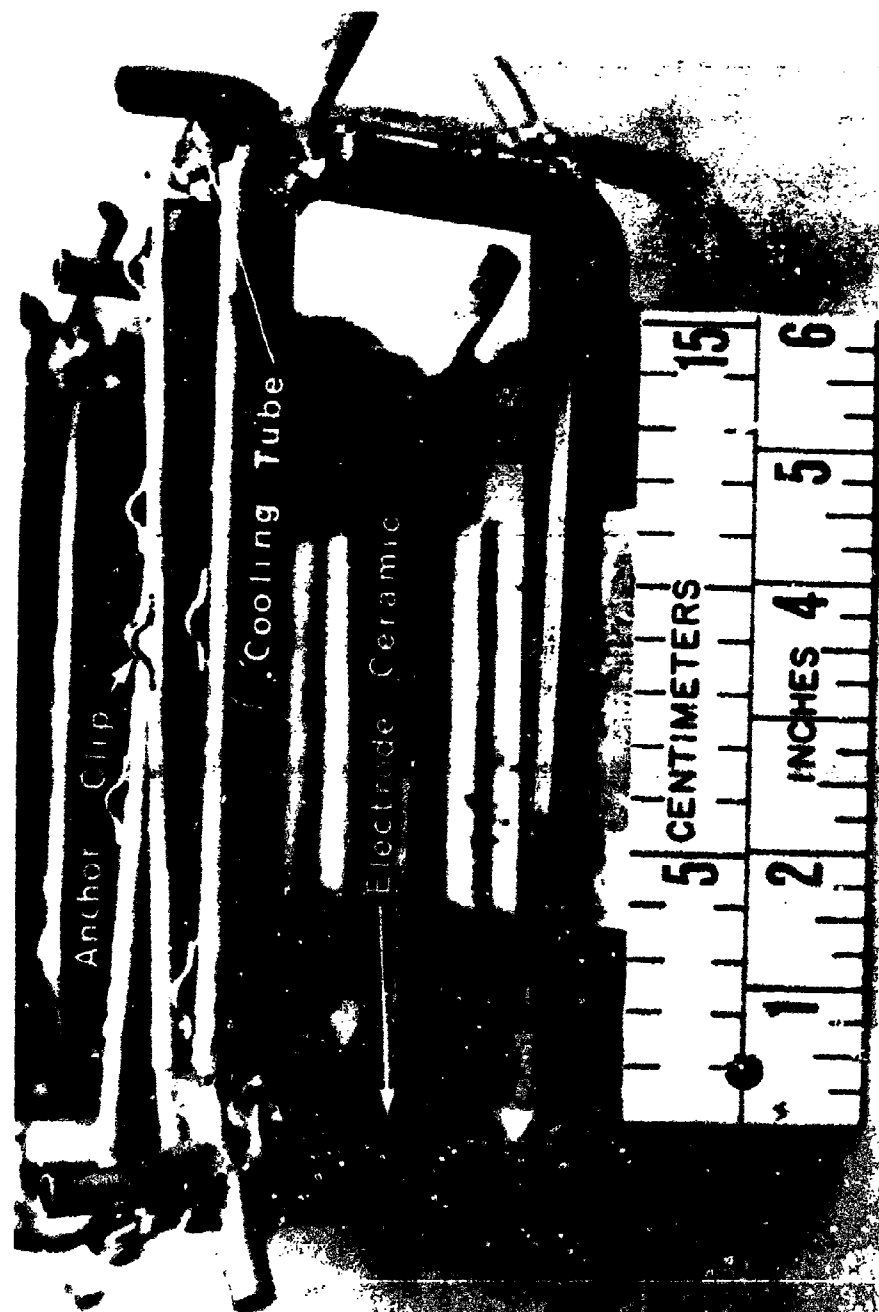


Figure 34. Electrode Frame with Electrode Ceramic Emplaced.

The formulation and batch size selected for the insulator ceramic was:

75 g	-	alumina powder
12 ml	-	water glass (calcium silicate)
4 ml	-	distilled water

Following the mixing of the water glass and water in a small graduated cylinder, the required mass of the alumina was obtained and placed in a mixing container. Next, the binder liquid was added, and the mixture stirred into a uniform ceramic mixture with a small flat metal spatula.

Because of the wires and shims used to position and constrain the frames on the mandrel, the emplacement of the insulator ceramic was a multi-step process. Working on the top side of the assembled channel, the accessible gaps were filled with ceramic using spatulas and air dried for about 20 minutes before rotating the channel and proceeding to the next side. Next, the assembly was baked for two hours at 330-355 K. After allowing the frames to cool, the shims and wires were removed and the ceramic emplacement continued. Following a second bake and cool-down cycle, the gaps between the corners of the frames were filled, one at a time, with the corner being filled when it was positioned on top. After the third bake/cool-down, final repairs and touchups were made. A fourth bake completed the emplacement. Figures 35 and 36 show the emplacement in progress and completed, respectively. Fortunately, the fine nature and low viscosity of the insulator ceramic mixture precluded the need for vibratory de-aeration. Periodic rodding and tamping with the metal tools resulted in a dense, smooth ceramic.

5. FINAL FRAME ASSEMBLY, CASE FABRICATION AND FINISHING OPERATIONS

a. Final Frame Assembly

The final frame assembly was one of the most important tasks in the fabrication of the lightweight MHD channel. Once the frames were in position



Figure 35. Emplacement of the Alumina Insulator Material.

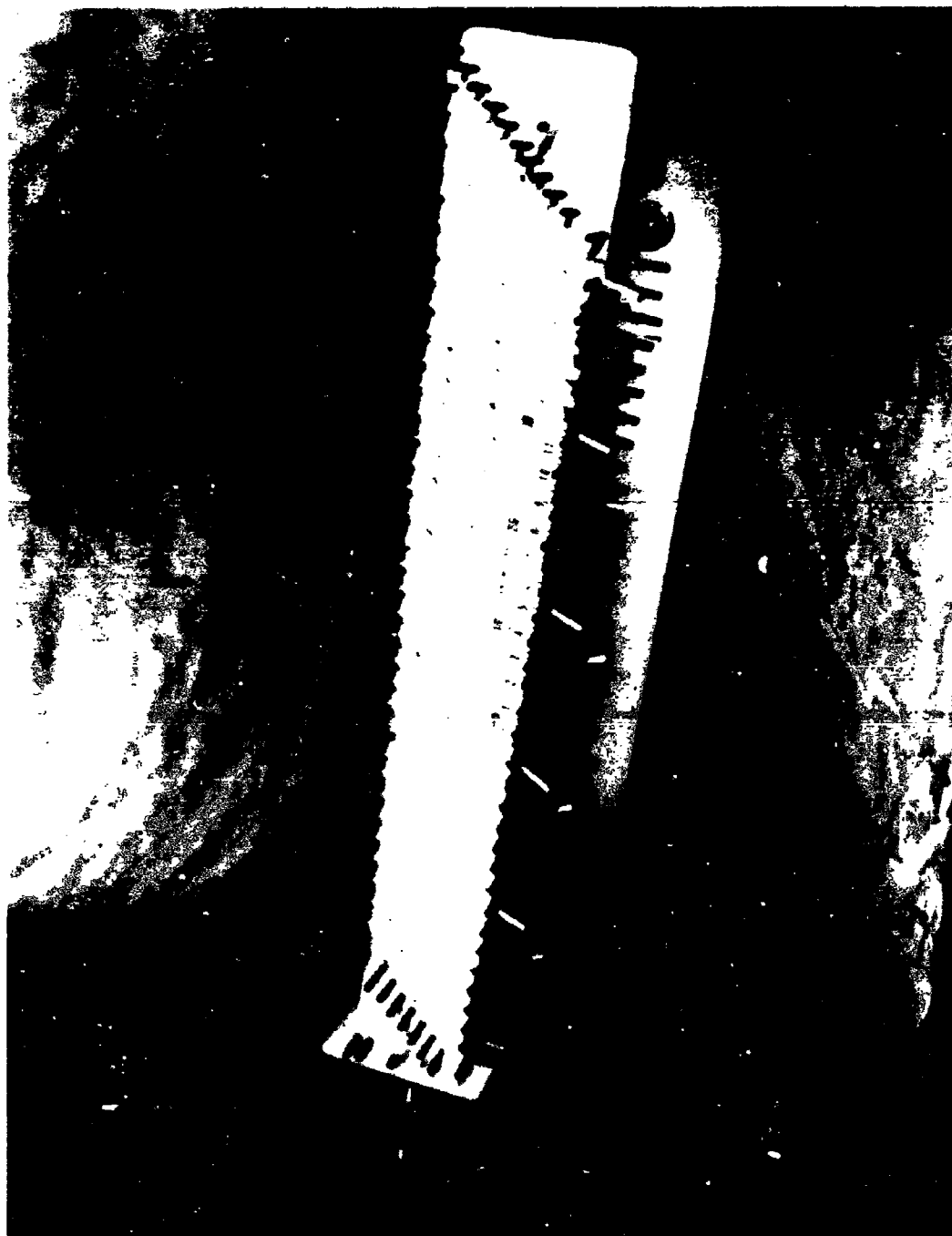


Figure 36. Lightweight MHD Channel with Ceramic Emplaced.

on the mandrel with restraining wires and shims, they could not be moved. This restriction required the electrode frame fit-up to be done methodically and with care.

Critical to successful fit-up was the mandrel. In addition to the uses mentioned in Section III-3, the mandrel served to establish the smooth inner contour of the channel until the glass epoxy shell was fabricated to support the frames. By using a locating gauge (see Figure 37), the nominal location of any one of the seventy frames was automatically established. For each frame the gauge was secured to the mandrel by pins and a unique pair of holes. The downstream edge of the gauge was the theoretical upstream face of the frame.

The fit-up procedure for the lightweight MHD channel began by mounting the mandrel in a vertical position to a workbench on the exit (large) end. To facilitate the removal of the frames after the case curing, liquid mold release was applied to the exterior surfaces of the mandrel. Following the installation of the exit duct, the frames, starting with the largest one, were fitted to the mandrel. Steel and aluminum shims were placed between the frames to guarantee proper spacing while wire was used to secure each frame (see Figure 37) to the exit duct via the cooling tube ends. This operation required an optimization among the following: 1) the nominal frame location, 2) interframe gaps, 3) the slant angle of the frame, and 4) the frame to mandrel gap.

Because the frame manufacturing tolerances were not held sufficiently close to the design specification to permit compliance with all four of these conditions, the fit-up sequence required several weeks of work, the remanufacture of several frames and custom fitting (filing, sanding and cold forming) of many others. In addition, three complete frame fit-ups were required before the fit-up effort showed that any further gains in optimization would not be cost-effective. Figure 38 shows the final assembly nearing completion.

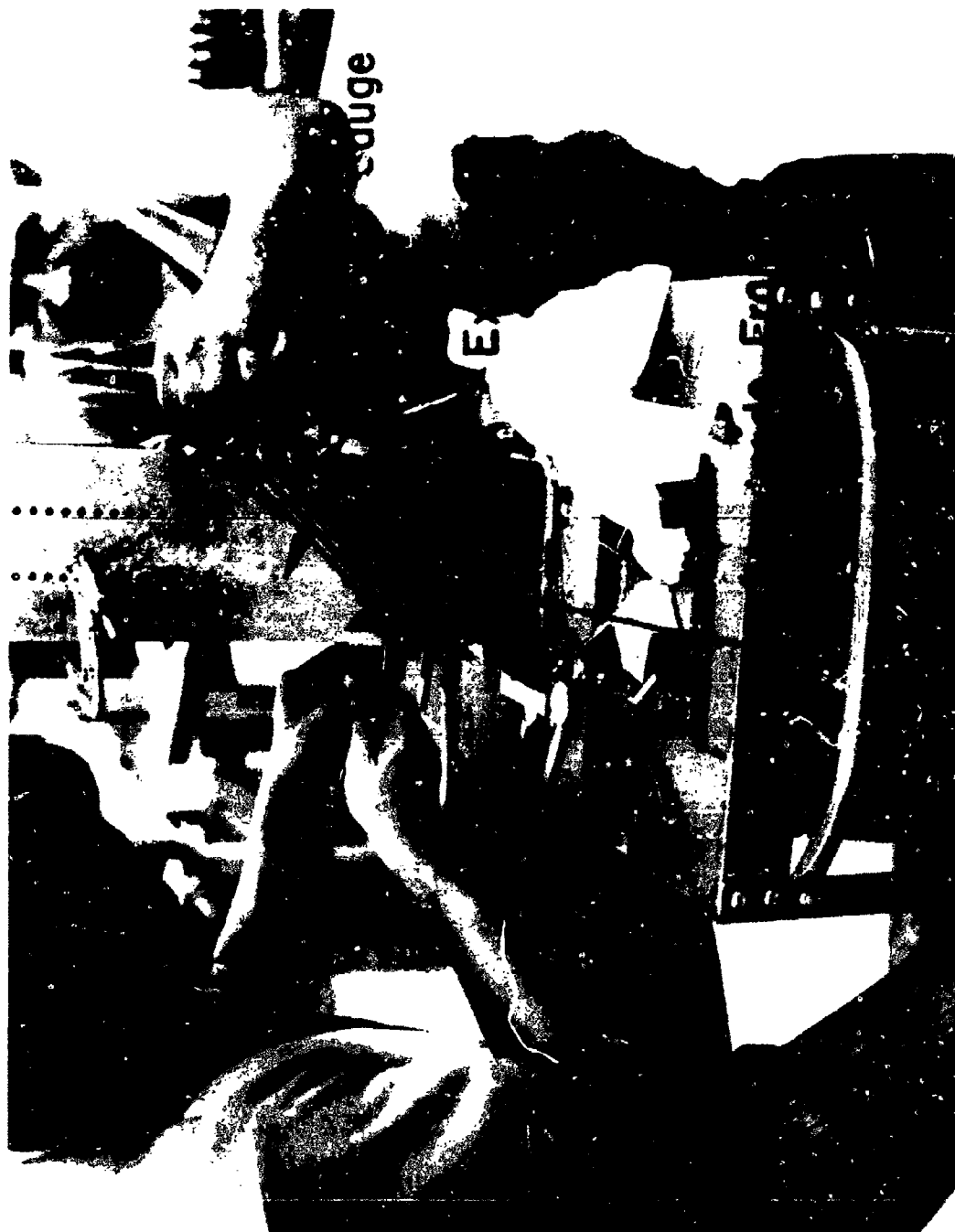


Figure 37. Final Frame Fitup in Process.

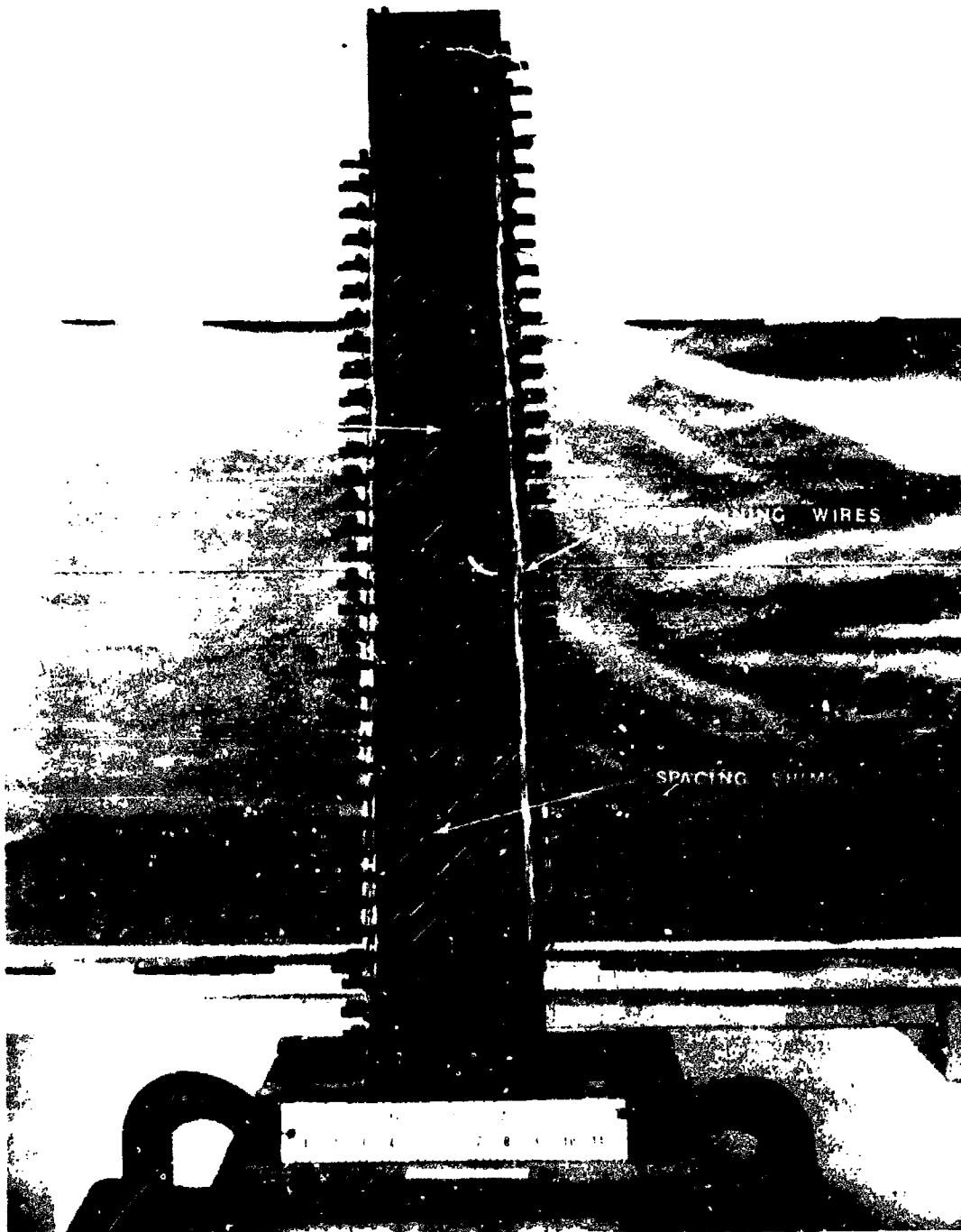


Figure 38. Final Assembly of Frames on the Mandrel.

The end result of this work was that although the frame position and angle were held quite close to the nominal design values, the interframe gaps, especially at the top and bottom walls, were not. Gaps ranged from 1.3 mm to 3.8 mm versus a design value of $1.57 \text{ mm} + 0.05 \text{ mm} - 0.00 \text{ mm}$. The variance was attributed to the technique of frame manufacture and the lack of inspection - in particular the frame thickness at the top and bottom. Also, the frame to mandrel gaps, nominally 0-0.25 mm, were oversize, particularly at the top and bottom of the frames. All interframe gaps and frame/mandrel gaps were documented so that a reconstruction of frame locations could be made if necessary. Following the installation of the inlet duct, the entire frames/mandrel assembly was mounted into the winding fixture.

Second in importance to the mandrel, the combination winding fixture and oven was also utilized for a variety of efforts. The fixture was basically a box constructed of steel angles and 9.5 mm thick Transite sheets. The box was made in two halves, which were readily separable. The lower half contained self-aligning ballbearings, which supported the trunnions, bolted to each end of the mandrel. This half also contained an electric motor with an infinitely variable speed control and a reversing switch. A "V" belt and pulleys transmitted power to one of the mandrel trunnions. The upper half of the box contained several large strip heaters, a small blower, baffles, a light, two view ports, and two thermocouples. A temperature controller, which connected to one of the thermocouples and to a relay which switched the heaters on and off, provided a simple, reliable means to control oven temperature. The winding fixture was used as a work station for ceramic and silicone rubber implantation, a lathe for the filament winding of the case, and an oven for curing the ceramic and epoxy resin.

At the same time the frames/mandrel assembly was mounted in the fixture, two other operations were performed. Large teflon flanges were mounted to the end of the mandrel to provide surfaces against which the fiberglass filaments could be wound. In effect these flanges defined the ends of the case. Small tapered

Buna-N plugs were also inserted in the cooling tube ends to prevent any foreign matter from entering the tubes and reducing the water flow rate. At this point in the fabrication process, the insulator ceramic was installed as described in Section III-4. Figure 36 shows the frames/mandrel assembly mounted in the winding fixture, just after the insulator ceramic has been installed.

b. Case Fabrication Assembly

The case of the lightweight MHD channel consisted of a filament wound fiberglass/epoxy resin shell which was separated from the frames by a 0.8 mm to 1.5 mm thick layer of silicone rubber, which formed the "hot gas barrier". The frames were secured to the case with four "anchors" made of beryllium-copper wire and soldered to the frame fins.

The first step in fabricating the case was to install a 0.8-1.5 mm thick layer of self-leveling, room temperature vulcanizing (GE RTV 112), silicone rubber to the exterior of the frames. As was the case with the insulator ceramic application, this was a multi-step operation. The sides were coated one at a time, with 30-minute waiting periods before rotating the mandrel. Next, the RTV was applied to the corners, one edge at a time. After allowing the silicone rubber to cure for 24 hours at room temperature, the excess material was cut away with knives.

Next, short lengths of 12.7 mm x 9.5 mm silicone rubber tubing were installed on the ends of the cooling tubes. The purpose of the tubing, which was later removed after curing of the shell, was to mold a cavity in the case around each cooling tube. The cavity was then filled with self-leveling RTV silicone rubber. This formed, in effect, a continuation of the hot gas barrier.

Before the details of the case fabrication are discussed, a description of the materials and tools required is necessary. The epoxy resin system used consisted of Shell Epon 828 (100 parts by mass), Miller-Stephenson NMA nadic methyl anhydride curing agent (100 parts by mass) and Miller-Stephenson DMP-30 acid-based accelerator (2 parts by mass).

Fiberglass was used in three forms: roving (Volan A treated, 60 ends of 150 continuous filaments, "G" filament), woven roving (same specifications as roving, but woven into a mat of 81 g per 1000 cm²), and woven fabric (Volan A treated, satin weave, 30 g per 1000 cm²).

The case derived the bulk of its strength from the fiberglass roving. The woven roving was primarily filler material, which provided a great deal of bulk to the case; whereas the fabric was used as a filler layer, primarily for cosmetic purposes.

A dispenser reservoir and mechanism was used to wet the roving and then remove the excess epoxy. The roving was manually guided as it passed over the rollers and the rotation of the mandrel was also manually controlled. The roving tension was adjusted during the winding process to insure that the tension was always sufficient to provide a "tight," filament winding. The continuous rotation of the mandrel during the winding process minimized the amount of epoxy which dripped onto the base of the winding fixture. Brushes were used to wet both the woven roving and fabric during the winding process. Special serrated rollers were also used to pump out any air bubbles introduced by the winding and lay-up processes.

The next step after the RTV installation was the fabrication of the "interface layer" of fiberglass. This layer provided the bond between the hot gas barrier and the case. Since uncured silicone rubber was about the only material which would satisfactorily bond to cured silicone rubber, the following technique was employed. To each side of the frames/mandrel assembly, two layers of large rectangular pieces of woven fiberglass fabric, semi-soaked with RTV silicone rubber, were attached. They were allowed to cure 24 hours at room temperature. When wetted with epoxy resin, these layers of glass cloth became the "interface" between the rubber and case.

Using a curved sail-maker's needle, 125 mm long tassles of roving were fastened to the anchors by threading through the interface layer. These tassles were eventually meshed into the case to provide a secure bond between the anchors and the shell. Figure 39 shows these tassles in place. Epoxy resin was applied next to make them stand up while the roving was wound around them.

In order to monitor the case buildup, initial measurements were made on each Teflon winding flange from the outside edge down to the interface layer. Periodic measurements were made and compared with these initial figures to provide the case thickness at any time during the filament winding process.

Using a bristle brush, a generous amount of epoxy resin was applied to the interface layer, thoroughly soaking it. The layer was then rolled using the serrated rollers to remove excess air.

The roving winding was initiated by tying the roving to a cooling tube at the inlet end of the assembly. Then, using the motor to rotate the mandrel, a layer was wound from inlet to outlet to inlet with no bias and no serpentine. (Note: bias refers to the angle between the wound-on roving and a vertical plane; serpentine refers to the routing of the roving around the two tubes at the frame corners in an "S" shaped manner.) The tassles were then trimmed to 25 mm length and kept erect throughout the following steps.

Again, roving was wound inlet to outlet to inlet with no bias or serpentine. Next, many small pieces of waver roving were added to the frame corners, to hasten the case buildup. Then roving was added at a 45 deg bias, no serpentine, from inlet to outlet. Then from outlet to inlet at a 135 deg bias with no serpentine. Next, several layers of woven fabric were added to fill many of the voids.

The steps described above were repeated as many times as necessary to build up the case as uniformly as possible. The bias was changed to fill in gaps between adjacent roving windings, while filler pieces of woven roving and serpentine winding were used to fill in gaps around the tube ends.



Figure 39. Lightweight MHD Channel Before Filament Winding.

About two-thirds of the way through the winding process, the tassles were flattened and rolled thoroughly into the case. In addition, anchor plates, used to secure the front end of the channel to the combustor nozzle, were wound into the case at the top and bottom of the inlet end.

Following more winding and filling, the case thickness was measured again. As the case thickness approached the design goal (3 mm - 5mm thick in the corners and 6 mm - 10 mm thick at the midspan of the sides), the final layer of roving was applied. This layer of roving was applied somewhat tighter and drier than preceding layers. This was done for cosmetic reasons and also to absorb as much of the extraneous epoxy resin as possible. Following a final rolling, the roving end was cut off and buried within the shell. A final brushing removed most of the excess material and smoothed over the case exterior. Next, two dial thermometers were attached to channel assembly to monitor cure temperature (one to a cooling tube and one to the mandrel). The winding fixture motor was turned on and adjusted to rotate the channel at about 7-10 rpm to prevent epoxy from dripping from the shell.

The top half of the winding fixture/oven was set in place and the heaters turned on. The total cure for the case was ≈ 20 hours, which included a 6-8 hour warmup and 14 hours at 370 K. Temperature readings were read and recorded every half hour throughout this period. Following the shutdown of the heaters, the top of the fixture was removed and the channel allowed to cool very gradually. Figure 23 shows the channel following the cooldown.

c. Finishing Operations

The channel finishing operations consisted of sealing the cavities around the cooling tubes, sealing the area around the entrance and exhaust ducts at the ends of the channel, removing excess epoxy, RTV, foreign matter, etc. from the exterior of the channel, and finally, repairing and finishing the interior of the channel once it had been removed from the mandrel.

Following the attachment of the cooling tube fittings (see Section III-6), the first finishing operation was to remove the temporary tube end seals of silicone rubber tubing from the cooling tubes, and then clean and abrade the resultant cavities. This was effectively done with a pencil-type sand blaster possessing a nozzle small enough to be placed within the cavities. The purpose of abrading was to promote good adhesion between the glass/epoxy shell and the RTV rubber. Following a cleaning with a mild alcohol solvent, the seals were cast in place, one corner at a time with a 30-minute waiting period before rotating mandrel, using a self-leveling RTV silicone rubber. After a 24-hour cure excess RTV was cut away, and the case was washed down with alcohol to remove foreign matter.

At this point the mandrel was removed to inspect the hot gas surface. After removing the self-aligning bearings, the assembly was carefully lifted out of the winding fixture onto a work bench. The channel was supported by wooden blocks on the bottom of the case and the trunnions were unbolted. Next, the channel was upended onto the exit end and supported by wooden blocks placed under the case end. The mandrel was then tapped downward very gently with a plastic hammer. Because of the taper on all four sides of the mandrel, the loose fit between the frames and mandrel, and the Teflon and mold release coatings, the mandrel was easily removed. The channel was then supported horizontally so that a detailed inspection of the interior could be made.

This inspection revealed that the interior surfaces were unsatisfactory. While the electrode ceramic was in place and required only minor repair, the insulator ceramic had worked into the gaps between the frames and the mandrel. The end result was a very uneven hot gas surface with wide patches of alumina between the frames. There were also many voids in the alumina-regions where the frame/mandrel gaps were not completely filled with alumina.

The first step to improve the interior was to level the alumina as much as possible. This difficult task required the use of double cut files, a hand-held

grinder with hardened grinder bits and aluminum oxide paper. Following this task and a thorough vacuuming, the gaps in the electrode ceramic were filled using small spatulas with extension handles and inspection mirrors. One side of the channel at a time was repaired with work proceeding from each end of the channel. At this time all pressure tap holes were cleared with short lengths of hardened music wire, secured in pin vises, using a rotary drill-like motion.

After curing the electrode ceramic with a lamp at 340-360 K for three hours, the insulator ceramic was repaired and cured in a similar manner. At this point the alternate bands of ceramics were essentially void free and uniform in width. However, the interior surfaces were not smooth. The poor frame-to-mandrel fit created "waves" in all four sides of the channel which were completely undesirable and required repair. As a final interior finishing operation, a coat of insulator ceramic was applied to the entire interior surface; thin enough to not seriously impair channel operation, yet thick enough to smooth out most of the waviness of the surfaces. This was accomplished with a small tool similar to a hoe, and a trowel. Then the alumina was cured, finish sanded and vacuumed.

Next, beads of non self-leveling RTV silicone rubber were applied to grooves in the case around the inlet duct and the exhaust duct, thereby completing the hot gas barrier. Finally, interior bore measurements at the inlet and exhaust faces were measured with vernier calipers and recorded.

6. COOLING SYSTEM

The building of the cooling system for the lightweight MHD channel and diffuser involved the fabrication of fittings, interconnecting tubes and manifolds; and the installation of fittings, ferrules and flexible cooling tubes. The specifics of the cooling system design have been described in Section II-5.

a. Channel Cooling

The fabrication of the electrode frame cooling tubes was discussed in Section III-3 and will not be repeated here.

The fittings which connected the flexible cooling tubes to the frame and duct cooling tubes were custom screw machine products made of brass. Two configurations were used: straight, and 90 deg elbow. One end was barbed to provide a grip for the flexible tubing while the other was bored to provide a 0.08 mm - 0.13 mm clearance fit over the frame and duct tube ends for soldering.

The flexible tubing used to connect the intake and exhaust manifolds to the frame and duct cooling tubes and also to connect some frame half-loops in series was made of nylon. The tubing was 9.5 mm O.D. with a 1.3 mm thick wall and rated for 28 atm.

The majority of the interconnections between frame half-loops and between duct cooling tubes were made with standard 90 deg elbow "sweat type" copper fittings and lengths of formed copper tubing; and with custom brass fittings and lengths of formed copper tubing. The custom brass fittings were essentially blocks with holes drilled in two adjacent sides to form a 90 deg bend in the cooling water path. They were used primarily at the exhaust end of the channel where interference problems with the MHD generator magnet were of prime concern.

The manifolds for cooling the channel were made from 76 mm O.D. copper tubing, fitted with end caps and barbed fittings. All joints and connections were brazed.

The first step in building the cooling system was to precut the nylon tubing. Next, ferrules were made from thin wall aluminum tubing. The barbed fittings were pretinned with solder at the sweat end and pressed into the nylon tubing. A ferrule was slipped over the tubing at the center of the barbed region. Using a Maxwell MagneformTM machine with a circular field shaper, each ferrule was securely clamped in place through the process of magnetic forming.

The second operation was to solder all the interconnecting elbows and copper tubes in place. Heat shields were used to protect the case shell from the soldering torch flame. This was done before the tube end seals were cast in place since the heat would destroy the seal (see Section III-5). All elbows and copper tubes were pretinned. After the tubes were soldered to the elbows, the elbows were soldered to the frame and duct tube ends. See Figure 40 for a view of the inlet end of the channel.

The next operation was the most complex step: the soldering of the barbed fittings to the frame cooling tubes. Again, this was done before the tube end seals were cast in place. Because of the high thermal conductivity of the copper, a torch was also required for this operation. Numerous asbestos heat shields were used to protect the nylon tubing and the channel case. Heat sinks were used to protect the clamped end of the tubings. For this operation, each frame tube end was carefully heated. Next, the appropriate tubing/fitting assembly was placed over the tube end and correctly oriented while heating continued. Once the solder wicked freely around the joint, the torch was quickly removed. While a satisfactory technique was developed, some of the tubes were damaged and had to be replaced and some joints required resoldering. The end result however, was a leakproof joint at each connection.

Throughout this operation, the routing of the tubes was a prime concern (see Figure 41). A sizing gage, simulating the envelope into which the channel had to fit, was used to establish the optimum placement of the tubes.

Finally, all the tube ends were tagged to indicate the frame half loop or duct loop the end was connected to and whether the end was an inlet or outlet line. For example, 47A1 described the inlet tube for the "A" half-loop of frame #47 and "BI" described the inlet tube for path B in the exhaust duct.

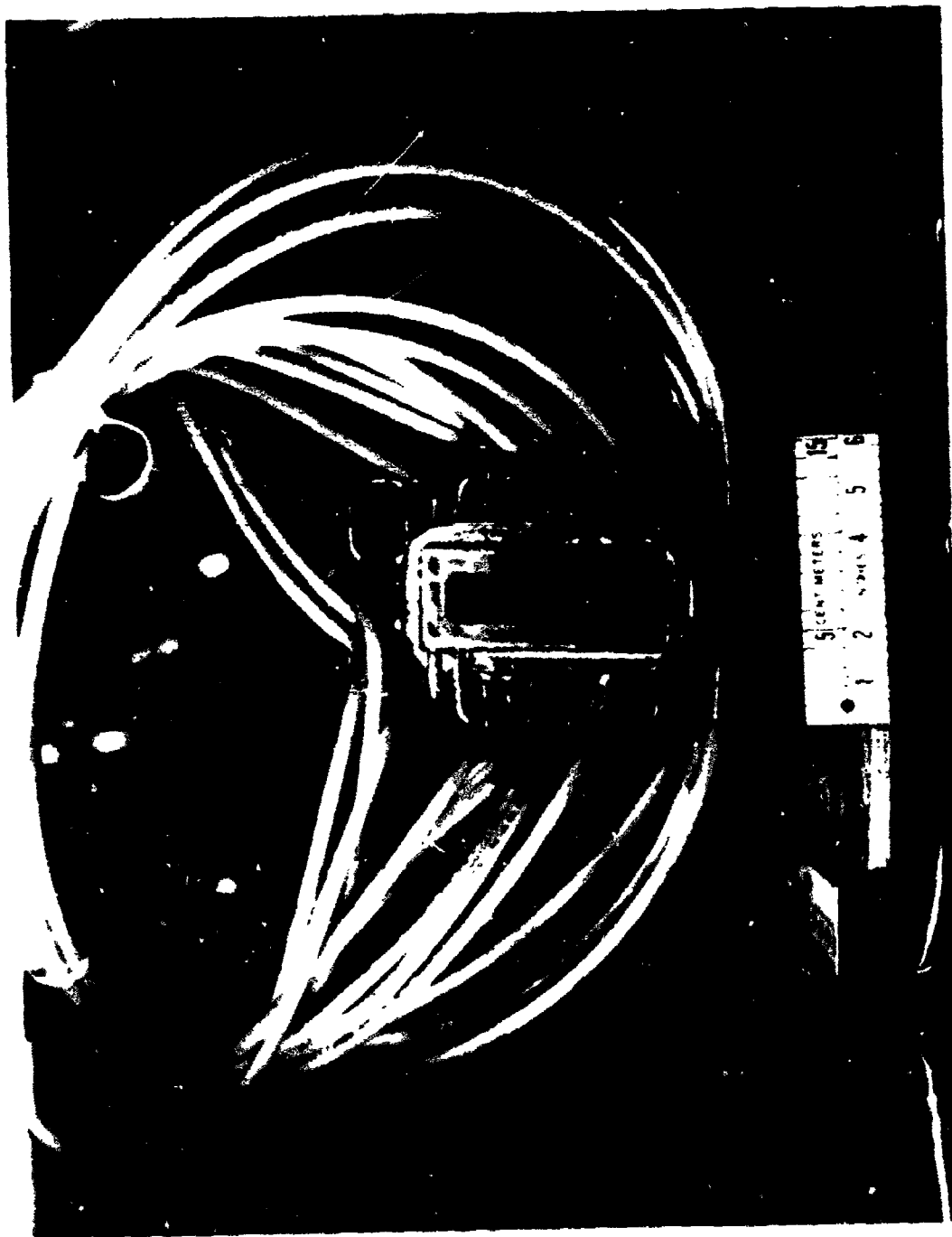


Figure 40. Inlet End of Lightweight Channel.

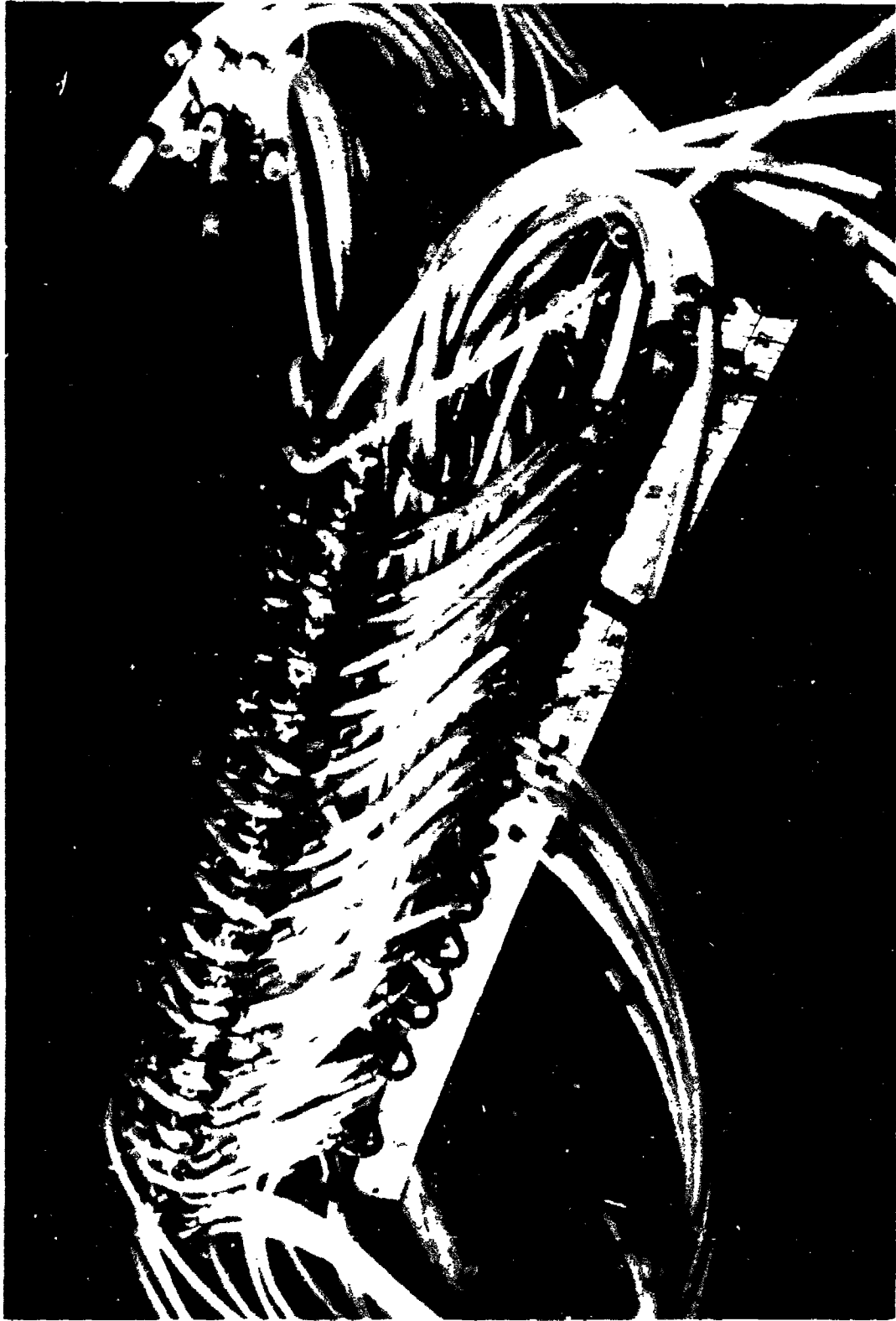


Figure 41. Finished Lightweight MHD Channel.

All of the manifolds were shipped with the channel, but were unconnected. The final connections were more readily made with the channel installed using standard compression type clamps to secure the tubing to the barbed manifold fittings.

b. Diffuser Cooling

The fabrication of the diffuser cooling tubes is discussed in Section III-7 and will not be repeated here.

The fittings which connected the flexible cooling tubes to the diffuser copper tubes were custom screw machine products made of brass and copper sweat elbows. Two configurations were used: straight, and 90 deg elbow. One end of each fitting was barbed to provide a grip for the flexible tubing while the other was bored to provide a 0.08 mm - 0.13 mm clearance fit over the diffuser tube ends.

The flexible tubing used was the same type used on the channel but was 13 mm O.D. with a 1.6 mm thick wall. The pressure rating was 28 atm. The interconnections between the diffuser half-loops were made with formed copper tube fittings shaped like the letter "C". A collar with an I.D. large enough to accept the O.D. of both the fitting and the diffuser tube was fabricated and soldered to the fitting.

The manifolds (two inlet and two outlet) were fabricated in the same fashion as the channel manifolds. The only difference was the diameter (102 mm) and the number of barbed fittings.

The first step in fabricating the diffuser system was to precut the nylon tubing. Next, after tinning the sweat end of each interconnection, the interconnects were soldered in place. In order to protect the silicone rubber case, heat sinks and shields were used. Next, the barbed fittings were attached in a similar manner (see Section III-7). Finally, each barbed fitting was tagged in order to facilitate installation.

The manifolds and tubing were shipped with the diffuser, but were unattached. Final attachment was best done at installation using standard compression clamps to secure the tubing to the barbed fittings.

7. DIFFUSER FABRICATION

a. Shell Fabrication

The basic shell of the lightweight MHD diffuser (see Figure 9) consisted of a straight section, a diverging section, and an entrance flange. The two sections were fabricated from 1.2 mm thick copper using development patterns. Each section contained a longitudinal seam at the top and bottom. The seams and the sections were joined together with a high temperature braze alloy.

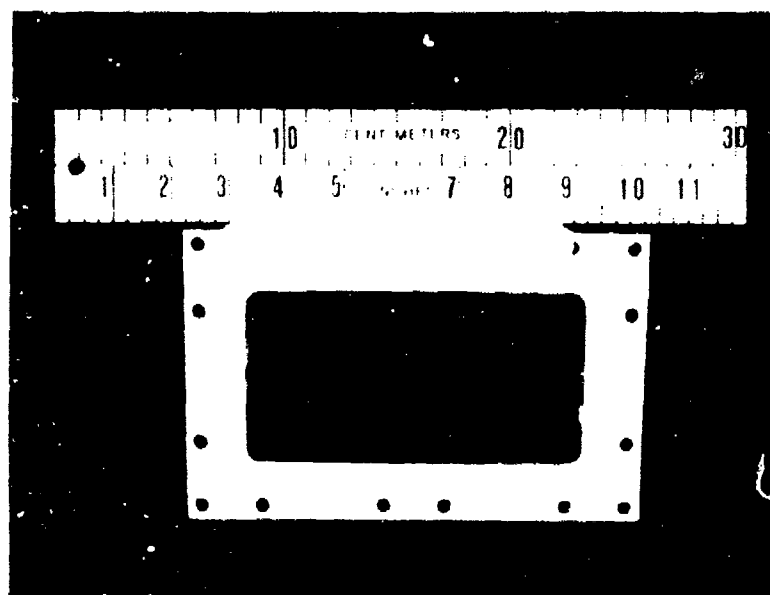
The entrance flange, containing the bolt holes for attaching the diffuser to the channel, was machined from 2.4 mm thick copper and was also brazed to the shell. Finally, all braze joints were ground flush with the copper and the shell was thoroughly sandblasted and degreased. Figure 42 shows both ends of the completed shell.

b. Pressure Taps

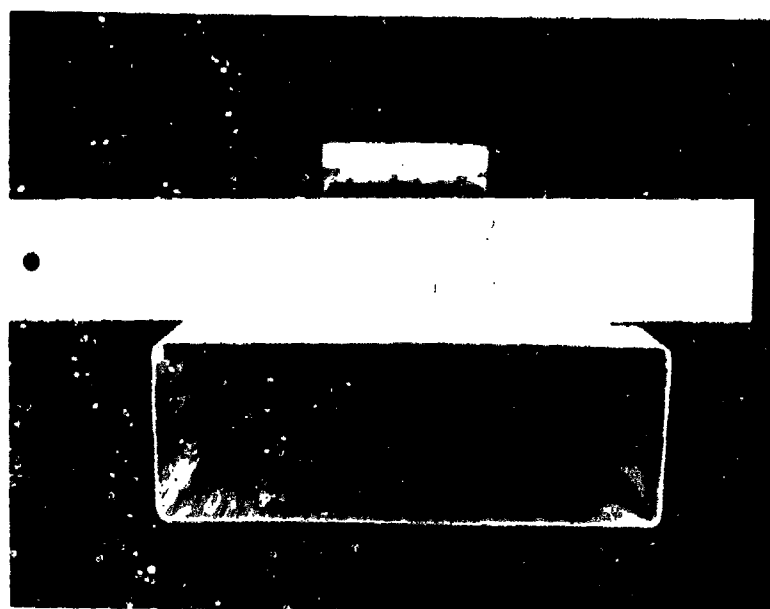
To monitor the gas static pressure, six pressure taps were fabricated and installed. These were later connected to pressure transducers. The taps were turned from #303 stainless steel rod, 6.3 mm in diameter. A 0.8 mm diameter hole was drilled through the length of the rod providing a passage for the pressure measurement. Six holes were drilled in the bottom side of the shell and the pressure taps were silver soldered in place.

c. Cooling Tubes

The cooling tubes for the diffuser were fabricated from 8.0 mm O.D. x 0.8 mm wall copper tubing. The original plan was to fabricate forty-four loops from this tubing and solder them to the shell. During the assembly of the first



(A) Inlet End



(B) Exit End

Figure 42. Inlet and Exit Ends of Lightweight Diffuser Shell.

few cooling loops, the difficulty in maintaining intimate contact between the loops and all four sides of the shell became quite apparent. A solution to this problem was to create each loop using two "L" shaped "half-loops" and later interconnect them with custom formed fittings (see Section III-6). With this approach a close fit between the tubes and the shell was easily achieved.

In addition to the change described previously, thermal analysis indicated that the area of contact between the tubes and shell needed to be increased. This was accomplished by flattening the tubing into a "D" shape before forming the "L" shaped half-loops. A die was machined from steel to accomplish this (see Figure 43). Pressure was provided by a 22,000 N cam-driven punch press.

The eighty-eight half-loops were then soldered to the shell in planes perpendicular to the hot gas flow path. Four different spacings between the loops were used in order to accommodate the varying thermal loads imparted to the shell by the hot plasma. Figure 10 shows about 50% of the tubes in place on the shell.

d. Ceramic Felt

In order to protect the silicon rubber blanket (see Section III-6.e) from the hot copper shell, moldable lightweight ceramic felt was applied to all four sides of the diffuser. The felt was supplied in air tight plastic bags in roll form and was easily cut and shaped because of its moist condition. However, once the felt was air dried for several hours, it hardened. A second advantage of this lightweight yet bulky material was that it provided a relatively flat base for the rubber, thereby facilitating the application process. At this point plastic plugs were snapped on the ends of the tubes to prevent silicone rubber from entering. See Figure 44.

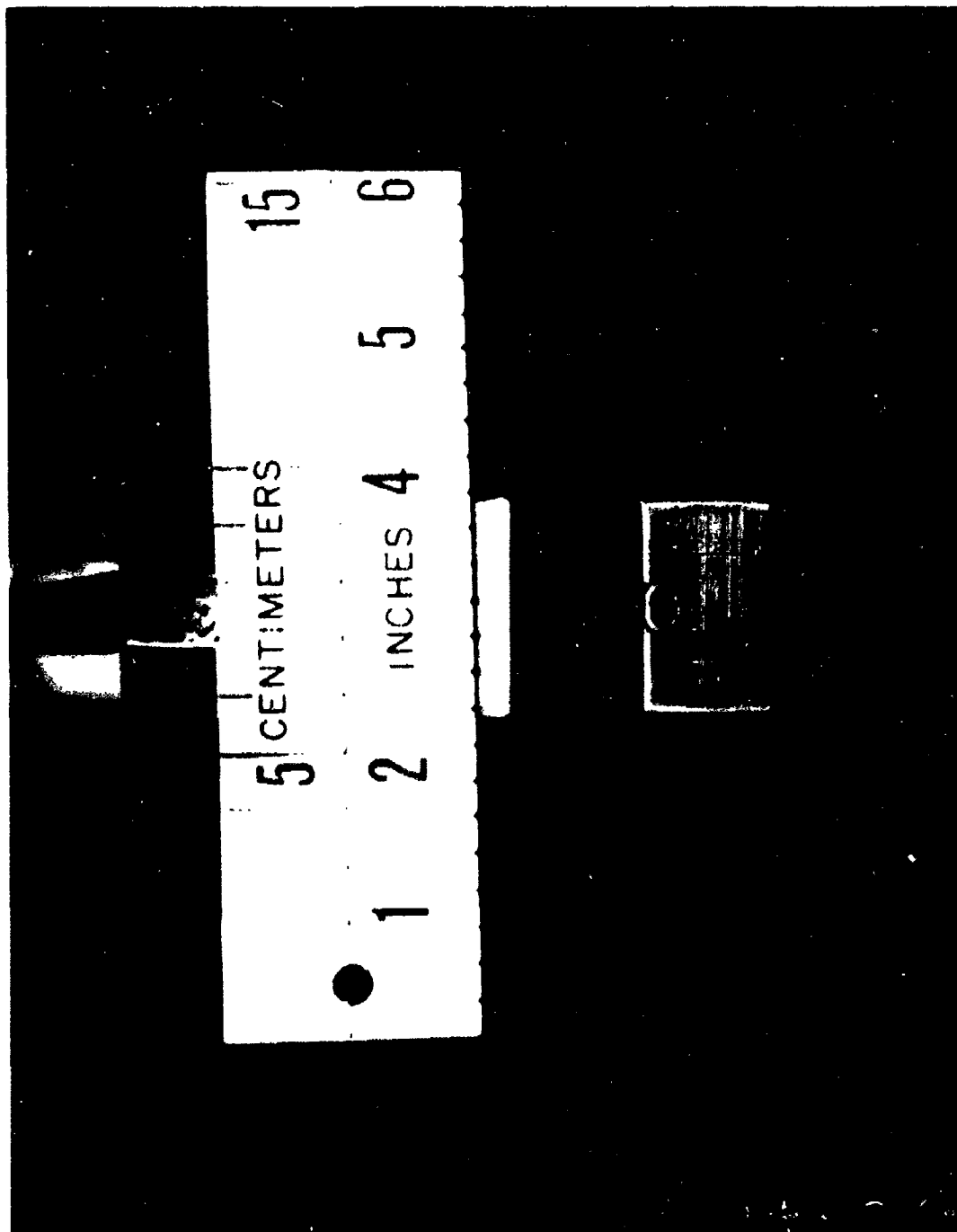


Figure 43. Diffuser Cooling Tube Tooling.

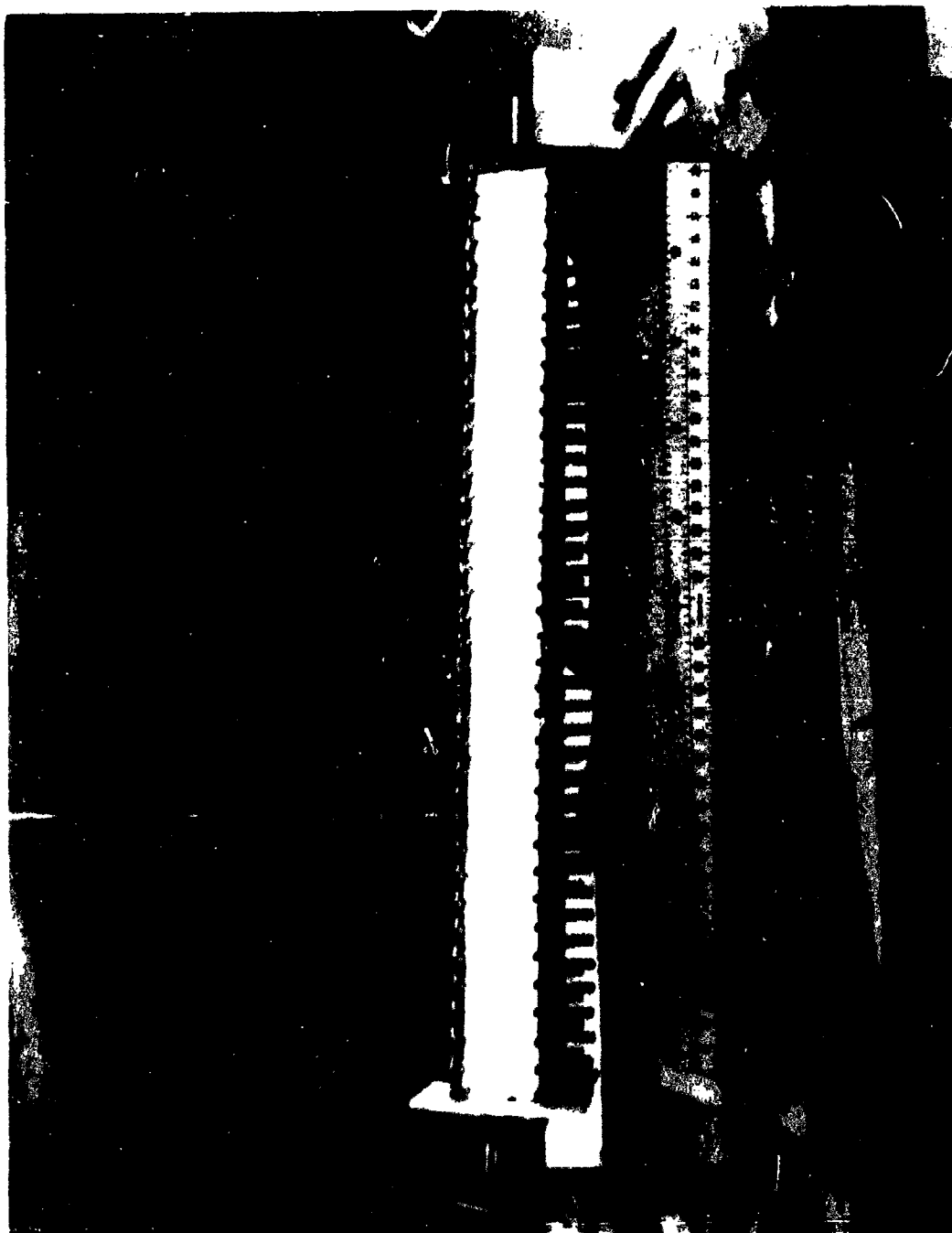


Figure 44. Lightweight MHD Diffuser.

e. Silicone Rubber Blanket

The final step in building the lightweight MHD diffuser was to apply an exterior blanket of blue RTV silicone rubber. This was done not only for cosmetic purposes, but also to secure the felt in place. While there was a slight adhesive bond between the felt and the copper, the felt would have fallen off when handled if the rubber had not been applied.

The specific material used was supplied in two parts: a combination dye/activator and the uncured rubber. Following a thorough mixing, the material was applied to the diffuser, one side at a time while the diffuser was mounted horizontally. After a 24-hour cure, the diffuser was turned 90 deg to expose the next side. The rubber was somewhat self-leveling so that a fairly smooth, uniform application was possible to achieve. After the sides had been covered, the corners were filled and cured. Throughout the application small "dams" were made using flexible zinc chromate tape to contain the rubber to one side, or to one corner, until the cure was completed.

Following this operation, the cooling tube fittings were attached. Figure 45 shows the completed diffuser.

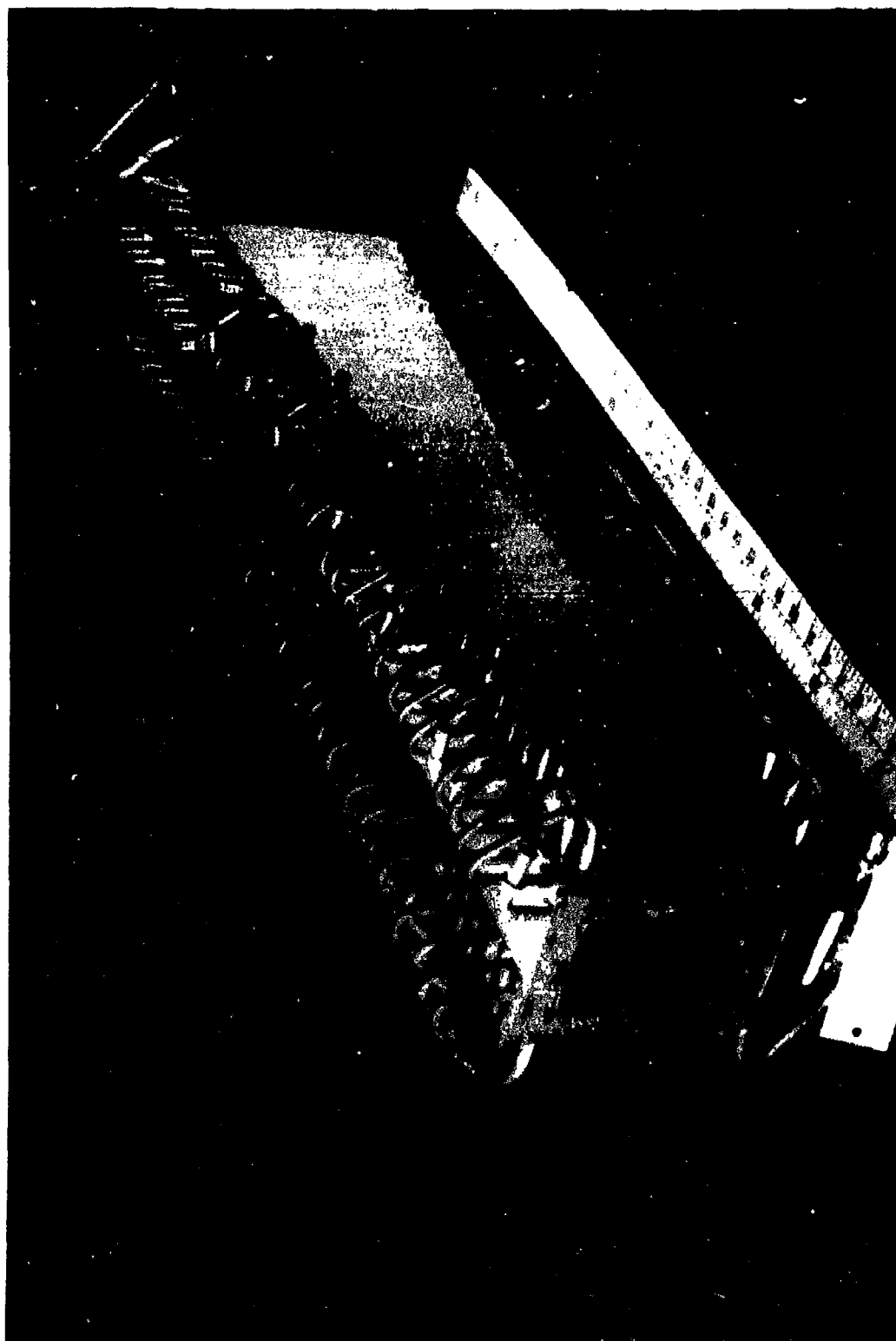


Figure 45. Completed Lightweight MHD Diffuser.

SECTION IV

MHD GENERATOR TESTING PROGRAM

1. WATER FLOW TESTS

a. Introduction

Of all the tests performed on the lightweight MHD channel and diffuser during fabrication, none were more important than the water flow tests. These tests measured the pressure drop in each cooling passage at the water mass flow rate required to remove the nominal thermal load imposed on the channel and diffuser by the hot plasma. In the case of the channel, these flow tests were done twice - before and after the final frame fit-up. In addition, prior to the case wind and cure, each passage was checked for any obstructions. The diffuser was flow checked once following the attachment of the cooling tube fittings (see Section III-6).

b. Test Set-Up and Operation

A very simple, yet reliable test apparatus to measure the pressure drop for a given water velocity was designed, fabricated, and checked out. A pressure vessel with one end modified to accept the multiple fluid flow lines provided the high pressure water supply. The three fluid feed lines in one end of the pressure vessel were: 1) a low pressure water feed with a valve; 2) a high pressure air supply with a pressure gauge and a quick disconnect fitting; and 3) a high pressure water exhaust line with a fast action ball valve. In addition to the pressure vessel hardware, a second pressure gauge, connecting hoses, water collection container, timer, and platform scale were utilized. The pressure vessel was filled with tap water at a pressure of ≈ 2 atm, and subsequently pressurized to a higher pressure by the high pressure air line. The half-frame or multiple half-frame cooling loop under test was then connected between the high pressure water line and the second

pressure gauge. The hoses were connected to this gauge and the water collection container. Using the timer, test runs of known duration were made and the mass of water collected in the container during the test was determined. From the diameter of the tubing and the data collected during the test, the velocity of the water was calculated. This value was then compared to the velocity which would theoretically produce the required convective film coefficient.

The system pressure drop was also measured and was subtracted from the pressure drop across the cooling path to yield the "cooling loop pressure drop." Using quick disconnect connections to the half-frames and a consistent sequence of operations, the water flow tests provided the hydraulic data which were later used to predict the cooling water requirements for the channel and diffuser.

c. Channel Flow Tests

The water flow tests for the channel consisted of the pressure and flow checking of each of the seventy frames before the final fit-up, the checking of each frame for any flow obstructions after the final fit-up, and the pressure and flow checking of each of thirty-eight cooling paths after the case fabrication and cooling tube attachment. The first of these tests permitted a first approximation of the cooling system design while the last provided final raw data for the final design described in Section II-5.

d. Diffuser Flow Tests

Following the attachment of the interconnecting fittings and nylon tubing to the eighty-eight "half-loops" of the diffuser, pressure and flow checks were made on each of the forty-four cooling paths. The raw data was used to verify the final design (Section II-5).

2. VACUUM TESTS

Proper operation of the lightweight MHD generator demanded a gas tight channel. Even the slightest leak could easily lead to the destruction of the generator because of the pressures and temperatures of the plasma. Therefore, a reliable, effective method to check the gas seals of the channel case following the case curing and sealing operations was required. Because of the tightness of the continuous seam brazing of the diffuser shell joints (see Section III-7) and the fact that the gas static pressure in the diffuser is near atmospheric, only the channel was leak-checked.

The tightness of the case was checked by creating a partial vacuum within the channel and monitoring any changes in pressure with respect to time. A piston type vacuum pump with a capability of evacuating gas from a chamber down to a pressure of 2 Torr, a low pressure gauge with a range of 0 to 50 Torr in 0.2 Torr increments, and flat aluminum plates were connected together. Using RTV silicone rubber as the "in place" gasket, the plates were used to seal off both ends of the channel. One of the plates was modified before use to accommodate the suction line from the pump. An initial run was made to check out the system using a previously fabricated experimental glass/epoxy shell. No problems were encountered.

Because the proper operation of the lightweight channel demanded a leak-free seal, strict criteria for the gas tightness of the case were imposed. The case was required to hold a vacuum below ten Torr for ten minutes.

The plates were connected to the channel and the gas evacuation was initiated. After a few minutes the lowest pressure was achieved, and the suction line was closed off, isolating the channel vacuum from the pump. Several leaks were immediately detected as the gauge needle rose steadily. A few leaks were located at the end plates, but most of the leaks were at the cooling tube end seals.

These leaks were quickly and effectively sealed by applying more RTV silicone rubber. Following a room temperature cure, the gas evacuation was repeated. Only a few leaks remained. After repair the channel was retested and found to be gas tight, as defined by holding a vacuum below ten Torr for ten minutes.

3. AFAPL EXPERIMENTAL TEST PROGRAM

The MHD test program for the lightweight channel/diffuser system was conducted by the Air Force in the AFAPL facility located in Building 71, Area B, Wright-Patterson Air Force Base, Ohio with MLI advice and consultation. The hardware was installed in the facility for testing according to the test plan developed by MLI. During the test program, one hundred twenty-five hot fire tests of average duration of five seconds were conducted. A full series of tests, including thermal, low magnetic field and full power tests, were completed. The test series is to be reported in greater detail in a separate technical report by AFAPL.

a. Facility Description

The overall schematic of the facility is shown in Figure 46. Figure 47 presents the details of the demineralized cooling system used to cool the MHD channel. The descriptions of the reactant feed system, the exhaust system, the magnet system, the control, the instrumentation, and the data acquisition system, and the electrical load and power take-off system have been presented previously and will not be repeated here.^{1,3}

The facility was equipped with a water-cooled load resistor network to provide a main load resistance of 0-32 ohms and air-cooled grading resistor network elements ranging from 0 to 15 ohms. The maximum power dissipation capacity by the facility resistance network was 600 kW.

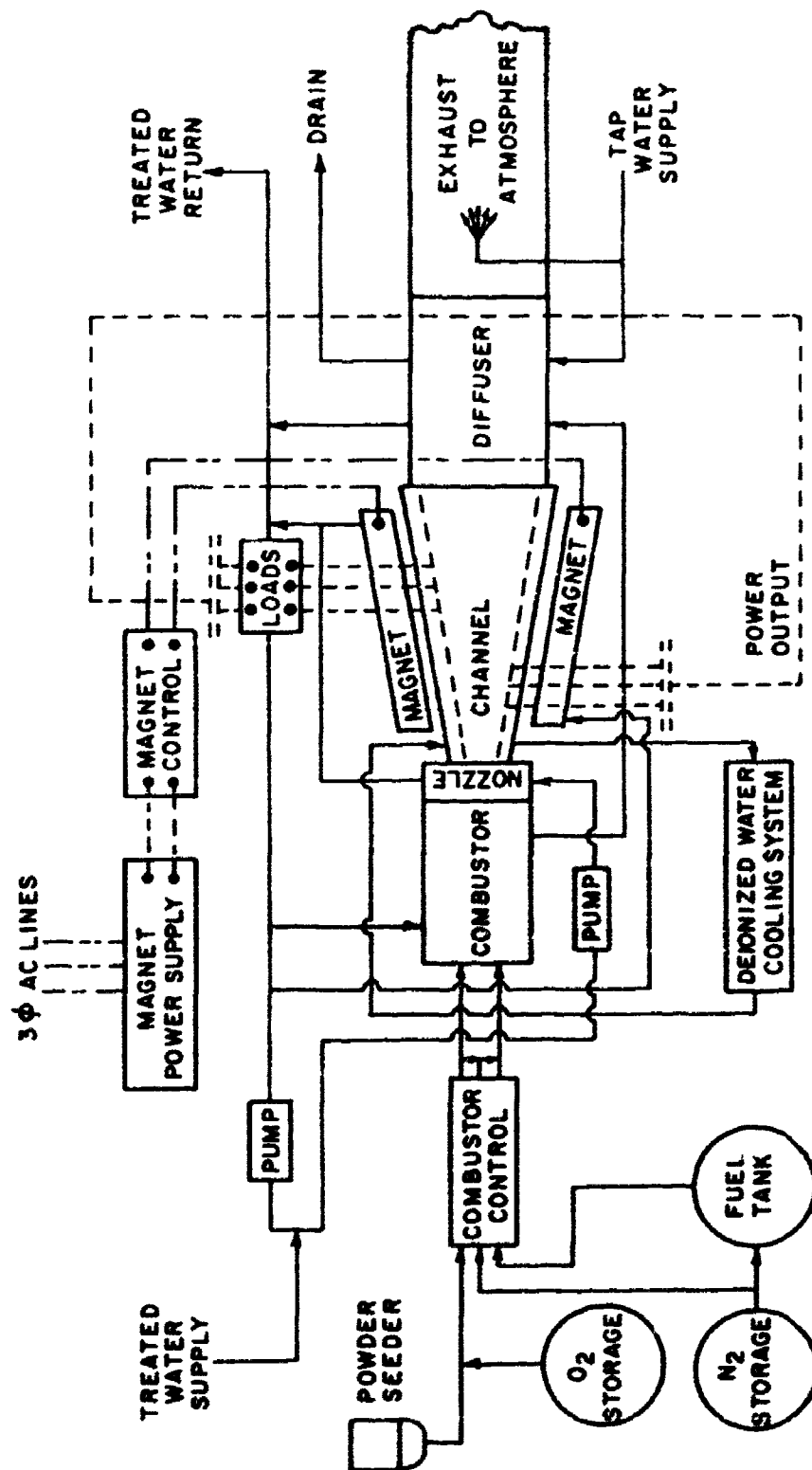


Figure 46. Schematic Illustration of the Major Systems of the AFAPL MHD Generator Facility.

The instrumentation system provided measurements of temperature, pressure, voltage, current, mass flow rate, and vibrations. Two data acquisition systems were available to record the data - a 100 channel, high speed data system with a throughput data rate of 16.7 kHz and a 100 channel low speed data system with a throughput data rate of 40 Hz. These two systems were augmented for this test program by a remote data acquisition unit of the Air Force Flight Dynamics Laboratory to record the accelerometer signals.

The nominal operating conditions of the AFAPL test facility are given in Table 4. The flexibility of the facility operation permitted testing over a range of oxygen/fuel ratios, electrical loads, seed mass flow rates, total mass flow rates, and magnetic fields. Figure 48 shows a photograph of the channel/diffuser system installed in the test facility and ready for testing.

b. Test Plan Summary

The objectives of the lightweight channel test program were to demonstrate 200 kW of electrical power output and to complete a vibration analysis to determine the frequency and amplitude of the channel vibrations. Three types of tests were completed: 1) setup and calibration of the MHD test facility; 2) checkout testing of the MHD generator channel/diffuser system; and 3) MHD generator system performance tests.

The setup and calibration of the MHD test facility included the calibration of the pressure, temperature, mass flow rate, voltage, current, and accelerometer instrumentation. Also included was a combustor test to establish the combustor start up and shut down procedures, the emergency shut down procedures, and the control settings necessary for attaining the proper reactant mass flow rate. A vibration nodal analysis of the lightweight channel was completed at the Air Force Flight Dynamics Laboratory prior to installation in the MHD facility.

TABLE 4. OPERATING CONDITIONS

Reactants

Fuel	Toluene
Oxidizer	Gaseous O ₂
Seed	Powdered Cs ₂ CO ₃

Reactant Mass Flow Rate 0.3 kg/sec

Combustor Stagnation Pressure 10.0 atm Nominal

Channel Inlet Conditions

Mach No.	2.1
Static Temperature	2700 K
Static Pressure	0.95 atm

Peak Magnetic Field 2.3 Tesla

O/F Ratio Stoichiometric with range of 2.7 - 3.1

Seed Mass Flow Rate 4-8% of Reactant Mass Flow Rate

Start-Up Time < 1 sec

Mode of Operation Pulse or Continuous

Plasma Conductivity 10-20 mhos/m

Channel Cooling System 680 liters/min @ 7.8 atm (maximum output)

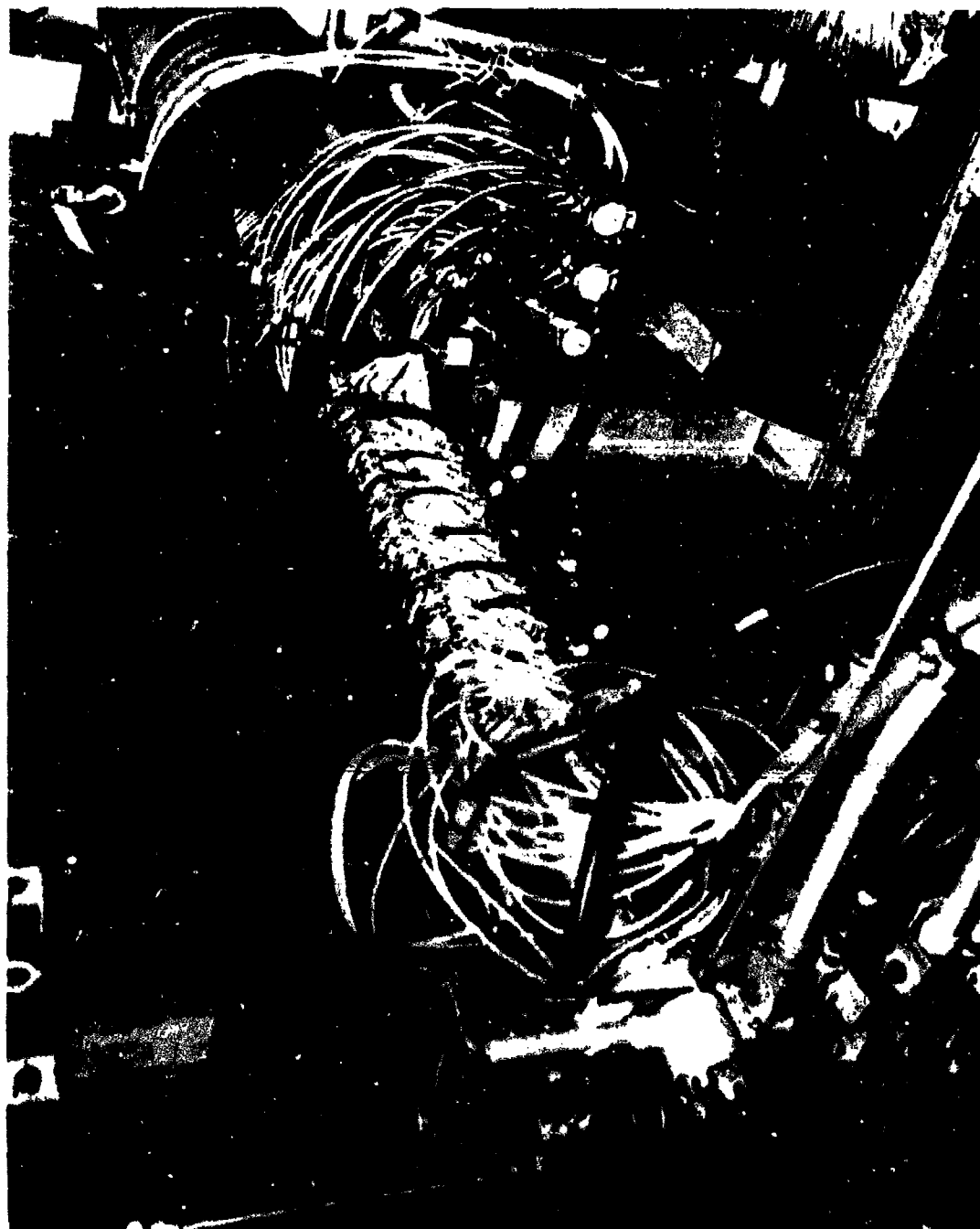


Figure 48. Lightweight Channel/Diffuser System Installed at the AFAPL MHD Facility.

The channel checkout tests of the MHD channel/diffuser were completed to establish the cooling water flow rates, the wall heat transfer rates, and the gas dynamic performance of the channel. Temperature, pressure, mass flow rate, and vibration data were recorded. A performance evaluation of the channel and diffuser cooling system, which compared the calculated predictions with the actual experimental values, was completed. This analysis also evaluated the overall performance and operating characteristics of the channel/diffuser system and verified that the components were properly installed and ready for the MHD test program.

The MHD channel/diffuser system performance tests were completed to demonstrate the feasibility of the construction techniques used to fabricate the channel/diffuser system and to verify the predicted performance levels. The first performance test was conducted at a reduced magnetic field to verify that the electrical circuit connections to each of the electrode frames were correct. After the low magnetic field test was successful, the design power level test program was completed.

c. Thermal Tests

Several thermal test runs were conducted to insure that adequate cooling water was available and that all control and operating systems were functioning properly. Four electrode frame cooling loops were instrumented with thermocouples. This instrumentation provided the heat flux at several axial locations in the channel. Figure 49 shows the measured axial heat flux distribution for the lightweight channel as well as other channels operated at the AFAPL facility.

During these thermal tests measurements were made of the static pressure distribution with no magnetic field applied. Figure 50 shows the pressure distribution for a mass flow rate of 0.6 kg/sec. The figure shows that the pressure recovery started in the diffuser inlet duct section rather than in the electrode region of the channel. This, of course, indicated a more favorable pressure recovery condition and insured channel/diffuser system operation near the design levels.

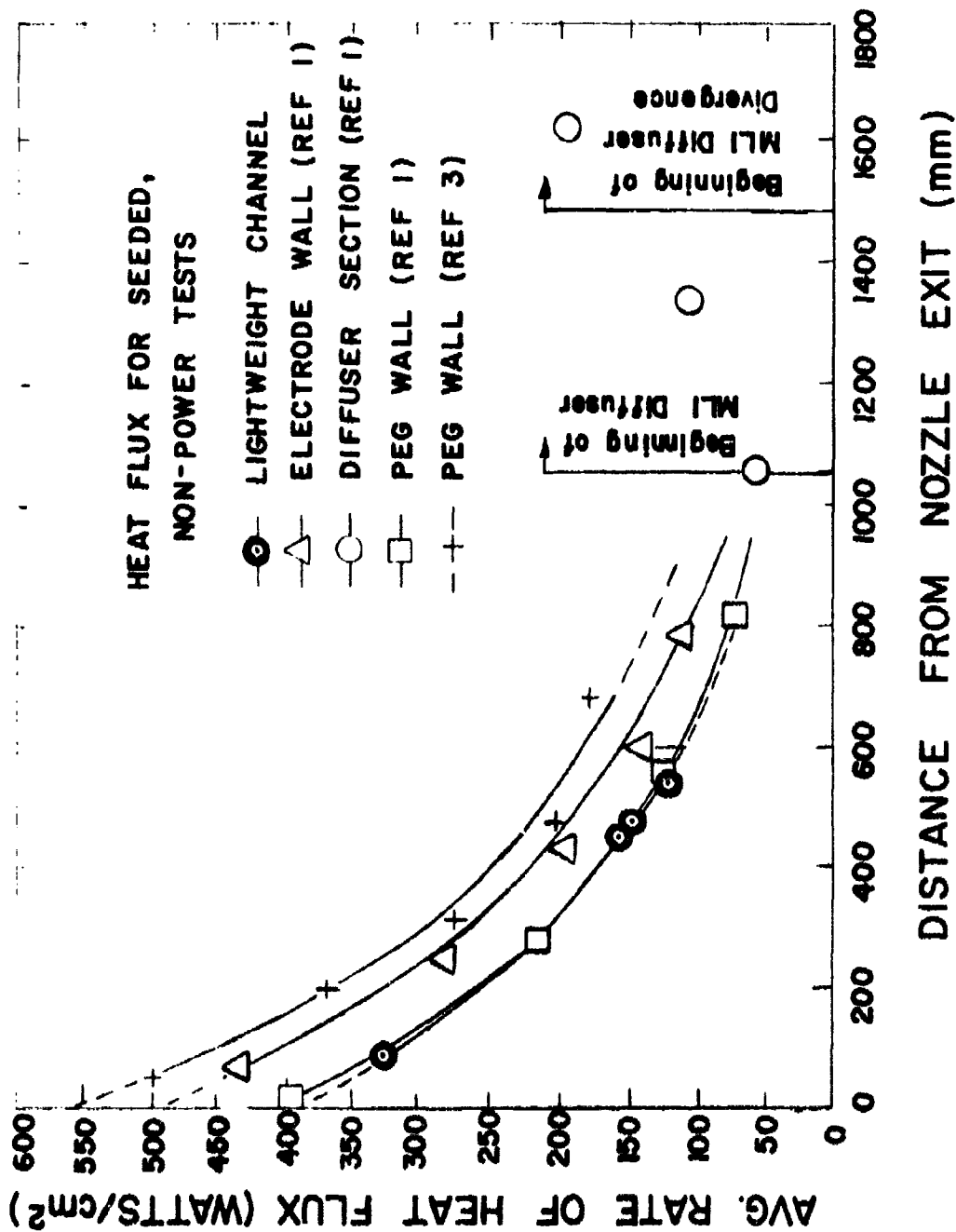


Figure 49. Axial Heat Flux Distribution for Test LWC 003.

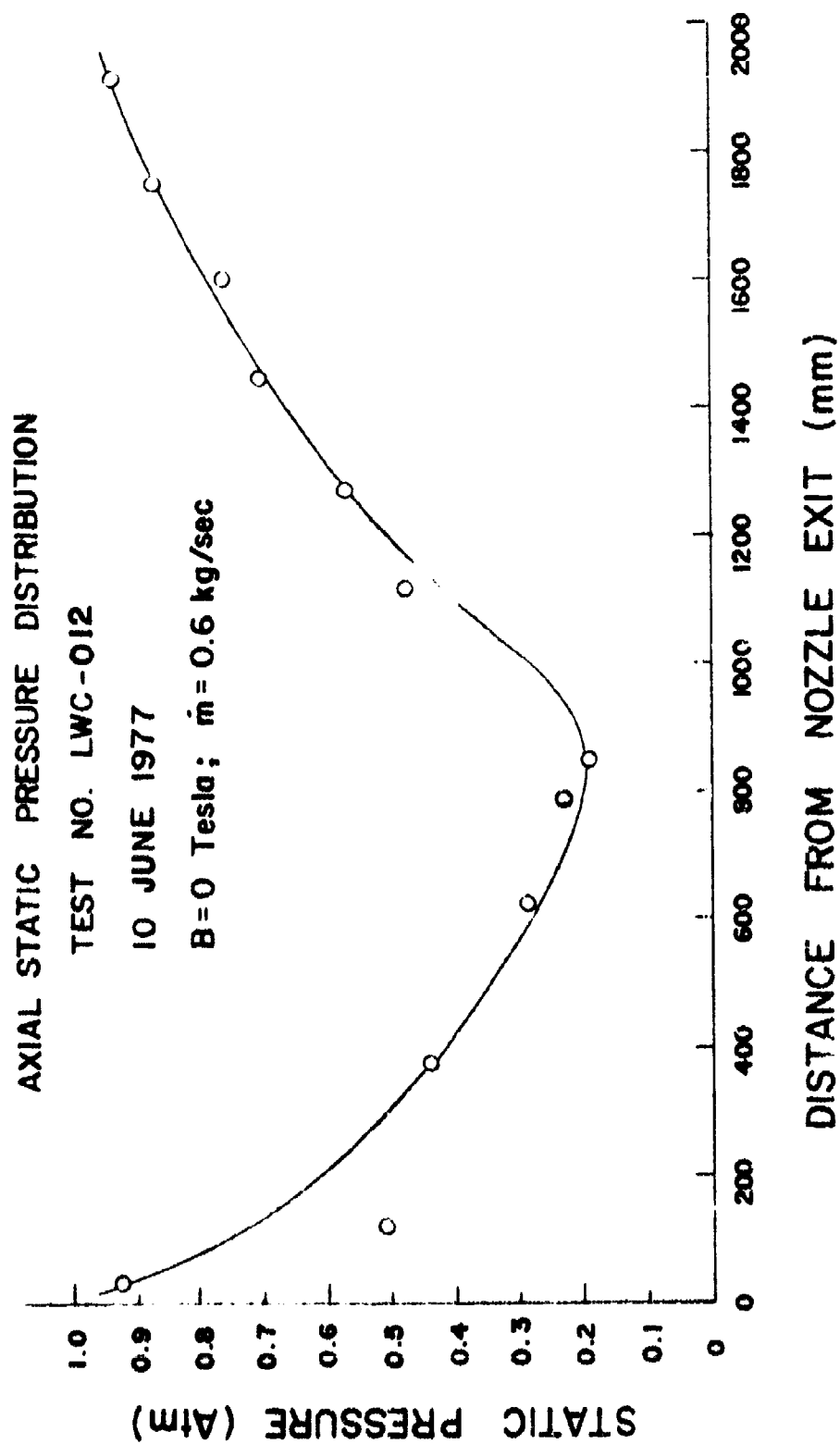


Figure 50. Axial Static Pressure Distribution for Test LWC 012.

Vibration measurements were also made during this initial thermal test. Additional vibration measurements were made throughout the test program during the non-power tests. The test description and the results of these tests are presented in Section IV-3.f.

d. Low Magnetic Field Tests

The initial low magnetic field power generation test was performed immediately after the conclusion of the thermal tests. This test was completed to check out the electrical performance of the MHD channel/diffuser system at low magnetic field levels. The magnet coil current was 400 A, which produced a peak magnetic field of 1.6 Tesla. The run duration was 4 seconds with a mass flow rate of 0.6 kg/sec. The load electrical power output for this test was 73 kW.

The electrical power takeoff connections used for the MHD power generation tests are shown in Figure 51. Twenty-four of the seventy electrodes were used as the power takeoff electrodes. The values of the grading resistors ranged from 1.0 to 10.6 ohms at the channel entrance and from 0.6 to 7.0 ohms at the channel exit. The values of these resistors were selected so that the generator performance was satisfactory in the end regions of the channel for these particular loading conditions.

More detailed results for this test are shown in the next two figures. Figure 52 shows the axial voltage distribution along the axial centerline. Because the diagonal conducting wall channel did not have any split frames, no transverse current measurements were possible. Likewise, transverse voltage measurements were also not possible. The axial static pressure distribution in the channel and diffuser is shown in Figure 53.

e. Power Tests

The full power generation test program was performed immediately after the conclusion of the thermal tests. This part of the testing program was significantly influenced by two events that occurred during the test program. These events and their impact are discussed below:



Figure 51. Schematic of the Electrical Wiring Diagram.

AXIAL VOLTAGE DISTRIBUTION

TEST NO. LWC-007

10 MAY 1977

$B = 1.6$ Tesla; $\dot{m} = 0.6$ kg/sec

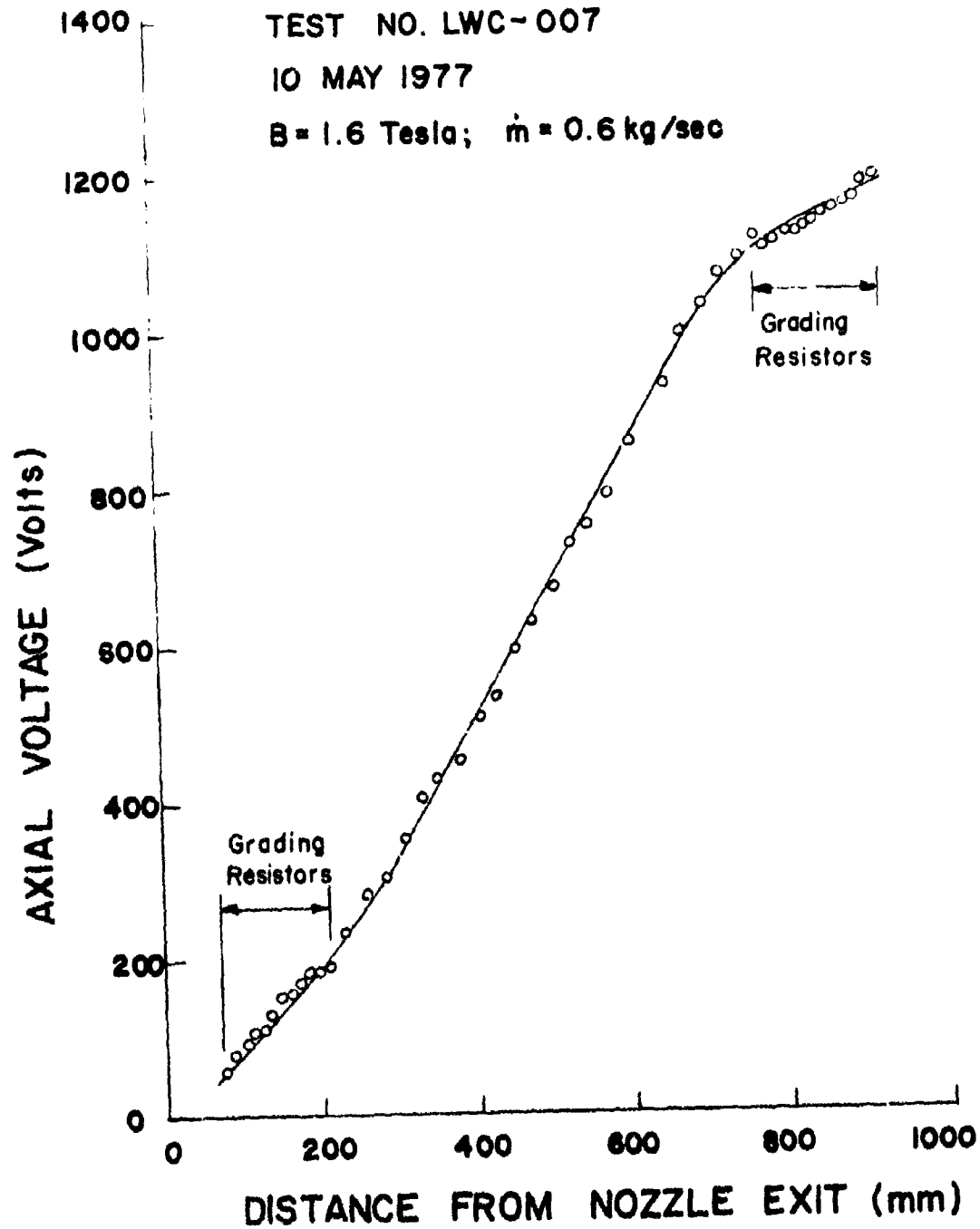


Figure 52. Axial Voltage Distribution for Test LWC 007.

AXIAL STATIC PRESSURE DISTRIBUTION

TEST NO. LWC - 007

10 MAY 1977

$B = 1.6$ Tesla; $\dot{m} = 0.6$ kg/sec

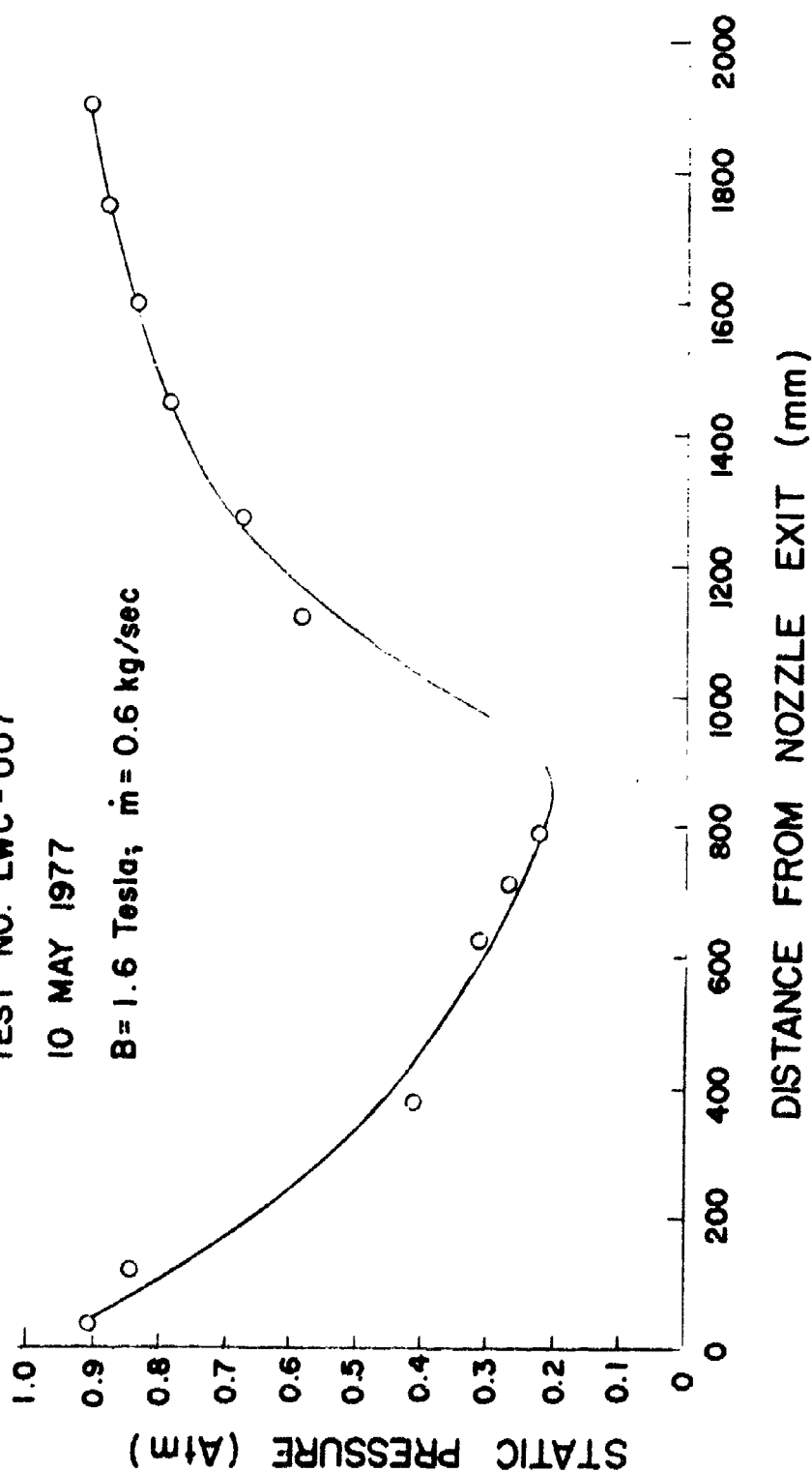


Figure 53. Static Pressure Distribution for Test LWC 007.

i) During the initial full power test, an electrical load bank failure occurred causing the channel to operate into a nearly short circuit condition for about two seconds. Since the electrical connections for the test were established for a load resistance of 10.6 ohms, the short circuit condition provided the potential for severely overloading some electrode pairs. This condition could have severely damaged these electrode pairs. After the load bank was repaired, a second full power test was attempted. Water leakage around the load bank during this test also caused a short circuit similar to the previous test.

ii) After the initial set of testing was completed, a complete review of the apparent variances in this test series was completed. This review covered four areas: seed system, fuel/oxidizer system, electrical connections, and the data system.

During the initial test series the full electrical output was not obtained until two seconds after the seed flow was initiated. This delay was attributed to the cesium carbonate grain size and seeder inertia. Previous tests had been conducted with a mix of grain sizes below a maximum upper limit. This test series was conducted with the cesium carbonate filtered between a maximum and a minimum grain size. By using a single screen to permit retention of about half very fine grains, the fast startup (less than 0.25 sec) capability was retained. The reason for this result was attributed to the fact that during the seeder startup transient the small grains moved more quickly and easily through the mechanical seeder.

A view of the fuel/oxidizer system revealed a defective fuel drain valve which caused the fuel flow to be substantially below the planned fuel flow rate. This valve was replaced and the fuel flow rate measuring system was recalibrated.

The electrical connections were reviewed in detail to establish that all electrical circuits were correctly connected. During this review two non-adjacent electrode frames were discovered to have been inadvertently connected while setting up for some vibration test measurements.

The subsequent test program that was conducted after these test facility problems were resolved established the required generator electrical performance of 200 kW. The test conditions were the nominal operating conditions of the test facility, as shown in Table 4. The total mass flow rate was 0.6 kg/sec with a stoichiometric combustion chamber mixture ratio. The cesium carbonate mass flow rate varied from 5-8% of the total mass flow rate. The peak magnetic field was 2.3 Tesla; Figure 54 shows the axial magnetic field distribution. The schematic of the electrical wiring diagram for the lightweight MHD generator performance testing is shown in Figure 51.

The test to date program consisted of 125 power and non-power test runs. Figure 55 shows the axial voltage distribution along the axial centerline for Run No. 122, which produced 195 kW of electrical power through the main load resistor. Approximately 20 kW additional electrical power was dissipated in the grading resistors. This power level was obtained at the nominal flow condition and stoichiometric mixture ratio. A comparison of the axial pressure distribution for a power and non-power run is shown in Figure 56. A photograph of the interior of the channel at the conclusion of the test program is shown in Figure 57. While the interior surfaces showed some evidence of erosion, the design power level of the channel was still obtainable at this point in the test program. At this writing the channel is still being operated by AFAPL to observe its life cycle.

f. Vibration Measurements

During sixteen non-power tests, vibration measurements were made by the Air Force Flight Dynamics Laboratory. The channel wall accelerations were sensed by twelve accelerometers, which were located as shown in Figure 58. After the

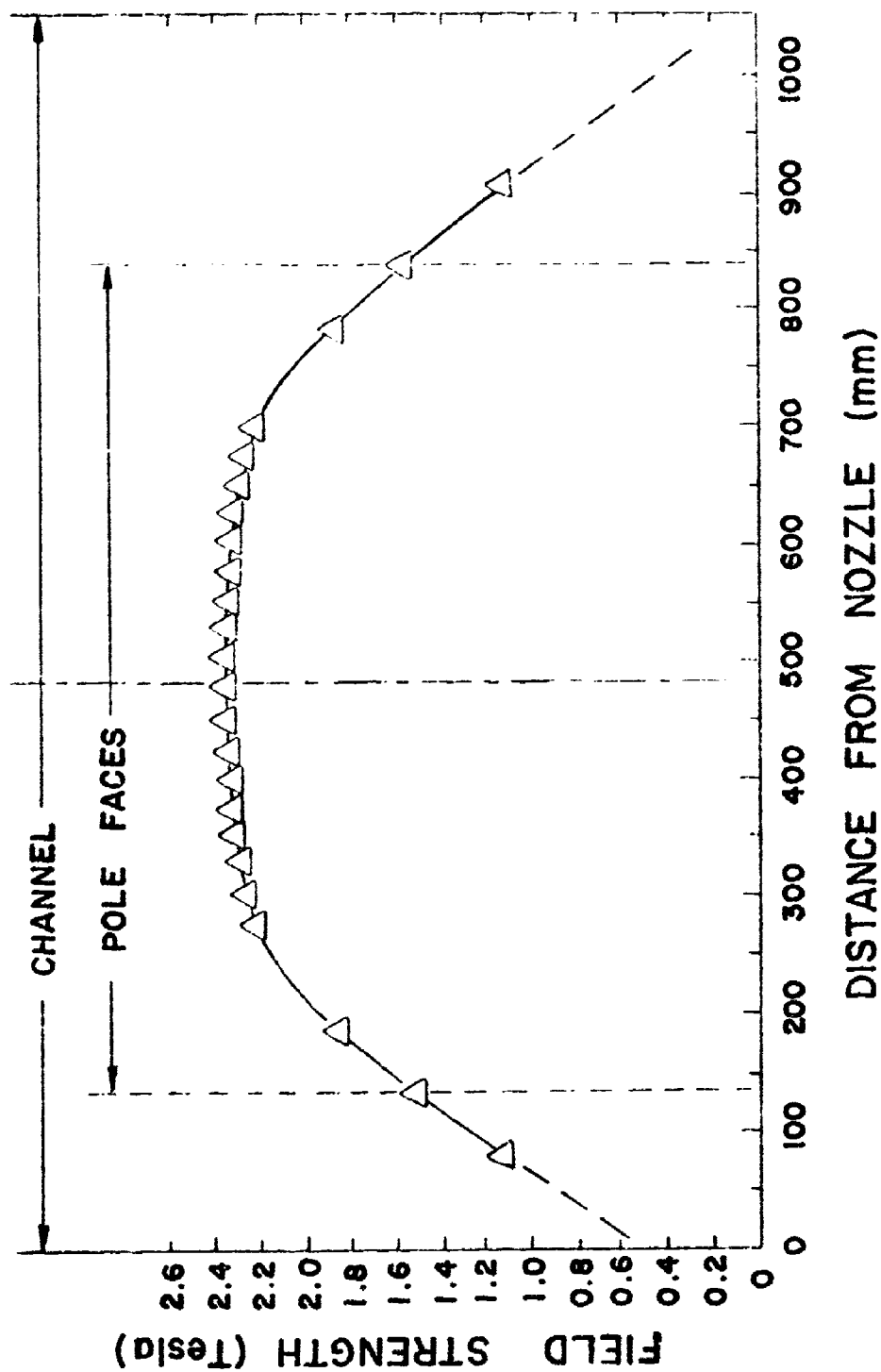


Figure 84. Magnetic Field Distribution for 2.3 Tesla Center Field for the AFAPL Magnet.

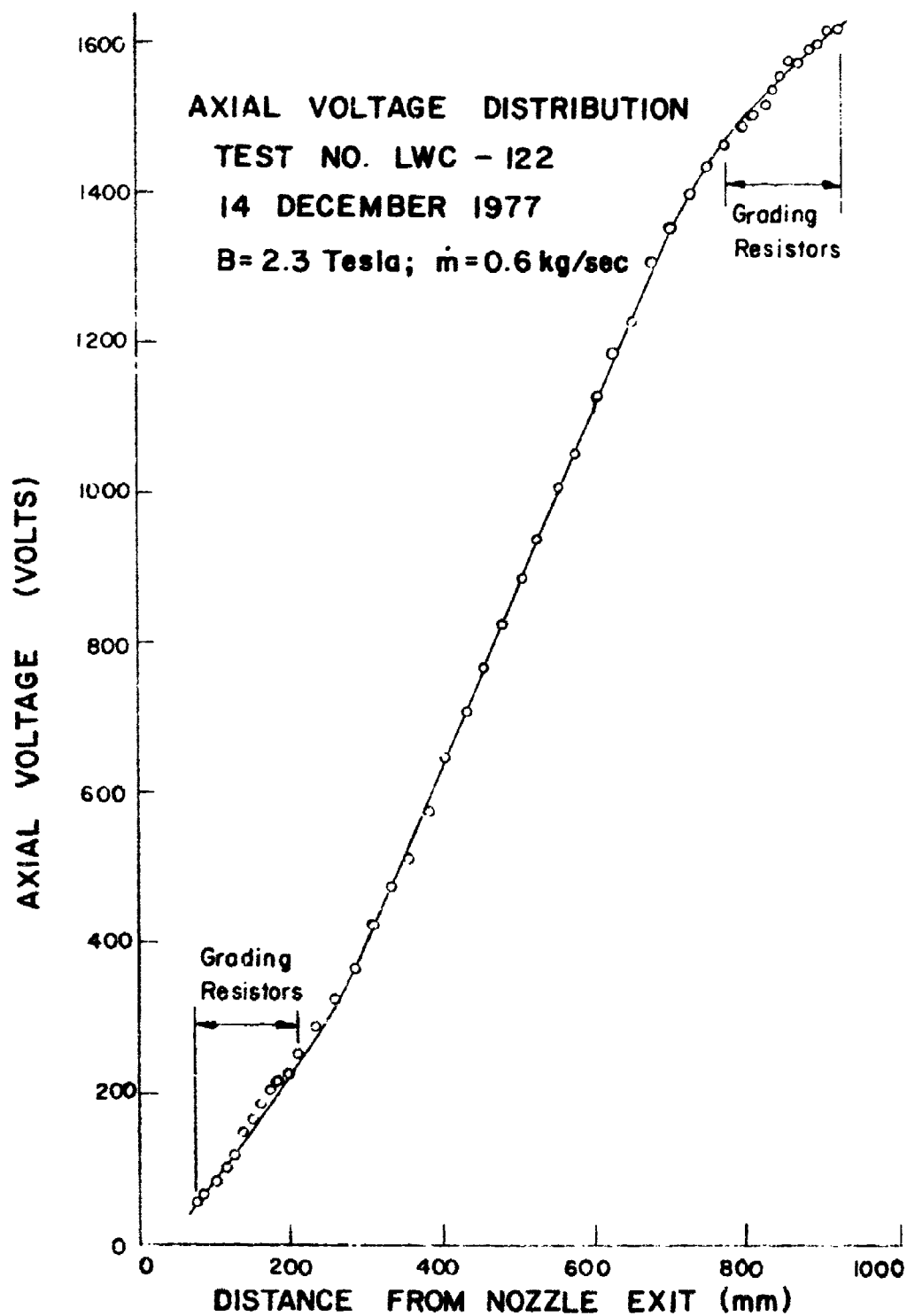


Figure 55. Axial Voltage Distribution for Test LWC 122.

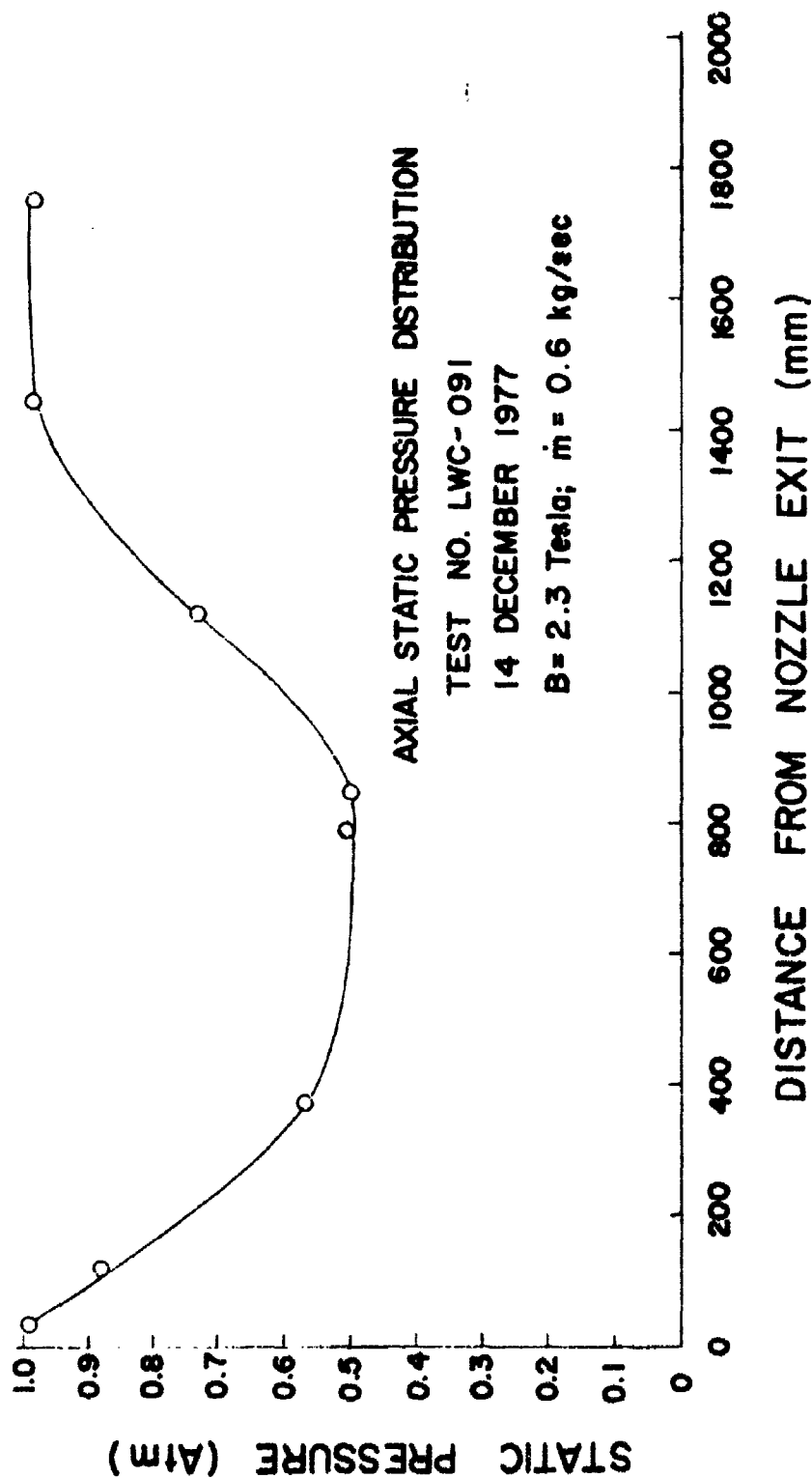


Figure 56. Axial Pressure Distribution for Test LWC 091.



Figure 57. Interior of Lightweight Channel at Test Program Conclusion.

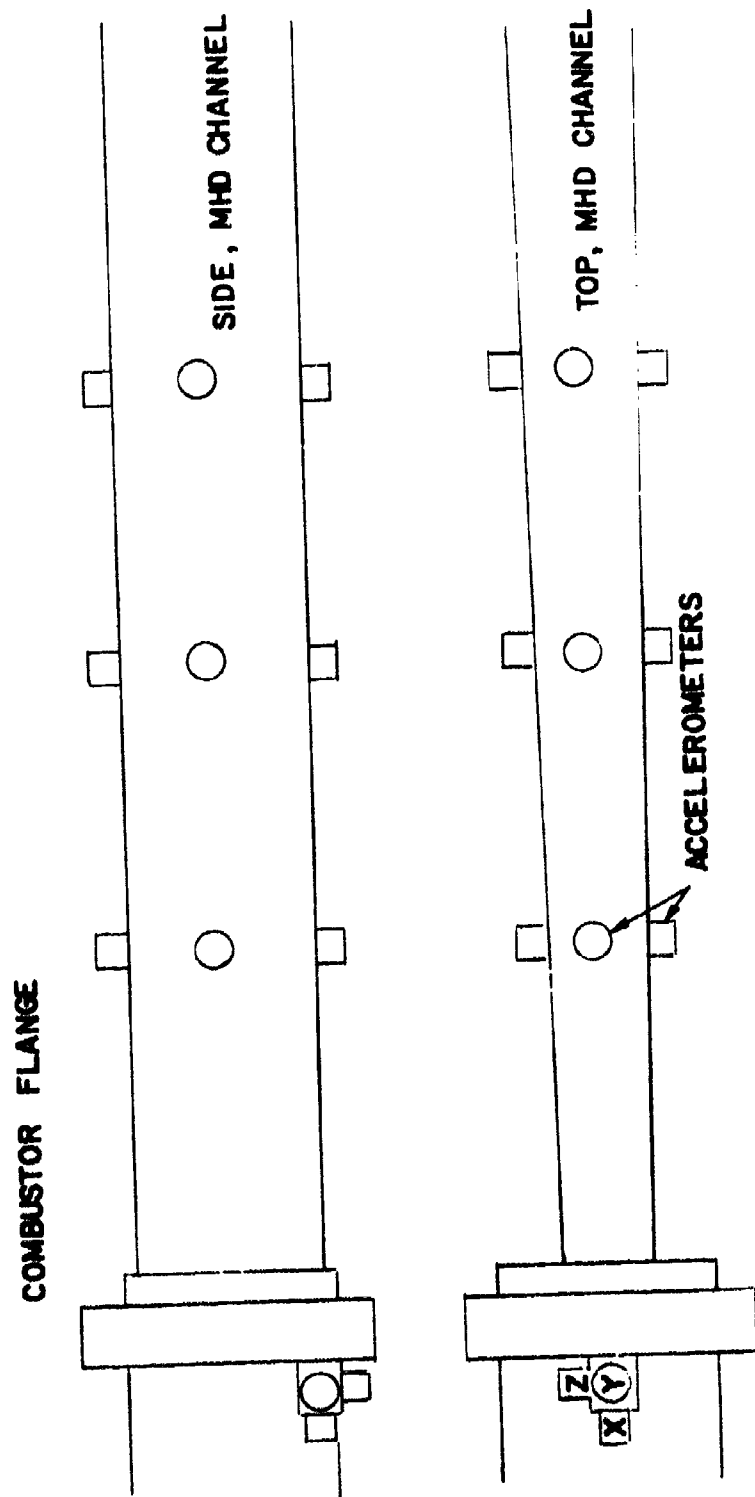


Figure 58. Schematic of Accelerometer Placement.

thirteenth run, additional x, y, and z accelerometers were mounted on the combustor outlet flange to sense the motion near the inlet end of the channel. Using Fast Fourier Transform analysis, power spectral density values were computed over the frequency range of 0 to 500 Hz, with a resolution of 1.22 Hz for each spectrum.

The highest measured value of spectral energy density was $0.06 \text{ g}^2/\text{Hz}$ at 53 Hz. Spectra of the various runs were very similar, and a typical spectra is shown in Figure 59. This result compares closely to the frequencies of 45 Hz and 115 Hz determined in the Air Force Flight Dynamics Laboratory nodal analysis laboratory and to the predicted resonant natural frequency of 56 Hz. The overall rms acceleration was also computed. The highest overall acceleration was 0.8 g. In order to assess the effect of the continued test program on the vibration responses, the data were analyzed at selected times over a long series of hot fire tests. No significant changes in the frequency or intensity of any mode were apparent nor was any change in the damping characteristics evident. The individual accelerometer frequency responses show several peaks which could be interpreted as overall vibration modes of the channel.

In order to distinguish between the bending and the breathing modes, the accelerometer signals on the opposing sides of the channel were combined by addition and subtraction. A typical result is shown in Figure 60 (addition) and Figure 61 (subtraction). No correlation between the motions of the opposing sides of the channel was evident. This result was attributed to highly damped structure of visco-elastic fiberglass coating. Hence, the four walls moved more or less independently.

The Air Force Flight Dynamics Laboratory completed additional data analysis to estimate the stress levels and thus the expected fatigue life of the structure. Each wall of the channel was assumed to be a beam with pinned ends, and each spectral peak was considered to be a measure of the sinusoidal motion which represented a mode of the structure. Based on these assumptions, an rms stress

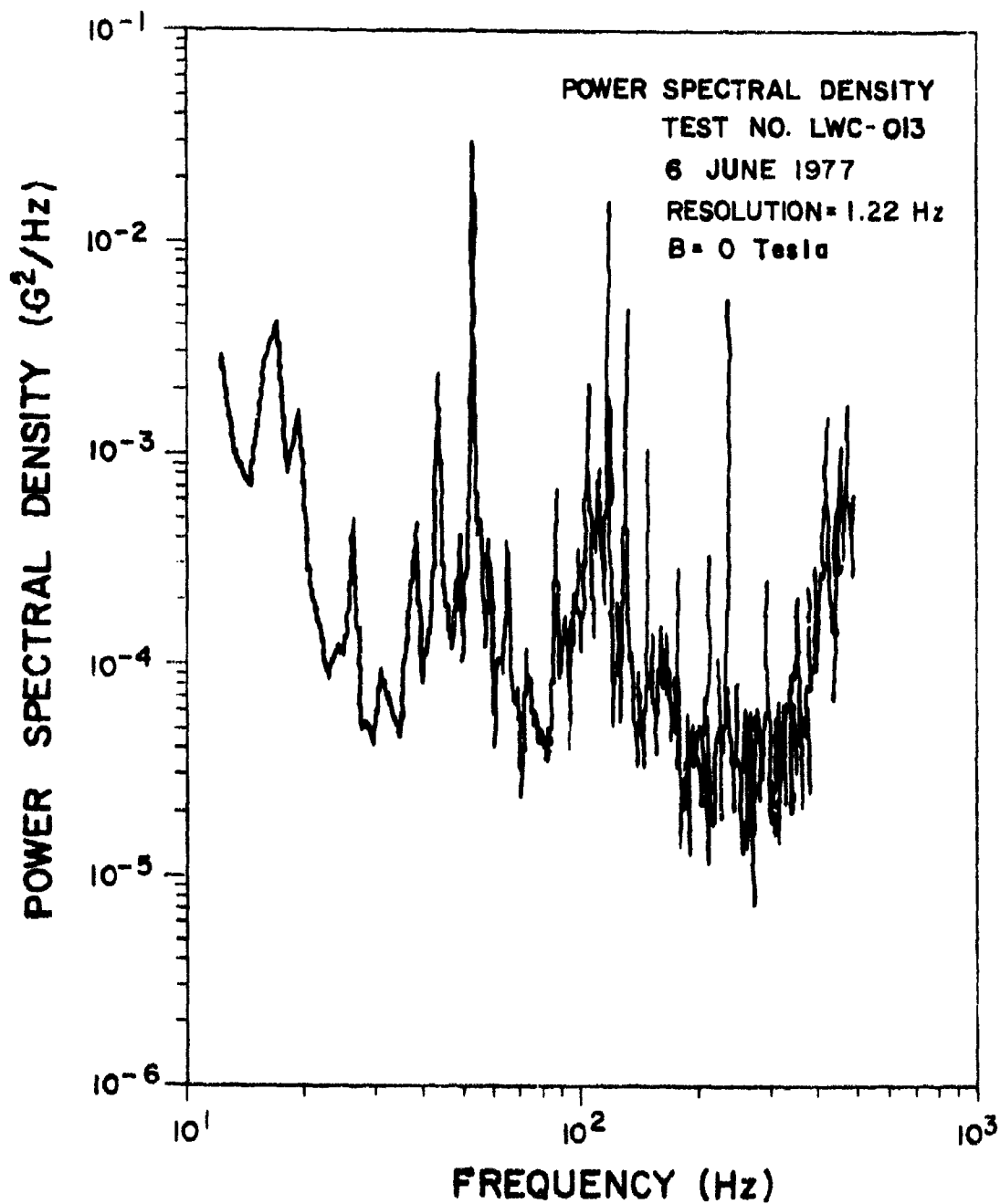


Figure 59. Power Spectral Density for Test LWC 013.

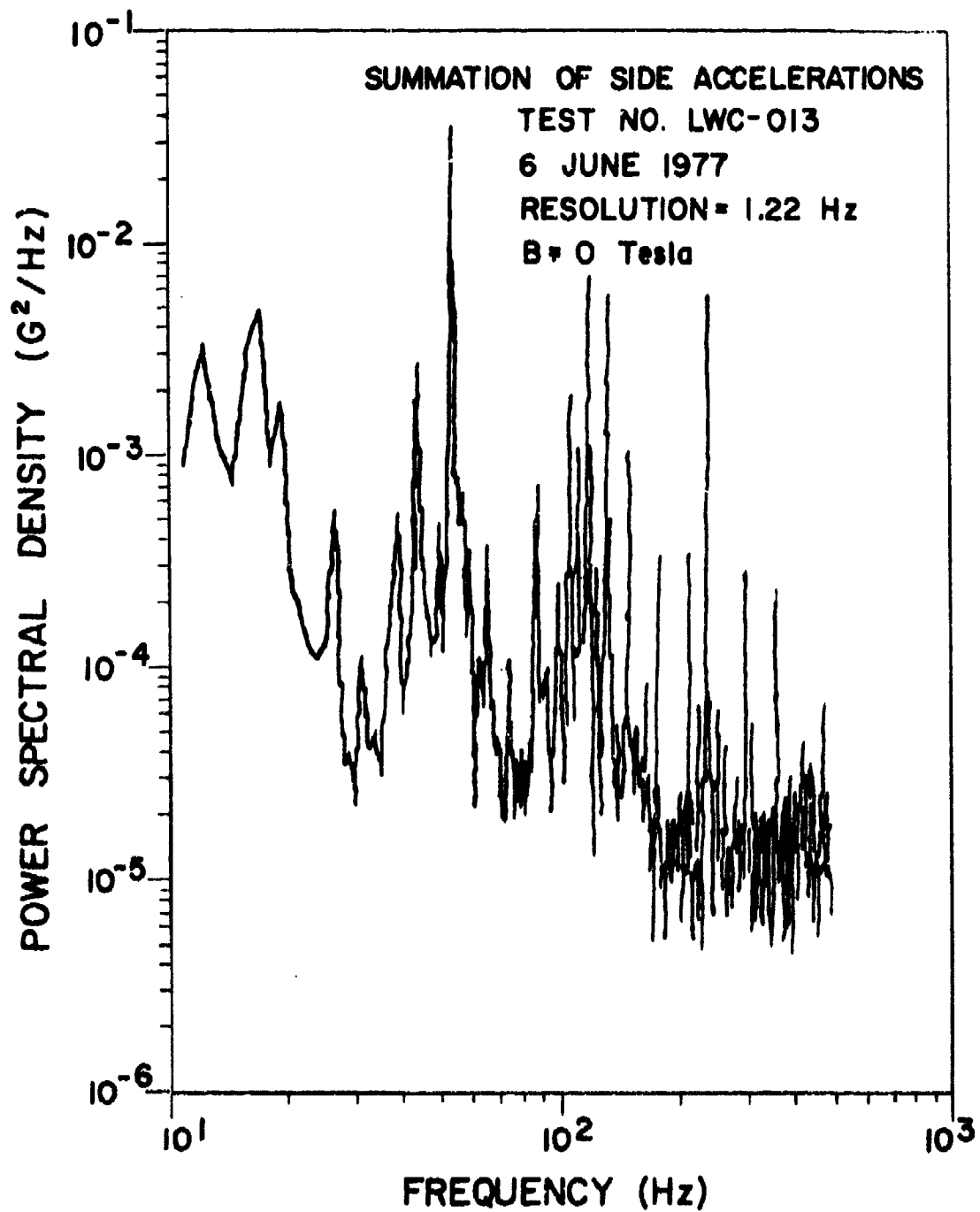


Figure 80. Summation Power Spectral Density for Test LWC 013.

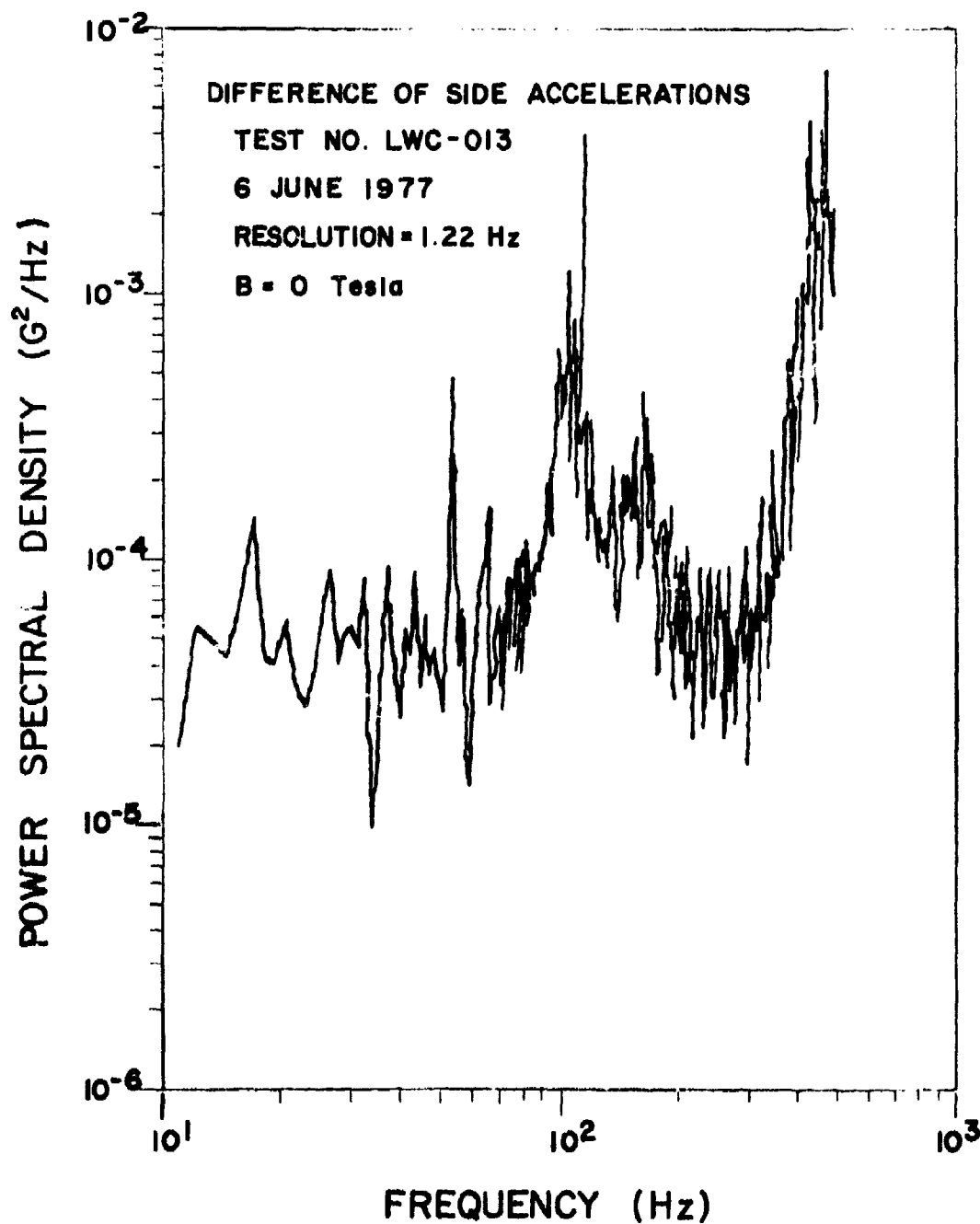


Figure 61. Difference Power Spectral Density for Test LWC 013.

level was calculated from the spectral peak accelerations. Depending upon the Young's modulus of elasticity used for the fiberglass composite structure, the channel fatigue life was estimated to be between 190 sec and 5 hours. This range of fatigue life can be reduced by a better estimate of the Young's modulus. Since the channel has completed over 600 sec of operation without any degradation of the channel wall structure, the channel has exceeded the estimated minimum life.

SECTION V

RELIABILITY AND MAINTAINABILITY ANALYSIS

1. INTRODUCTION

The purpose of the Reliability and Maintainability Analysis (RMA) was to eliminate or minimize the probability of occurrence of the failure modes that could have affected the system performance or operation. The channel/diffuser RMA was given careful consideration and study at all of the strategic phases of the design and fabrication efforts that occurred during this program. Although no testing was performed specifically for the purpose of the RMA, the channel/diffuser system tests have provided actual test information relating to this analysis.

In the subsequent sections of this chapter, each component is identified and analyzed with respect to its function, failure mode, failure effects, probability of failure, maintainability provisions and maintenance frequency. The results of this analysis, arranged in a criteria matrix, are presented in both qualitative and numerical form. The probability of failure, based on the design system operation within the performance requirements of the contract, was given an estimated numerical rating of percent probability of failure. A rating less than 5% implied that the failure was not likely to occur within the design life of the component while a rating greater than 95% implied that the failure was most likely to occur.

Since the channel/diffuser system has successfully completed 125 hot fire tests of average duration of five seconds, the RMA conducted at the conclusion of the test program was based on the actual test results. While the actual test sequences were not identical to the original design specifications, the total run time and the number of thermal cycles exceeded the initial channel/diffuser system design specifications. During the test program no total component failures were experienced.

However, the performance of some of the components degraded with use. This degradation was reflected in the RMA. For example, a 15% degradation in the performance of a component was shown in the RMA as a 15% probability of failure.

The channel/diffuser system components were grouped according to their functions: electrode system, cooling system, gas seals, channel and diffuser cases, and instrumentation and electrical. Each subsection presents the results of the RMA for each of the five system components.

2. ELECTRODE SYSTEM

The electrode system components were the electrode frame assemblies, the electrode screen, the electrode ceramic, and the insulator ceramic. Of these the electrode ceramic and the insulator ceramic have the highest probability of failure of the electrode system components. The insulator ceramic was particularly vulnerable because of the ceramic susceptibility to cesium carbonate penetration, and hence, the ceramic became more of an electrical conductor than was desired. The electrode ceramic also was susceptible to the same type of damage from impurities, thus decreasing the performance of the electrode ceramic. Table 5 provides a summary of the results of the RMA for the electrode system.

3. COOLING SYSTEM

The cooling system components were the water manifolds for the channel and diffuser, the cooling tubes for the channel electrodes, the cooling tubes for the diffuser wall, and the water hoses for the channel and diffuser. Of these the water hoses and connections for the channel and diffuser have the highest probability of failure of the cooling system components. The problem was most severe at the connections where minor leaks could occur after prolonged usage. Table 6 provides a summary of the results of the RMA for the cooling system.

TABLE 5. ELECTRODE SYSTEM RMA

Component Identification	Component Function	Failure Mode	Failure Effects	Probability of Failure	Maintainability Provisions	Maintenance Frequency
Electrode Frame Assemblies	Extract energy from plasma	Burnout because of excessive temperatures	Decrease power output	< 5%	Cut through case and replace frame	Seldom
Electrode Screen	Conduct electric current and heat	Thermal erosion	Decrease current flow	< 5%	Require re-placement of electrode frame	Seldom
Electrode Ceramic	Electric current collector and emitter	Spalling and erosion	Increase Electrode voltage drop	15%	Cast replacement ceramic from inside of channel	Periodic with operation, as required
Insulator Ceramic	Prevent electric current flow between frames	Spalling, erosion and contamination by conductive seed and moisture	Decrease output voltage	15%	Cast replacement ceramic from inside of channel	Periodic with operation, as required

TABLE 6. COOLING SYSTEM RMA

Component Identification	Component Function	Failure Mode	Failure Effects	Probability of Failure	Maintainability Provisions	Maintenance Frequency
Water Manifolds, Channel and Diffuser	Distribute and collect channel/diffuser coolant	None	N/A	0%	N/A	N/A
Cooling Tubes, Channel Electrodes	Control electrode temperature	Leaks	Degrade performance Possible electrical short to ground.	< 5%	Repair or replace	Seldom
		Blockage	Overheating	< 5%	Remove blockage	Seldom
Cooling Tubes, Diffuser Wall	Control diffuser wall temperature	Leaks	Possible electrical short to ground.	< 5%	Repair or replace external tubes	Seldom
		Blockage	Overheating and melting tube to wall solder joint.	< 5%	Remove blockage	Seldom
Water Hoses, Channel and Diffuser	Transfer coolant water between manifold and channel and diffuser	Leaks at connections after prolonged operation, blockage	Component destruction through burnout, if coolant lost or blocked.	< 5% with proper operation	Tighten or replace hoses and/or fittings	Seldom

4. GAS SEALS

The gas sealing system components were the nozzle/channel interface seal, the channel/diffuser interface seal, and the channel cooling tube gas seals. The probability of failure for each of these three components was approximately equal, and if properly installed, failure was not likely to occur during the design life. After prolonged periods of operation, leaks may develop from the effects of repeated thermal and mechanical cycling. Table 7 provides a summary of the results of the RMA for the gas sealing system.

5. CHANNEL AND DIFFUSER CASES

The case system components were the composite channel case and the diffuser shell. Within the design cycle life neither component was likely to fail. A summary of the results of the RMA for the channel and diffuser case system is given in Table 8.

6. INSTRUMENTATION AND ELECTRICAL

The instrumentation and electrical system components were the accelerometers, the channel and diffuser pressure transducers, the channel and diffuser static pressure taps, the channel case and cooling water thermocouples, and the electrical wiring. Of these the channel and diffuser pressure taps and the channel case and cooling water thermocouples had the highest probability of failure of the instrumentation and electrical system components. The static pressure taps were particularly vulnerable to blockage from the products of combustion. The blockage was easily removed, and the only loss was the test data from that pressure transducer for only the tests conducted while the blockage was present. The thermocouples may also fail because of overheating or the breakage of the wire leadouts. These thermocouples were easily disconnected and replaced by a new one whenever a failure occurs. Table 9 provides a summary of the results of the RMA for the instrumentation and electrical system.

TABLE 7. GAS SEALS RMA

Component Identification	Component Function	Failure Mode	Failure Effects	Probability of Failure	Maintainability Provisions	Maintenance Frequency
Interface Seal, Nozzle/Channel	Prevent leakage of pressurized hot gas	Leaks may occur after prolonged operation from the effects of temperature, pressure, and thermal expansion	Hot gas might degrade composite channel case and damage adjacent non-metallic components.	< 5% (if properly applied at assembly)	Reassemble channel to nozzle with new application of silicone rubber sealant	Very low
Interface Seal, Channel/Diffuser	Prevent entrance of atmospheric air	Leaks may occur after prolonged operation from the effects of temperature, pressure, and thermal expansion	Substantial air leakage into gas flow stream would degrade generator performance and decrease output	< 5% (if properly applied at assembly)	Reassemble diffuser to channel with new application of silicone rubber sealant	Very low
Gas Seals, Channel Cooling Tubes	Prevent gas leakage	Leaks may occur after prolonged operation from the effects of temperature, pressure, and thermal expansion	Degrade performance, damage adjacent non-metallic components	< 5%	Reapply silicone rubber to repair seals	Seldom

TABLE 8. CHANNEL AND DIFFUSER CASES RMLA

Component Identification	Component Function	Failure Mode	Failure Effects	Probability of Failure	Maintainability Provisions	Maintenance Frequency
Composite Case, Channel	Main structural member of channel and primary pressure vessel	Progressive cracking with extended number of run cycles	Loss of structural integrity	< 1% (within the design number of cycles)	Fiberglass-epoxy composite is readily repaired	Seldom
Shell, Diffuser	Main structural member of diffuser and primary pressure vessel	Burnout because of localized thermal problem (e.g. cooling tube blockage)	Decrease power output	< 1% (within the design number of cycles)	Out away RTU blanket and ceramic felt, repair burned area, install new felt and RTV.	Seldom

TABLE 9. INSTRUMENTATION AND ELECTRICAL RMA

Component Identification	Component Function	Failure Mode	Failure Effects	Probability of Failure	Maintainability Provisions	Maintenance Frequency
Accelerometer	Measure vibrations imparted to the case	Overheating because of localized thermal problem	Loss of measurement	< 1% (if properly installed and operated)	Replace transducer	Seldom
Pressure Transducers, Channel and Diffuser	Measure gas pressure	Most likely mode: mechanical abuse resulting in external damage	Loss of measurement	< 1% (if properly installed and operated)	Replace transducer	Seldom
Pressure Taps, Channel and Diffuser	Conduct pressure pulse to transducer	Blockage from products of operation	Loss of pressure measurement	40%	Remove blockage with flexible probe	As Required
Thermocouples, Channel Case and Cooling Water	Measure temperature of case and cooling water	Burnout because of excessive temperatures or lead breakage because of abuse	Loss of measurement	10%	Remove and replace thermocouple, or disconnect leads and install a replacement nearby	Low
Electrical	Conducts electrical current from frames to load bank	Overheating because of electrical current overload	Loss of output power	< 1% (if properly sized and installed)	Verify proper connections and installation	Low

SECTION VI

CONCLUSIONS AND RECOMMENDATIONS

In this MHD development program the feasibility of the novel lightweight channel/diffuser design and fabrication techniques have been successfully demonstrated. This novel channel concept has successfully completed over 125 hot fire tests and produced, during test number 122, over 200 kW of total electrical output power. This result clearly demonstrated the durability of the channel/diffuser system. The data from the vibration analysis have clearly indicated no degradation in the filament wound, epoxy coated fiberglass shell as a structural member or pressure vessel. During the test program the generator was also operated successfully at several off-design conditions. With respect to performance, no serious degradation of the channel occurred as a result of this off-design operation.

The results of this channel development program have provided the basis for a continuing effort in the development of lightweight, high performance MHD generator development. Another development program underway at the present time has provided the next step in this evolution - the design of MHD hardware for multi-megawatt electrical output power levels.¹⁴ The technical effort of that activity can eventually lead to compact, transportable MHD generator systems capable of producing tens of megawatts of electrical output power. Such power levels will result in an increase in the pertinent performance parameters such as enthalpy extraction ratio, volumetric efficiency, and specific power density, and these increases are not unreasonable extrapolations of the results of the current programs.

¹⁴ AF Contract F33615-76-C-2104, "High Power MHD System."

Along with this channel development effort, parallel programs leading to the development of lightweight superconducting magnets, lightweight power conditioning systems, and advanced electrode/insulator systems should be implemented. These programs would be implemented to fully develop the potential of the lightweight, transportable, high power MHD generator power supply systems.

APPENDIX

SAFETY AND HAZARDS ANALYSIS

CHANNEL AND DIFFUSER

1. INTRODUCTION

This operating Safety and Hazard Analysis (SHA) for the lightweight channel and diffuser tests at Air Force Aero Propulsion Laboratory was conducted in accordance with Section 5.8.2 of MIL-STD-882 of 15 July 1969. A SHA for the AFAPL-MHD KIVA-I facility was used as a reference for the preparation of this report¹. The analysis was performed to determine safety requirements for personnel, procedures, and equipment used in installation, maintenance, support, testing, transportation, storage, operations, emergency escape, egress, rescue, and training during all phases of intended use as decided in the system requirements. Engineering data, procedures, and instructions developed from the engineering design and initial test programs were used in support of this effort. Results of these analyses provided the basis for:

- 1) Design changes where feasible to eliminate hazards or provide safety devices, and safeguards
- 2) The warning, caution, special inspections, and emergency procedures for operating and maintenance instructions including emergency action to minimize personnel injury
- 3) Identification of a hazardous period time span and actions required to preclude such hazards from occurring
- 4) Special procedures for servicing, handling, storage, and transportation.

¹⁵ AF Contract F33615-75-C-2043, "Alternate Fuels for MHD Applications."

2. AREAS TO BE CONSIDERED FOR THE CHANNEL AND DIFFUSER

The following areas, which are required to be reviewed by Section 5.8.2.1 of MIL-STD-882, were reviewed to determine their applicability. This SHA was conducted for the channel/diffuser system only. For the SHA for the complete facility, the AFAPL-MHD KIVA-I facility SHA should be consulted.

- A. Isolation of Energy Sources - Applicable**
- B. Fuels and Propellants - Not Applicable**
- C. System Environmental Constraints - Not Applicable**
- D. Explosive Devices - Not Applicable**
- E. Compatibility of Materials - Applicable**
- F. Transient I, Electrostatic, EMR, Ionizing Radiation - Applicable**
- G. Pressure Vessels and Plumbing - Applicable**
- H. Crash Safety - Not Applicable**
- I. Safe Operation and Maintenance - Applicable**
- J. Training and Certification in Operations and Maintenance - Applicable**
- K. Egress, Rescue, Survival - Not Applicable**
- L. Life Support Requirements - Not Applicable**
- M. Fire Ignition and Propagation Sources and Protection - Applicable**
- N. Resistance to Shock Damage - Not Applicable**
- O. Fail Safe Design Considerations - Applicable**
- P. Environmental Factors, Layout, Lighting, Safety Implications in Manual Systems - Not Applicable**
- Q. Safety from Vulnerability Standpoint, Armor, Fire Suppression, Redundancy - Not Applicable**
- R. Protective Clothing, Equipment or Devices - Applicable**
- S. Lightning and Electrostatic Protection - Not Applicable**
- T. Human Error Analysis of Operation Function and Tasks - Applicable**

3. COMPONENT IDENTIFICATION BY HAZARD AREAS

The subsystem hazard analysis per 5.8.2.2 identifies all components and equipment comprising each subsystem whose failure could result in hazardous conditions. Those components are identified below by the hazard area noted above.

- A. Isolation of Energy Sources
 - 1. Electrical signals and signal power
 - 2. MHD Power
 - a. Channel Electrodes
 - b. Insulation/Isolation for Diffuser
- B. Fuels and Propellants - Not Applicable
- C. System Environmental Constraints - Not Applicable
- D. Explosive Devices - Not Applicable
- E. Compatibility of Material
 - 1. Liquids
 - a. Hard Water - corrodes carbon steel fittings, restricts coolant flow; contains suspended material, plugs coolant channels.
 - b. Treated Water - corrodes carbon steel fittings, restricts coolant flow.
 - c. Electrolytic Action - deteriorates brasses, steels.
 - 2. Solids
 - a. Cs_2CO_3 - penetrates channel insulator and electrode ceramic material.
- F. Transient Current, Electrostatic Discharge, EMR, Ion Radiation
 - 1. Current Surges
 - a. Unsteady MHD operation
 - b. Load switching
 - c. Arcing to ground

- 2. Static Discharge - Not Applicable
- 3. Electromagnetic Radiation
 - a. Unsteady MHD operation
 - b. Load switching
- 4. Ionizing Radiation - Not Applicable
- G. Pressure Vessels and Plumbing
 - 1. Pressure gauge
 - 2. Pressure Transducers
 - 3. High Pressure H₂O System
 - a. Pipes, hoses, fittings
- H. Crash Safety - Not Applicable
- I. Safe Operation and Maintenance
 - 1. Use of check list
 - 2. Safety planning for tests
 - 3. Regularly scheduled, progressive maintenance
- J. Training and Certification in Operation and Maintenance
 - 1. Certification - Not Applicable
 - 2. Operators and technician trainees should operate under direction of past operators.
- K. Egress, Rescue and Survival - Not Applicable
- L. Life Support Requirements - Not Applicable
- M. Fire Ignition and Propagation Sources and Protection
 - 1. Ignition Sources
 - a. Damaged channel or diffuser
 - b. Short circuits, sparks
 - 2. Fire Propagation Sources
 - a. All combustible materials in presence of gaseous oxygen
 - 3. Fire Protection - Not Applicable
- N. Resistance to Shock Damage - Not Applicable

- O. Fail Safe Design Considerations
 - 1. Electrode frame cooling system
 - 2. Ceramic insulators
- P. Environmental Factors, Layout, Lighting, Safety Implications in Manual Systems - Not Applicable
- Q. Safety from Vulnerability Standpoint - Not Applicable
- R. Protective Clothing, Equipment, Devices
 - 1. Protective gloves, goggles, and dust masks when handling electrode and insulating ceramics and seed contaminated components and materials.
- S. Lightning and Electrostatic Protection - Not Applicable
- T. Human Error Analysis of Operator Functions and Tasks
 - 1. Impossible to evaluate as all functions are error prone.

4. HAZARD ANALYSIS BY COMPONENTS

- A. Isolation of Energy Sources
 - 1. Electrical Signals and Signal Power (5, 10, 15, 28 Vdc)

Hazard Potential: Numerous exposed cables

Hazard: Loss of power, damaged power supplies, fire

Cause: Short circuits because of abrasion and/or cutting of insulated cables by normal activity

Correction/Prevention: All signal cables and signal power should be encased within flexible protective sheaths and routed through cable ways. All electrical power requirements should be reviewed to insure a safe shutdown under electrical power failure conditions.
 - 2. MHD Power - Characteristically a noisy dc signal of 2500 V dc maximum and 300 A dc maximum, but not simultaneously.
 - a. Channel Electrodes

Hazard Potential: Voltage instrumentation leads from various electrode frames to the voltage divider located in test cell.

Hazard: Short circuit to ground through various paths.
Fire, explosion of various devices, electrocution.

Cause: Insulation breakdown, voltage divider breakdown arc over in voltage divider, arc over to manifolds or instrumentation.

Correction/Prevention: Extreme care to assure sufficient voltage potential gap between high voltage sources and conductors or wet and/or dirty surface. Need high voltage, high current shunt to earth ground or signal side of the voltage divider.

b. Insulation/Isolation for Diffuser

Hazard Potential: High voltage end of the channel (diffuser is secured with bolts having insulating sleeves and phenolic rod ends - the diffuser rests on a one-inch thick insulator).

Hazard: Short circuit to ground through various paths, fire, explosion of various components, electrocution.

Cause: Insulation breakdown, arc over to coolant manifold or instrumentation leads, dirty or wet insulation surfaces.

Correction/Prevention: Extreme care taken to assure unbroken or cracked insulations, maintain insulating surfaces in a clean and dry condition - need fuse shunts for all high voltage end instrumentation leads to shunt arc over current to earth ground.

B. Fuels and Propellants - Not Applicable

C. Systems Environmental Constraints - Not Applicable

D. Explosive Devices - Not Applicable

E. Compatibility of Liquids and Solids

1. Hard Water

Hazard Potential: Hard water is used wherever possible for coolant.

Hazard: Corrosion, burnout of components.

Cause: Carbon steel parts and pipe are corroded by hard water, causing decreased heat flow rates. Suspended material clogs flow passages.

Correction/Prevention: All hard water lines should have large filter screens for removal of suspended material. All fittings and tubing should be stainless steel or copper.

2. Treated Water

Hazard Potential: Treated water is used wherever higher quality water is needed, but de-ionized water is not required.

Hazard: Corrosion, burnout of components.

Cause: Carbon steel parts and pipe are corroded by the treated water, causing reduced heat flow rates where coolant lines have been restricted. Corrosion particles can obstruct coolant passages.

Correction/Prevention: All treated water lines should have large filter screens for removal of corrosion particles. Screens should be inspected regularly. All fittings and tubing should be stainless steel or copper.

3. Electrolytic Action

Hazard Potential: Dissimilar metal materials in contact with water.

Hazard: General deterioration of components - leaks and weakening of joints.

Cause: Highly dissimilar materials can be expected to sustain electrolytic activity.

Correction/Prevention: Care should be taken in specifying materials to reduce electrolytic potential. Materials, where possible, should be treated with inorganic protective coatings to reduce electrolytic activity.

4. Cs_2CO_3

Hazard Potential: Cs_2CO_3 is required to achieve the proper plasma conductivity, but material is corrosive to electrode/insulator system ceramic materials.

Hazard: General deterioration of the insulator ceramic eventually leading to electrical shorts between electrode frames.

Cause: Cs_2CO_3 penetration into the castable ceramics.

Correction/Prevention: Controlled shutdown procedure at conclusion of test where seed flow termination leads hot gas flow termination by more than one second. Operation with the minimum Cs_2CO_3 flow rate to achieve required plasma conductivity.

F. Transient Current, Electrostatic Discharge, EMR, Ion Radiation

1. Current Surges

a. Unsteady MHD Operation

Hazard Potential: Operation of the MHD generator primarily involves unsteady operation.

Hazard: No direct hazard without a failure of another type additionally.

Cause: Natural operation of MHD generator.

Correction/Prevention: None known at this time.

b. Load Switching

Hazard Potential: Operations involving load switching.

Hazard: Large arcs (open to atmosphere) drawn by opening circuits. Source of ignition. No direct hazard without additional failure.

Cause: Normal operation.

Correction/Prevention: Load switches might be housed in an inert atmosphere.

2. Static Discharges - Not Applicable

3. Electromagnetic Radiation

a. Unsteady MHD Operation

Hazard Potential: Unsteady generation of power is normal, but unusual or strong surging occurs.

Hazard: Electrical shocks, data biasing, computer errors, adverse test sequence influence.

Cause: Rapid variation of power can cause transient and randomly induced voltages during periods of strong MHD generator surging. The result is loss of data, erroneous data, or erroneous computer operation. Extreme cases could conceivably cause minor electrical shocking from ungrounded metal objects and erroneous test sequence signal.

Correction/Prevention: All metallic objects should be grounded to earth ground - all cabling should be shielded and grounded to earth ground. All cabinetry for computers, controls, etc., should completely enclose the components and be grounded to earth ground.

b. Load Switching

Hazard Potential: Operations involving load switching.

Hazard: Same as Unsteady MHD Operation.

Cause: Rapid variation of loading by load switching can cause randomly induced voltages.

Correction/Prevention: Same as for Unsteady MHD Operation.

4. Ionizing Radiation - Not Applicable

G. Pressure Vessels and Plumbing

1. Pressure Gauges

Hazard Potential: Bourdon tube gauges are used for calibration, setting points, and monitoring critical pressures.

Hazard: Explosive rupture of the gauges, incorrect indication response to applied pressure.

Cause: Overpressurization, incorrect calibration, malfunctioning, deterioration.

Correction/Prevention: Periodic inspection and calibration, shatterproof plexiglass shields over gauges.

2. Pressure Transducers

Hazard Potential: Strain gauge pressure transducers are used to monitor various pressures.

Hazard: Incorrect readings (indications).

Causes: Incorrectly positioned calibration valves, transducer shorting (water leaks can do this), improper or obsolete amplifier calibration settings.

Correction/Prevention: Transducer connections should be protected from short circuiting influences. Check lists must be strictly adhered to in valve positioning. Transducer amplifiers must be calibrated prior to each test run to reduce drift errors.

3. High Pressure Water System

a. Pipes, hoses, fittings, valves

Hazard Potential: Water is routed through copper pipe, re-inforced nylon tubing, copper tubing and brass barbed fittings.

Hazard: Ruptures, leaks, clogging.

Cause: Overpressure, deterioration of materials or joints, corrosion.

Correction/Prevention: System should be provided with pressure-relieve valves and/or vents; lines should be leak tested and flow tested periodically.

H. Crash Safety - Not Applicable

I. Safe Operation and Maintenance

1. Use of Check List - Check lists for system operation must be strictly adhered to.
2. Safety Planning for Tests - Each test must be analyzed concerning expected operation of the test cell and where deviations from normal operation are to be expected. These deviations must be thoroughly analyzed to provide safety precautions in areas where abnormal operation may create unsafe conditions.
3. Regularly Scheduled Progressive Maintenance - All items of hardware involved in operation should be placed on a table of periodic maintenance operations which should include regular inspection.

J. Training and Certification in Operation and Maintenance

1. Certification - Not required.
2. Operators and trainee technicians should receive on-the-job training and operate the system under the direction of persons experienced in its operation.

K. Egress, Rescue and Survival - Not Applicable

L. Life Support Requirements - Not Applicable

M. Fire Ignition and Propagation Sources and Protection

1. Ignition Sources

a. Channel or Diffuser

Hazard Potential: High temperature combustion gases.

Hazard: Burnout of components.

Cause: Burn-through or deteriorating gasketing plus burn-through of electrode frame insulation and channel composite case have the potential to burn the magnet coil insulation causing short circuiting.

Correction/Prevention: No simple means of interlocking against burnouts is possible; it is necessary that the operator know what to expect and what to look for and shut down the system through the dead man switch in these events.

b. Short Circuits or Sparks

Hazard Potential: Ignition of combustible products present as vapors in the test cell.

Hazard: Overloaded electrical circuits or open arc current concentrations.

Cause: Overheating caused by electrical conditions forcing electric current through a reduced number of circuits. Sparks caused by shorting of high voltage components to ground.

Correction/Prevention: Verify that all electrical connections are properly installed and that all lug/terminal connections are securely attached. Review operation to insure that all water sprays, test leads, etc. do not provide short circuit or grounding conditions.

2. Fire Propagation Sources

a. All Combustible Materials in Presence of Gaseous Oxygen

Hazard Potential: Oxygen rich atmosphere.

Hazard: Metal oxidation.

Cause: Hot metal components exposed to oxygen rich conditions during channel operation.

Correction/Prevention: Operate components with the surface temperatures below the combustion temperature of the component.

N. Resistance to Shock Damage - Not Applicable

O. Fail Safe Design Considerations

1. Electrode Frame Cooling System

Hazard Potential: Overheating of electrode frames and adjacent case area.

Hazard: Loss of cooling system integrity without interlock signal.

Cause: Reduced water flow rate because of leaks and/or partially blocked tubes.

Correction/Prevention: Cooling water flow rates should be interlocked with the operating system to cause a system shutdown if proper water flow rates are not maintained.

2. Ceramic Insulators

Hazard Potential: Degradation of the insulator material.

Hazard: Electrode frame short circuit.

Cause: Seed penetration of the insulator ceramic.

Correction/Prevention: Controlled shutdown procedure at conclusion of test where seed flow termination leads hot gas flow termination by more than one second. Operation with minimum Cs_2CO_3 flow rate to achieve required plasma conductivity.

P. Environmental Factors, Layout, Lighting, Safety Implications in Manual Systems - Not Applicable

Q. Safety from Vulnerability Standpoint - Not Applicable

R. Protective Clothing, Equipment, Devices

1. Protective gloves, goggles, and dust masks when handling electrode and insulating ceramics and seed contaminated materials.

Hazard Potential: Cesium carbonate or cesium nitrate compounds are used as seeding agents. Ceramic materials used in channel electrodes.

Hazard: Cesium compounds are extremely caustic and can cause severe skin burns as well as lung irritation. Cesium and its oxides form caustic hydroxides on contact with moisture. Ceramic materials are irritants to skin, eyes, and lungs.

Cause: During operation of the channel and diffuser, deposits form on the walls due to condensation of seed and slight corrosion of the walls.

Correction/Prevention: Protective clothing, when handling all ceramic and seed materials such as cesium and potassium compounds, should include gloves, goggles, and a dust mask as a minimum. The same precautions should be observed when handling the internal surfaces of the channel and diffuser after system operation with seed materials.

S. Lightning and Electrostatic Protection - Not Applicable

T. Human Error Analysis of Operator Functions and Tasks

1. Hazards involved in operator functions are impossible to evaluate; therefore, it is imperative that check lists be carefully prepared and strictly adhered to. The use of interlock bypasses to facilitate test operations is extremely hazardous and should not be used except for "dummy" test, calibration checks, and other non-combustion type tests.

REFERENCES

1. Shanklin, R.V., Lytle, J.K., Nimmo, R.A., Buechler, L.W., and Hehn, H.W., "KIVA-I Extended Duration MHD Generator Development," AFAPL-TR-75-27, June 1975.
2. Brogan, T.R., Aframe, A.M., and Hill, J., "Preliminary Design of a Magneto-hydrodynamic Channel for the USSR U-25 Facility," Final Report, Contract No. 14-32-001-1733, ERDA, November 1974.
3. Sonju, O.K., Teno, J., Lothrop, J.W., and Petty, S.W., "Experimental Research on a 400 kW High Power Density MHD Generator," AFAPL-TR-71-5, May 1971.
4. Sonju, O.K., Teno, J., Kessler, R., Lontai, L., and Meader, D.E., "Status Report of the Design Study Analysis and the Design of a 10 MW Compact MHD Generator System," AFAPL-TR-74-47, Part II, June 1974.
5. Coffin, L.F., Internal Stresses and Fatigue in Metals, Rossweiler, G. and Grube, W., Elsevier Publishing Co., 1959.
6. Majors, H., "Comparison of Thermal Fatigue with Mechanical Fatigue Cycling," ASTM STP 165, 1954.
7. Manson, S.S., "The Challenge to Unify Treatment of High Temperature Fatigue," ASTM STP 520, 1973.
8. Dietz, A.G.H., Composite Engineering Laminates, MIT Press, 1969.
9. Broutman, L.J. (Ed.), Composite Materials, Vol. 5, Academic Press, 1974.
10. Jacobsen, L.C., Ayre, R.S., Engineering Vibrations, McGraw Hill, 1958.
11. Kreith, F., Principles of Heat Transfer, International Textbook Co., 1961.
12. "User Information Manual for MITAS (Martin Marietta Thermal Analyzer System)," Publication No. 86615000, Rev. A; Cybernet Service Control Data Network; September 1972.
13. Anon., "Flow of Fluids Through Valves, Fittings, and Pipes," Crane Company Technical Paper No. 410, 1970.
14. Swallom, D.W., Sonju, O.K., Meader, D.E., and Becker, H., "High Power Magnetohydrodynamic System," Final Report on Air Force Contract No. F33615-76-C-2104, June 1978.
15. Alternate Fuels for MHD Applications, "Safety and Hazards Analysis Report," from Air Force Contract No. F33615-75-C-2043, 1976.

LIST OF ABBREVIATIONS, ACRONYMS, AND SYMBOLS

A	Ampere
A	Area
AFAPL	Air Force Aero Propulsion Laboratory
atm	Atmosphere
B	Magnetic Field Strength
c	Speed of Sound
CDA	Copper Development Association
cm	Centimeter
d	Tube Diameter
dc	Direct Current
deg	Degree
E	Young's Modulus
EMR	Electromagnetic Radiation
f	Frequency
g	Gravitational Acceleration
g	Grams
h	Water/Metal Surface Heat Transfer Film Coefficient
h	Corner Thickness of Case
Hz	Hertz
I_{xx}	Moment of Inertia About Principal Central Axis
I. D.	Inside Diameter
K	Kelvin
KIVA-I	MHD Test Facility at AFAPL
kg	Kilogram
kHz	Kilohertz
kW	Kilowatts

LIST OF ABBREVIATIONS, ACRONYMS, AND SYMBOLS

L	Length
LWC	Lightweight Channel
m	Meter
\dot{m}	Mass Flow Rate
min	Minute
ml	Milliliters
mm	Millimeter
MHD	Magnetohydrodynamic
MIL-STD	Military Standard
MITAS	Martin Marietta Thermal Analyzer System
MLI	Maxwell Laboratories, Inc.
MW	Megawatt
N	Newton
NA	Not Applicable
N _{all}	Number of Cycles
No.	Number
O. D.	Outside Diameter
OFHC	Oxygen-Free High-Conductivity
p	Pressure
Q	Total Heat Transfer Rate
r	Channel Radius of Gyration
R	Corner Radius of Case
RMA	Reliability and Maintainability Analysis
rpm	Revolutions per Minute
RTV	Room Temperature Vulcanizing

LIST OF ABBREVIATIONS, ACRONYMS, AND SYMBOLS

sec	Second
SHA	Safety and Hazards Analysis
T	Temperature
T_w	Water Temperature
v	Velocity
V	Volts
w	Frame Width Parallel to Gas Flow
W_{case}	Mass of Case
W_{frames}	Mass of Frames
\bar{y}	Distance from Centroid to Section Extremity
Z_{xx}	Section Modulus About Principal Axis
α	Coefficient of Thermal Expansion
ϵ	Total Strain
ϵ_1	Circumferential Membrane Strain
σ	Bending Stress
σ_1	Membrane Stress
σ_2	Axial Stress
σ_{TU}	Ultimate Tensile Strength
σ_{TY}	Yield Strength
ν	Poissons Ratio
ΔP	Pressure Difference
ΔT	Temperature Difference